

**Phenomenological Consequences of QCD
Bremsstrahlung Processes in RHIC and LHC**

By

Raktim Abir

(Enrolment Number PHYS05200704015)

**Saha Institute of Nuclear Physics
Kolkata**

*A thesis submitted to the
Board of Studies in Physical Sciences
in partial fulfilment of requirements
for the degree of*

Doctor of Philosophy

of

Homi Bhabha National Institute



October, 2013

Homi Bhabha National Institute

Recommendations of the Viva Voce board

As members of the Viva Voce Board, we certify that we have read the dissertation prepared by Raktim Abir entitled "QCD Bremsstrahlung Processes and their Phenomenological consequences in RHIC and LHC" and recommend that it may be accepted as fulfilling the dissertation requirement for the Degree of Doctor of Philosophy.

D. K. Srivastava

Date : 6/11/2013

Chairman : Dinesh K. Srivastava

Munshi

Date : 06/11/2013

Guide / Convener : Prof. Dr. Munshi G. Mustafa

Jane Alam

Date : 6/11/2013

Member 1 : Jane Alam

Sourav Sarkar

Date : 08/11/2013

Member 2 : Sourav Sarkar

P. Mitra

Date : 6.11.13

Member 3 : Partha Mitra

Date :

Member 4 :

External Examiner : Subrata Pal Subrata Pal

Date : 06/11/13

Final approval and acceptance of this dissertation is contingent upon the candidates submission of the final copies of the dissertation to HBNI.

I hereby certify that I have read this dissertation prepared under my direction and recommend that it may be accepted as fulfilling the dissertation requirement.

Munshi

Date : 06/11/2013

Guide : Prof. Dr. Munshi G. Mustafa

Statement by Author

This dissertation has been submitted in partial fulfillment of requirements for an advanced degree at Homi Bhabha National Institute (HBNI) and is deposited in the Library to be made available to borrowers under rules of the HBNI.

Brief quotations from this dissertation are allowable without special permission, provided that accurate acknowledgement of source is made. Requests for permission for extended quotation from or reproduction of this manuscript in whole or in part may be granted by the Competent Authority of HBNI when in his or her judgment the proposed use of the material is in the interests of scholarship. In all other instances, however, permission must be obtained from the author.

Raktim Abir
Raktim Abir

Declaration

I declare that the investigation presented in the thesis has been carried out by me. The work is original and has not been submitted earlier as a whole or in part for a degree / diploma at this or any other Institution / University.

Raktim Abir
Raktim Abir

To My Parents,

... who value education above all else.

Acknowledgement

The time spent in writing a doctoral Thesis provides a rather unique opportunity to look back and gain a new perspective on several years of work. In doing so, I feel the need to thank the many people who have contributed in different ways to the realization of this work. I wish to express my sincerest gratitude to my PhD supervisor Prof. Munshi G. Mustafa, for generously sharing with me his scientific caliber and experience, which has permitted me to continuously improve my skills while allowing the progressive development of my independence. But even more, I thank him for his persistent support, and for being gifted with a firm enthusiasm and a solid guidance which really help to transform even the frantic work as an enjoyable experience. It is also a real pleasure for me to thank Prof. Dinesh K. Srivastava. Aside from his outstanding ability to execute research works, I am grateful to him for having closely followed my activity, thus allowing me to benefit from his very large experience and knowledge.

I thank Prof. Carsten Greiner, Dr. Mauricio Martinez, Dr. Umme Jamil, Jan Uphoff who has always been exceedingly generous in sharing their time in plenty of stimulating scientific discussions and collaboration related to work contained in this thesis. With all these people I am really indebted for having given an invaluable contribution to this work and, even more, to my formation as a young researcher. I would also like to thank Prof. Partha Mitra, Prof. Jane-e Alam, Prof. Subhasis Chattopadyay and Prof. Sourav

Sarkar for their generous help and support.

I wish to thank my colleagues with whom I have shared my PhD experience. The warm friendship and affection I have been received from them, particularly the members of 363 of Saha Institute, is always a charming experience I have gone through during the past few years. And will remain an asset of my life.

I wish to express my deep sense of gratitude to my parents, Enamul Kabir and Husnehana Begum, and brother Neelim Abir for their immense patience, love, affection, encouragements and support. I am indebted to my parents for giving me the freedom to choose my own career and for constantly providing me the ideological and emotional support at every stage of my life. It is only because of their kind wishes that I could complete this work.

Also my friends in my private life truly deserve my most sincere gratefulness for being close to me during these years and for helping me in times of trouble.

Last but not least, I thank Naznin. You have been at my side and believed in me during these years, and your enduring love is a privilege that I really hope to deserve. I regard every achievement in my life as a success of ours.

Raktim Abir

Publications

Journal Articles

- *SU(3) color singletness, Z(3) symmetry, Polyakov Loop and dynamical recombination.*,

Chowdhury Aminul Islam, **Raktim Abir**, Munshi G. Mustafa, Sanjay

K. Ghosh, Rajarshi Ray.

arXiv:1208.3146 [hep-ph].

Accepted in **J. Phys. G (2013)**.

- *Jet-parton inelastic interaction beyond eikonal approximation,*

Raktim Abir,

arXiv:1301.1839 [hep-ph],

Phys. Rev. D 87, 034036 (2013).

- *Heavy Quark Energy loss and D mesons at RHIC and LHC energies,*

Raktim Abir, Umme Jamil, M. G. Mustafa and D. K. Srivastava,

arXiv:1203.522 [hep-ph],

Phys. Lett. B 715, 183-189 (2012).

- *Soft gluon emission off a heavy quark revisited,*

Raktim Abir, Carsten Greiner, Mauricio Martinez, Munshi G. Mustafa

and Jan Uphoff,

arXiv:1109.5539 [hep-ph],

Phys. Rev. D 85, 054012 (2012).

- *Generalisation of Gunion-Bertsch Formula for Soft Gluon Emission,*
Raktim Abir, Carsten Greiner, Mauricio Martinez and Munshi G. Mustafa,
arXiv:1011.4638 [hep-ph],
Phys. Rev. D 83, 011501 (2011) (Rapid Communication).
- *Colour-singlet clustering of partons and recombination model for hadronization of quark-gluon plasma,*
Raktim Abir and M. G. Mustafa,
arXiv:0905.4140 [hep-ph].
Phys. Rev. C 80, 051903 (2009) (Rapid Communication).

Preprints

- Color synchrotron off heavy flavor jet deluges the "dead cone",
T. Bhattacharyya, S. Mazumder and **Raktim Abir**,
arXiv:1307.6931 [hep-ph].
- *On the critical exponent of η/s and a new exponent-less measure of fluidity ,*
Raktim Abir and M. G. Mustafa
arXiv:1001.0692 [hep-ph].

Contents

1	Introduction	21
1.1	Prelude	21
1.2	Emergence of Chromodynamics	23
1.3	QCD Phase Diagram	28
1.3.1	QCD Lagrangian and running coupling	28
1.3.2	Existence of a new state of matter	30
1.4	Experimental Observables	32
1.4.1	Soft sector observables : Anisotropic flow	32
1.4.2	Hard sector observable : Jet quenching	34
1.5	Chronicles of in-medium jet energy loss	36
1.5.1	Collisional energy loss	36
1.5.2	Radiative energy loss	39
1.5.3	Radiative loss of heavy flavor	44
1.6	Essential features of jet models	46
1.6.1	Medium modeling in jet models	46
1.6.2	The unphysical ‘leakage radiation’	50
1.6.3	Kinematic approximations in jet models	51

1.7	Stripping eikonal-collinear constrains	54
1.8	Outline of Thesis	55
2	Gluon-Gluon Scattering	59
2.1	Inelastic Gluon-Gluon Scattering ($gg \rightarrow ggg$)	61
2.2	Gluon multiplicity distribution	67
2.3	Generalization to $2 \rightarrow n$, $n > 3$	70
2.4	Discussion	72
3	Quark-Quark Scattering	73
3.1	Inelastic Quark-Quark Scattering ($qq' \rightarrow qq'g$)	74
3.1.1	Hierarchy in momentum scales	76
3.1.2	Matrix Elements, Amplitude and Cross-section	77
3.2	Inelastic gluon-gluon fusion ($gg \rightarrow ggg$)	83
3.3	Results and Discussion	85
4	Heavy Flavor Bremsstrahlung	89
4.1	Spectrum without collinear approximation	91
4.2	Gluon multiplicity distribution	95
4.3	Discussion	99
5	Energy loss of Heavy Quark	101
5.1	Radiative Energy Loss	107
5.1.1	Hierarchy and momentum cuts	109
5.1.2	Maximal rapidity integration :	110
5.2	Improved energy loss expression:	111

5.3	D Mesons at RHIC and LHC	113
5.3.1	Heavy quark production in pp collisions	113
5.3.2	Initial Conditions and Evolution of the Medium	114
5.4	Results and Discussion	118
5.5	The endeavour	124
6	Summary	127
A	Collider Variables	135
B	Gluon Kinematics	141
C	Matrix Elements	143
D	Color Factors	151
E	L^2 Dependence	153
Literature		157
		185

Synopsis

According to most prevailing *scientific* model for evolution of our universe, the early universe was filled with quantum fields maintaining its homogeneity and isotropy. With an incredibly high energy density, temperature and pressure the universe was expanding and cooling very rapidly. At approximately 10^{-35} s after the birth (with temperature about $\sim 10^{28}$ K) certain phase transitions caused *cosmic inflation* during which the universe grew exponentially. When inflation stopped at about $\sim 10^{-10}$ s after birth, ultra hot baby universe (with temperature about $\sim 10^{15}$ K) for the first time goes to a phase where one of its gradually dominating component supposed to be the *quark-gluon plasma*, a state where quarks and gluons are almost free to roam around and be in a state of plasma. The cosmic phase consists of quark-gluon plasma starts from an era of electro-weak phase transition (electric and weak force decoupled) till roughly $10 \mu\text{s}$ when quarks become confined into protons and neutrons at about $\sim 10^{12}$ K temperature. It is likely that those extreme temperatures are last seen in nature only in those elusive first few μs after the *Big Bang*. However, extraordinary global scientific effort recreates them for only about thousands of times a second in particle accelerators such as Relativistic Heavy Ion Collider (RHIC) at Brookhaven National Laboratory (BNL) in New York and Large Hadron Collider (LHC) at Conseil European pour la Recherche Nuclaire (CERN) in Geneva. At these temperatures, 10,000 times hotter than the centre of the sun, nuclear force becomes the dominant force over rest three fundamental force *viz.* electromagnetic, weak and gravitational. Experiments both at RHIC and LHC help

to learn about the fundamental and non-trivial emergent many-body plasma dynamics of the quarks and gluons that make up 99% of the mass of the *optically visible* universe. Collisions of ultra relativistic heavy-ion beams in the said experiments create a hot and dense medium comparable to the conditions in the early universe. One can try to determine the properties of this *quark-gluon plasma* through various hard probes, for instance tomographical probs. Tomographic measurement of those signatures is extremely crucial in order to determine the properties of the quark and gluon plasma, and eventually probe the first few moments of birth of this universe. momentum particles by studying the nuclear modification factor and suppression of back-to-back correlations. This *jet tomography* is supposed to be one of the most prominent signatures that signify presence of the partonic degrees of freedom in the hot QCD matter. Overwhelming evidences of this signature

Constituent *quark number scaling*[108] of elliptic flow and *jet quenching*[110] are supposed to be the most prominent signatures that favour the partonic degrees of freedom in the deconfined QCD matter. Jet tomography is the most powerful femtoscope for seeing into the very heart of the physics of heavy ion collisions. In particle physics, a jet is a narrow cone of particles produced by highly energy quarks and gluons. On very rare occasions, in a heavy ion collision extremely energetic particles are created which interact with the hot soup of deconfined QGP matter, subsequently becoming a jet of particles. It is the interactions between the high energy particle and the QGP medium that provide the most direct probe of the fundamental degrees

of freedom in a quark-gluon plasma: one hopes to tease out the properties of the QGP by comparing theoretical predictions based on assumptions for the relevant physics of the interactions to experimental measurements of these jets of particles.

Therefore the qualitative, and most certainly quantitative, extraction of the properties of QGP from jet tomography requires a well-controlled understanding of how high momentum particles lose energy as they propagate through the hot nuclear matter. As they propagate the energy of the high momentum partons is *reorganized* through collisional scatterings and *reduced* through medium induced gluon radiations, the latter being the dominant mechanism in this hot medium, the quark-gluon plasma. First evidence of parton energy loss has been observed at RHIC from the suppression of high momentum particles by studying the nuclear modification factor and suppression of back-to-back correlations [3]. Overwhelming evidences of this signature coming from dedicated heavy-ion experiments viz., STAR and PHENIX/RHIC/BNL, ALICE/LHC/CERN established the fact that, the primordial hot soup of nuclear matter, produced in those experiments, indeed contain partonic degrees of freedom (before freeze out to hadrons in later stage) instead of hadronic degrees of freedom throughout. Observation of strong suppression of inclusive yields of high momentum hadrons and semi-inclusive rate of azimuthal back-to-back high momentum hadron pairs relative to p-p collisions, are expectations from jet quenching. Both of them are extensively explored in collisions of Au-Au nuclei at $\sqrt{s} = 200$ A GeV

in RHIC. Fresh evidence for *jet quenching* has also been observed recently in Pb-Pb collision at ALICE.

Any phenomenologically peppy theory of jet, to study its quenching due to gluon emanation, in a hot and dense deconfined quark-gluon medium requires understanding of medium induced parton energy dispoession beyond the limit of eikonal kinematics. Strong modification of the internal architecture of the jet shower, in the form of energy degradation of most energetic partons as well as effects on the transverse momentum broadening and in-jet gluon multiplicity, in general are governed by both inelastic (radiative dispoession of energy) and elastic processes (collisional dispoession of energy). QCD based analytical analysis of quenching of jets remain clogged so far to *soft and eikonal* limits of parton kinematics. Studies of the predominant inelastic process of medium induced gluon radiation so far have focused on this limit. According to *soft and eikonal* kinematic approximation energy of the leading projectile parton E is taken to be quite large compare to the energy of the radiated gluon ω , which in turn suppose to be much larger than transverse moments carried by the gluon (k_{\perp}) and the recoiling momentum of scattering centre (q_{\perp}) much smaller than the gluon energy,

$$E \gg \omega \gg k_{\perp}, q_{\perp} \gg m_{g,q} \gg \Lambda_{QCD} \quad (1)$$

The foundation analysis of radiative parton energy loss by Gyulassy and Wang [140], Baier, Dokshitzer, Mueller, Peigne and Schiff [143] and by Za-

kharov [151] are based on this approximation. Same legacy of soft and eikonal approximation is also being carried off by the next generation prevailing models of jet quenching *viz.* by Armesto, Salgado, Wiedemann (ASW) [7, 167, 166, 181, 165], Gyulassy, Levai and Vitev (GLV) [156, 158, 157], Wicks, Horowitz, Djordjevic and Gyulassy (WHDG) [182, 189], Wang and Wang (WW) [17, 170] and by Arnold, Moore and Yaffe (AMY)[19, 176, 21] and others. It is generally agreed that extrapolating calculations of parton energy loss from 1.9 to the full phenomenologically relevant kinematic range induces uncertainties that are much larger than the other known model dependent differences [198]. In this thesis I have addressed some key issues, for which the *standard jet quenching models* are still lacking.

Eikonal parton trajectory approximation constrains the leading parton of the jet to have energy E much larger than the transverse momentum of exchanged gluon q_{\perp} (with medium partons) as well as transverse momentum of the emitted gluon k_{\perp} *i.e.* $E \gg q_{\perp}, k_{\perp}$. The kinematic constraints $E \gg q_{\perp}, k_{\perp}$ referred in the literature as soft eikonal approximation neglects any change in parton trajectory due to multiple scatterings but assumes a straight line trajectory throughout. Hence it is not able to give sufficient transverse kick to deflect the parton from straight trajectory. In order to study *diffusion of jets* inside the hot matter it is crucial to overcome this approximation. We have revisited the issue in Feynman gauge and make attempt to relax this approximation for the process $gg \rightarrow ggg$ [201]. We found that the correction terms are important at various physical domains of tem-

perature, coupling constant and the energy of gluon-gluon scattering. This generalisation seems to be very apt for the phenomenology (*viz.* hot glue scenario, chemical equilibration of gluons, partonic matter viscosity, radiative energy-loss of energetic partons and jet quenching) of heavy-ion collisions and would improve the present understanding on various phenomena in this area. An attempt has been also been made to relax part of the eikonal approximation for the inelastic process $qq' \rightarrow qq'g$ [202]. For both $qq' \rightarrow qq'g$ and $gg \rightarrow ggg$ differential cross-sections in first order noneikonal approximation have been obtained. Primary estimation indicates (15-20%) reduction in the cross section due to first order non-eikonal effect for both the processes in the soft and intermediate parton energies. These cross-sections naturally reproduce eikonally approximated results in the eikonal limit for soft emission, i.e., $E \gg q_{\perp}, k_{\perp}$ and $q_{\perp} \gg k_{\perp}$. QGP produced at LHC where large virtuality scattering processes may be dominant one, seems to be less opaque to jets than predicted by constrained extrapolations from RHIC. There are however other views also, where another set of constrained extrapolations show considerable variation in the postdictions of RHIC-constrained scenarios with LHC data. Here this has been taken as a constraint and cause to disregard class of models which fail to predict/postdict correctly the uprising behaviour of nuclear modification factor rather than assigning it as a generic surprising feature of LHC data. Our results indicate some reductions in interaction strengths of jets due to non-eikonal effects, in soft and intermediate sector. In the soft sector when the problem is embedded into a hydrodynamically evolving density distribution this could lead to non-trivial effects. We

also show that wide back scattering with scattering angle more than $\simeq 0.52\pi$ is forbidden in case of $qq' \rightarrow qq'g$ when the emitted gluon is soft. This, however, is not the case for $gg \rightarrow ggg$.

Small angle or collinear gluon emission approximation tells that energy ω of the emitted gluon is much larger than its transverse momentum k_{\perp} *i.e.* $\omega \gg k_{\perp}$. This connotes the fact that the angle between the direction of propagation of leading parton and the direction of emitted gluon is small, as both of them supposed to be collinear. We have recalled the process $qQ \rightarrow qQg$ in Feynman Gauge, where q and Q denote light and heavy quarks (e.g. charm) quark, respectively, instead of usually employed light-cone gauge in this context. We derived a compact expression that contains a generalized suppression factor for gluon emission off a heavy quark through the scattering with a light parton. This improved generalized suppression factor is derived within perturbative QCD and valid for the full range of rapidity of the radiated gluon *i.e.* free from *small angle/collinear* gluon emission approximation for soft gluon emissions [203]. In the appropriate limit this expression reduces to the usually known *dead cone factor*[26, 179]. Our analysis shows that even though there is a suppression of radiative soft gluon emission due to the mass of the heavy quark in the forward direction, it is almost tantamount in the backward regions. Consequently present findings indicate that a heavy quark emits a soft gluon almost similar to that of a light quark. This result seems to have important consequences for a better understanding of heavy flavor

energy loss in heavy-ion collisions.

We obtained the radiative energy loss of a heavy quark akin to the Bethe-Heitler approximation by considering the most generalised gluon emission multiplicity expression derived. It commends that both energetic heavy and light quark lose energy due to gluon emission almost similarly and the mass plays a role only when the energy of the quark is of the order of it. The hierarchy used for simplifying the matrix element as well as for obtaining the gluon radiation spectrum imposes a restriction on the phase space of the emitted gluon in which the formation time is estimated to be less than the interaction time. This suggests that the LPM interference correction may be marginal. Further, we compare our results with the well know existing formalism and it is found to differ significantly. To compute the nuclear suppression factor for D-meson we consider both radiative and collision energy loss along with longitudinal expansion of the medium. The nuclear modification factor for D-meson with radiative energy loss obtained in the present formalism has an increasing trend at high transverse momentum and found to agree closely with the very recent data from ALICE collaboration at 2.76 ATeV [204]. The ALICE experiment in CERN have measured the *nuclear modification factor* R_{AA} of charmed mesons and heavy flavor mesons (in general) in semi-electronic channels at mid-rapidity regions. Measurements for R_{AA} have also been done for heavy flavored mesons in semi-muonic decay channels at forward rapidity regions. Fresh data from ALICE/LHC show features that appear to be in accordance with $pQCD$ energy loss predictions

: significant ascendancy of *nuclear modification factor* R_{AA} at LHC as a function of transverse momentum. This appears to be qualitatively different to the observed sluggish flatness at RHIC. Our results are in accordance with trends of R_{AA} both from RHIC as well as LHC. Since there is not a single adjustable parameters for us, the simultaneously good description of R_{AA} both at *RHIC* and at *LHC* in our model is rather encouraging. When the collisional counter part is added independently, the further suppression is obtained in the nuclear modification factor. This suggest the non-photonic single electron data at 200 AGeV RHIC energy requires contributions from collisional energy loss as well from B decay. However, it is necessary to obtain both radiative and collisional energy loss from the same formalism to minimize the various uncertainties, which is indeed a difficult task. Moreover, data at high transverse momentum region with improved statistics are required to remove prejudice on different energy loss and jet quenching models.

The LHC data provide stringent tests of jet quenching theory complementary to those at RHIC—for example, via the momentum dependence of heavy quark energy loss, which is predicted to be different in strongly and weakly coupled regimes of the QGP. The higher beam energy at LHC makes the rate of rare probes much higher than the RHIC. This opens a larger kinematic range for hadrons, photons and b quarks. Challenging theoretical advances, including higher-order jet calculations [201, 202, 203] and effective theories [222, 223, 224] that connect lattice simulations with transport processes, are

needed to extract reliable values for the energy loss parameters and color screening length in the plasma from high precision data. Major numerical advances will be required to solve the transport equations describing rapid formation of an equilibration QGP. Such advances will not only elucidate the physics of QGP but also address intellectual challenges of strong coupling in many areas of physics.

Exploration of hot QCD matter has made enormous progress during the past decade. Experiments have discovered a new high-temperature phase, the strongly coupled *quark-gluon plasma* (QGP), which persists to the highest temperature probed. Surprising features of the QGP include near perfect fluidity and extreme opaqueness to all coloured probes. The rapid developments of theoretical and experimental tools promise quantitative insights into the still mysterious properties of QGP during coming decade.

Bibliography

- [1] KAamodt *et al.* [ALICE Collaboration], “Elliptic flow of charged particles in Pb-Pb collisions at 2.76 TeV,” *Phys. Rev. Lett.* **105**, 252302 (2010) [arXiv:1011.3914 [nucl-ex]].
- [2] K. Aamodt *et al.* [ALICE Collaboration], “Suppression of Charged Particle Production at Large Transverse Momentum in Central Pb-Pb Collisions at $\sqrt{s_{NN}} = 2.76$ TeV,” *Phys. Lett. B* **696**, 30 (2011) [arXiv:1012.1004 [nucl-ex]].
- [3] X. -N. Wang, “Why the observed jet quenching at RHIC is due to parton energy loss,” *Phys. Lett. B* **579**, 299 (2004) [nucl-th/0307036].
- [4] M. Gyulassy and X. -n. Wang, “Multiple collisions and induced gluon Bremsstrahlung in QCD,” *Nucl. Phys. B* **420**, 583 (1994) [nucl-th/9306003].
- [5] R. Baier, Y. L. Dokshitzer, A. H. Mueller, S. Peigne and D. Schiff, “Radiative energy loss and p(T) broadening of high-energy partons in nuclei,” *Nucl. Phys. B* **484**, 265 (1997) [hep-ph/9608322].

-
- [6] B. G. Zakharov, “Radiative energy loss of high-energy quarks in finite size nuclear matter and quark - gluon plasma,” JETP Lett. **65**, 615 (1997) [hep-ph/9704255].
- [7] C. A. Salgado and U. A. Wiedemann, “A Dynamical scaling law for jet tomography,” Phys. Rev. Lett. **89**, 092303 (2002) [hep-ph/0204221].
- [8] C. A. Salgado and U. A. Wiedemann, “Calculating quenching weights,” Phys. Rev. D **68**, 014008 (2003) [hep-ph/0302184].
- [9] C. A. Salgado and U. A. Wiedemann, “Medium modification of jet shapes and jet multiplicities,” Phys. Rev. Lett. **93**, 042301 (2004) [hep-ph/0310079].
- [10] N. Armesto, C. A. Salgado and U. A. Wiedemann, “Medium induced gluon radiation off massive quarks fills the dead cone,” Phys. Rev. D **69**, 114003 (2004) [hep-ph/0312106].
- [11] N. Armesto, C. A. Salgado and U. A. Wiedemann, “Measuring the collective flow with jets,” Phys. Rev. Lett. **93**, 242301 (2004) [hep-ph/0405301].
- [12] M. Gyulassy, P. Levai and I. Vitev, “Jet quenching in thin quark gluon plasmas. 1. Formalism,” Nucl. Phys. B **571**, 197 (2000) [hep-ph/9907461].
- [13] M. Gyulassy, P. Levai and I. Vitev, “Reaction operator approach to non-Abelian energy loss,” Nucl. Phys. B **594**, 371 (2001) [nucl-th/0006010].

-
- [14] M. Gyulassy, P. Levai and I. Vitev, “NonAbelian energy loss at finite opacity,” Phys. Rev. Lett. **85**, 5535 (2000) [nucl-th/0005032].
- [15] M. Djordjevic and M. Gyulassy, “Heavy quark radiative energy loss in QCD matter,” Nucl. Phys. A **733**, 265 (2004) [nucl-th/0310076].
- [16] S. Wicks, W. Horowitz, M. Djordjevic and M. Gyulassy, “Elastic, inelastic, and path length fluctuations in jet tomography,” Nucl. Phys. A **784**, 426 (2007) [nucl-th/0512076].
- [17] E. Wang and X. -N. Wang, “Jet tomography of dense and nuclear matter,” Phys. Rev. Lett. **89**, 162301 (2002) [hep-ph/0202105].
- [18] X. -N. Wang and X. -f. Guo, “Multiple parton scattering in nuclei: Parton energy loss,” Nucl. Phys. A **696**, 788 (2001) [hep-ph/0102230].
- [19] P. B. Arnold, G. D. Moore and L. G. Yaffe, “Effective kinetic theory for high temperature gauge theories,” JHEP **0301**, 030 (2003) [hep-ph/0209353].
- [20] S. Jeon and G. D. Moore, “Energy loss of leading partons in a thermal QCD medium,” Phys. Rev. C **71**, 034901 (2005) [hep-ph/0309332].
- [21] G. -Y. Qin, J. Ruppert, C. Gale, S. Jeon, G. D. Moore and M. G. Mustafa, “Radiative and collisional jet energy loss in the quark-gluon plasma at RHIC,” Phys. Rev. Lett. **100**, 072301 (2008) [arXiv:0710.0605 [hep-ph]].

-
- [22] N. Armesto, B. Cole, C. Gale, W. A. Horowitz, P. Jacobs, S. Jeon, M. van Leeuwen and A. Majumder *et al.*, “Comparison of Jet Quenching Formalisms for a Quark-Gluon Plasma ‘Brick’,” *Phys. Rev. C* **86**, 064904 (2012) [arXiv:1106.1106 [hep-ph]].
- [23] R. Abir, C. Greiner, M. Martinez and M. G. Mustafa, “Generalisation of Gunion-Bertsch Formula for Soft Gluon Emission,” *Phys. Rev. D* **83**, 011501 (2011) [arXiv:1011.4638 [nucl-th]].
- [24] R. Abir, “Jet-parton inelastic interaction beyond eikonal approximation,” *Phys. Rev. D* **87**, 034036 (2013) [arXiv:1301.1839 [hep-ph]].
- [25] R. Abir, C. Greiner, M. Martinez, M. G. Mustafa and J. Uphoff, “Soft gluon emission off a heavy quark revisited,” *Phys. Rev. D* **85**, 054012 (2012) [arXiv:1109.5539 [hep-ph]].
- [26] Y. L. Dokshitzer, V. A. Khoze and S. I. Troian, “On specific QCD properties of heavy quark fragmentation (‘dead cone’),” *J. Phys. G* **17**, 1602 (1991).
- [27] Y. L. Dokshitzer and D. E. Kharzeev, “Heavy quark colorimetry of QCD matter,” *Phys. Lett. B* **519**, 199 (2001) [hep-ph/0106202].
- [28] R. Abir, U. Jamil, M. G. Mustafa and D. K. Srivastava, “Heavy quark energy loss and D-Mesons at RHIC and LHC energies,” *Phys. Lett. B* **715**, 183 (2012) [arXiv:1203.5221 [hep-ph]].
- [29] R. Abir and M. G. Mustafa, *Phys. Rev. C* **80**, 051903 (2009) [arXiv:0905.4140 [hep-ph]].

- [30] R. Abir and M. G. Mustafa, arXiv:1001.0692 [hep-ph].

- [31] C. A. Islam, R. Abir, M. G. Mustafa, S. K. Ghosh and R. Ray,
arXiv:1208.3146 [hep-ph].

List of Figures

1.1	Important epochs of the expanding universe after the Big Bang.	23
1.2	Running strong coupling constant.	29
1.3	The contemporary view of the QCD phase diagram.	31
2.1	The ratio R as a function of \sqrt{s} at the center of momentum frame of gluon-gluon scattering at $T = 200$ MeV and $\alpha_s = 0.3$.	68
2.2	The ratio R as a function of strong coupling, α_s	69
2.3	The ratio R up to $\mathcal{O}(t^3/s^3)$ is displayed as a function of T/T_c for temperature dependent α_s with two momentum scales $2\pi T$ (red curve) and $4\pi T$ (green curve). The corresponding results from Ref. [210] are represented by dotted (red) and dashed (green) curves.	70
3.1	Five tree level Feynman diagrams for the process $qq' \rightarrow qq'g$. In each diagram the thick and thin lines signify the fact that projectile and target partons are of different flavour.	76

3.2	Non-zero angular deviation from eikonal trajectory. Angle between incoming and outgoing momentum of projectile is θ_q and direction of emission of gluon with that of incoming momentum of projectile parton is θ_g	77
3.3	Inverse cross-section σ^{-1} vs. scattering angle θ	80
3.4	Typical estimation of noneikonal factors at $T = 300MeV$ with $\alpha = 0.3$ for the process $qq' \rightarrow qq'g$. First order noneikonal factors $\zeta_a = (1 + q_{\perp}^2/s)^{-2}$, $\zeta_b = (1 - 17q_{\perp}^2/9s)$, and the full contribution $\Gamma_{ab} = \zeta_a\zeta_b$	84
3.5	Typical estimation of noneikonal factors at $T = 300MeV$ with $\alpha = 0.3$ for the process $gg \rightarrow ggg$. First order noneikonal factors $\zeta_a = (1 + q_{\perp}^2/s)^{-2}$, $\zeta_b = (1 - q_{\perp}^2/2s)$ and the full contribution $\Gamma_{ab} = \zeta_a\zeta_b$	85
4.1	Five tree level Feynman diagrams for the process $Qq \rightarrow Qqg$. In each diagram the thick upper line represents the heavy quark (Q) whereas the thin lower line represents the background light quark.	92
4.2	The suppression factor \mathcal{D} from (4.10) as a function of θ and M/\sqrt{s}	97
4.3	The suppression factor \mathcal{D} from (4.10) as a function of θ for charm and bottom at two different energy ($E= 5$ GeV and $E= 10$ GeV).	99

5.1	A Monte Carlo simulation for the suppression factor in (5.2) (see text for details).	106
5.2	Energy of probe charm with distance traveled for radiative energy loss only [215].	112
5.3	Comparison of average energy loss for light quark and charm quark with mass 1.5 GeV in a deconfined quark matter produced in Pb-Pb collision at 2.76 ATeV in the present and DGLV formalisms. For both cases the characteristics of the deconfined matter are treated in the same footing, <i>i.e.</i> , the strong coupling $\alpha_s = 0.3$ and the average path length, $\langle L \rangle \approx 6.14$ fm, traversed by an energetic quark in a deconfined medium produced in such collisions.	117
5.4	Same as Fig. 5.3 but only for charm quark in Au-Au collision at 200 AGeV with $\langle L \rangle = 5.78$ fm.	117
5.5	Same as Fig. 5.4 in Pb-Pb collision at 5.5 ATeV with $\langle L \rangle = 6.14$ fm.	118
5.6	Collisional energy loss of charm quark in Pb-Pb collision at 2.76 ATeV and 5.5 ATeV at LHC, and 200 AGeV at RHIC energies.	120
5.7	Nuclear modification factor R_{AA} for D mesons with both collisional and radiative energy loss in Pb-Pb collision at 2.76 ATeV. Only the systematic error bars are shown here.	120
5.8	Nuclear modification factor, R_{AA} , for D mesons in Pb-Pb collision at 5.5 ATeV.	121

5.9	R_{AA} with only radiative energy loss for non-photonic single electron from the decay of individual D mesons and B mesons in Au-Au collision at 200 AGeV. Both systematic and statistical error bars are shown for STAR data whereas only systematic error bars are displayed for PHENIX data.	122
5.10	R_{AA} with collisional and radiative energy-loss for non-photonic single electron from the combined decay of both D and B mesons in Au-Au collision at 200 AGeV. Both systematic and statistical error bars are shown for STAR data whereas only systematic error bars are displayed for PHENIX data.	123
5.11	Same as Fig. 5.10 in Pb-Pb collision at 2.76 ATeV.	123
C.1	$\mathcal{M}_1 \otimes \mathcal{M}_1^\dagger$	143
C.2	$\mathcal{M}_3 \otimes \mathcal{M}_3^\dagger$	144
C.3	$\mathcal{M}_1 \otimes \mathcal{M}_3^\dagger$	145
C.4	$\mathcal{M}_1 \otimes \mathcal{M}_2^\dagger$	146
C.5	$\mathcal{M}_3 \otimes \mathcal{M}_4^\dagger$	147
C.6	$\mathcal{M}_1 \otimes \mathcal{M}_4^\dagger$	148
C.7	$\mathcal{M}_2 \otimes \mathcal{M}_3^\dagger$	148
C.8	$\mathcal{M}_2 \otimes \mathcal{M}_4^\dagger$	149
C.9	$\mathcal{M}_4 \otimes \mathcal{M}_4^\dagger$	150

Chapter 1

Introduction

1.1 Prelude

In the beginning, there was the Big Bang that created the Universe [1]. According to most prevailing, scientifically build and experimentally supported model on evolution of our universe, the early universe was filled with quantum fields maintaining its homogeneity and isotropy [2, 3, 4]. With an incredibly high energy density, temperature and pressure the universe was expanding and cooling very rapidly. To our current understanding, the universe then went through a series of phase transitions, which mark the most important epochs of the expanding universe after the Big Bang (Fig.[1.1]). At approximately 10^{-35} s after the birth (with temperature $\sim 10^{+28}$ K or $\sim 10^{+15}$ GeV) certain phase transitions caused cosmic inflation during which the universe grew exponentially. When inflation stopped at about $\sim 10^{-11}$ s (after birth), ultra hot baby universe for the first time goes to a phase where

one of its gradually dominating component supposed to be the *quark-gluon plasma*, a state where quarks and gluons are almost free to roam around and be in a state of plasma. At 10^{-10} s and at a temperature of $T \sim 100$ GeV ($\sim 10^{15}$ K) the electroweak phase transition took place where most of the known elementary particles acquired their Higgs mass [5, 6]. The cosmic phase consists of quark-gluon plasma starts from an era of electro-weak phase transition (electric and weak force decoupled) till roughly $10 \mu\text{s}$, when quarks become confined into hadrons at about a trillion degree centigrade temperature. In parallel to strong phase transition also the approximate chiral symmetry was spontaneously broken almost at same time (10^{-5} s) and temperature (~ 200 MeV or $\sim 10^{12}$ K). It is likely that those extreme temperatures are last seen in nature only in those elusive first few moments after the Big Bang. However, extraordinary global scientific effort recreates them in particle accelerators such as Relativistic Heavy Ion Collider (RHIC) at Brookhaven National Laboratory (BNL) in New York and Large Hadron Collider (LHC) at Conseil European pour la Recherche Nuclaire (CERN) in Geneva. At these temperatures, 10,000 times hotter than the centre of the sun, nuclear force essentially becomes the dominant force over rest three fundamental force *viz.* electromagnetic, weak and gravitational. Experiments both at RHIC and LHC help to learn about the fundamental and non-trivial emergent many-body plasma dynamics of the quarks and gluons that make up 99% mass of the optically visible universe [7]. Collisions of ultra relativistic heavy-ion beams in the said experiments create a hot and dense medium comparable to the conditions in the early universe when quarks and gluons

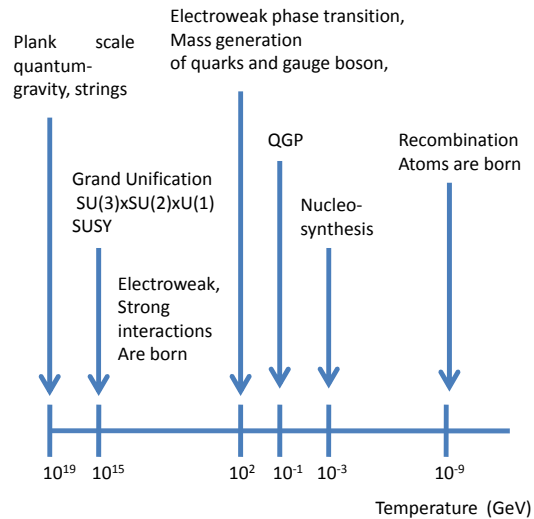


Figure 1.1: Important epochs of the expanding universe after the Big Bang.

are just popping up and roaming around in their era of liberation. With this great experimental endeavour across the world, one manage to recall some early moments of this lovely universe. Present thesis contains a few phenomenological aspects to those experiments as a teeny annexation to this great scientific effort.

1.2 Emergence of Chromodynamics

Revolution in materialistic understanding of fundamental constituents of nature, beyond the concept of ‘atom’, started slightly more than hundred years ago. In 1897, J. J. Thomson experimentally demonstrated that cathode rays

are basically the shower of negatively charged particles *electrons* [8]. Soon after (1911), Ernest Rutherford's famous large angle scattering experiment on gold foil showed that the majority of atomic mass being carried not by negatively charged electron but by positively charged nucleus [9]. Rutherford named the constituents of the hydrogen nucleus as *proton* [10]. Exactly 100 years ago, in 1913, N. Bohr offered the 'Bohr model' for hydrogen atom superseding the cubic model by Gilbert N. Lewis (1902), the 'Plum-pudding model' (1904) by J. J. Thomson, the 'Saturnian model' (1904) by Hantaro Nagaoka, and the 'Rutherford model' (1911) by E. Rutherford. In 1930, Viktor Ambartsumian and Dmitri Ivanenko found that, contrary to the prevailing opinion of the time, the nucleus cannot consist of protons and electrons. They proved that some neutral particles must be present besides the protons. J. Chadwick's discovery of neutral *neutron* in 1932, completed the discovery of the constituents of atoms [11].

Puzzle of keeping positively charged protons together in nucleus motivated H. Yukawa [12] in 1935 to develop a theory for the force that binds nuclei together. He proposed the existence of an as-yet unidentified particle whose mass in natural units is of the order of the nuclear radius, 1 fm^{-1} - the *pions*. Initially it was hard to separate *pion* from *muon* conclusively. Later definitive experiments [13, 14] was conducted that disentangled the pion from the muon. Soon *kaon* was discovered in a cosmic ray cloud chamber photograph [15]. Subsequently η , ϕ , and ω mesons were found and Λ baryon discovered.

M. Gell-Mann [16, 17], T. Nakano and K. Nishijima [18] and indepen-

dently Y. Ne'eman [19], described the proliferation of hadrons by organising them in multiplets that are representations of the flavour group $SU(3)$. This naturally led to predict the existence of the Ω^- baryon (discovered in 1964 [20]) by positing a new conserved quantity: strangeness [16, 17]. Exploring the amazing '*Eightfold Way*' to establish existence of subnuclear structure, Gell-Mann named these smaller, fundamental building blocks of hadrons as *quarks*, which originally comes from phrase "*three quarks for Muster Marks*" in *Finnegans Wakes* by James Joyce [21].

The quark model was awfully successful. Constituents having spin $1/2$ and fractional charge $2/3$ for the u and $-1/3$ for the d and s , naturally explained all known (even undiscovered) hadrons with all their mass-ordering. Current algebra techniques proposed the scaling laws of Form factors [22, 23] and soon experimentally found [24, 25]. These experiments also found wide-angle scattering from protons, which, in the line of E. Rutherford's earlier experiments with atoms [9], showed conclusively that nucleons have fundamental substructure.

Problems with the quark model at this time was two fold - quarks had not been observed and some baryons apparently violated the Pauli's exclusion principle despite being fermions. Mystery of Δ^{++} , composed of three u quarks with same spin was resolved by M. Y. Han with Y. Nambu and independently by O. W. Greenberg by proposing that quarks have an additional $SU(3)$ gauge degree of freedom [26], later known as *color*. Phenomenologically however one could presume that nature requires color neutrality to explain the non detection of isolated free quarks. M. Y. Han and Y. Nambu

also introduced gauge vector fields associated with the quark color charge so that quarks might interact via an octet of vector gauge bosons called *gluons*. Feynman then came up with his parton picture of deep inelastic scattering, a intuitive way of describing deep inelastic scattering in terms of point like object, the *partons* [27, 28]. To agree with data nucleons have to be made up of not just the three valence quarks, but also sea quarks [29] and gluons [30], which essentially warrant to describe the strong force binding the quarks in nuclei, by a theory of quantum fields.

The idea of a non-Abelian gauge theory was introduced by C. N. Yang and R. Mills [31], quantization was performed by L. Faddeev and V. Popov [32], and G.'t Hooft proved renormalizability of the theory [33]. Exploration of asymptotic freedom in the strong interaction field theory by D. Gross, D. Politzer and F. Wilczek, allowed physicist to make strict predictions of the outcome of many high energy experiments using quantum field theory techniques of perturbation theory [34, 35, 36, 37]. While no experiment has yet to directly observe a bare quark or gluon, first strong evidence about fundamental constituent elements of hadrons was obtained in deep inelastic scattering experiments at SLAC and PETRA for quarks from two jet events [38] and gluons from three [39] and four [40, 41] jet events.

Deluging experimental evidence for QCD as the theory of strong interactions revolutionized the understanding of nuclear force and gradually established quantum chromodynamics as most viable strong force theory with tantalizingly enriched phenomenological profile. At hard sector, logarithmic violations of Bjorken scaling in deep inelastic scattering were predicted

[35, 36, 42] and subsequently observed [43, 44]. Next-to-leading order (NLO) calculations reproduce the experimental data of prompt photon production [45]. Heavy quark jet production rates are calculated and agreed with experiment. These experiments become more and more precise culminating the verification of perturbative QCD at the level of few percent at LEP in CERN [46]. At soft momenta lattice calculations by K. Wilson [47] showed that effective potential between a q and \bar{q} inside a meson is essentially a linear one, which represents some kind of stiffness between particle and antiparticle at large distances, similar to entropic elasticity of a rubber band, leading to confinement or infrared slavery. On experimental side, several measurements demonstrate that nature in fact uses no more than three colors. The ratio of the cross sections, $\sigma(e^+e^- \rightarrow \text{hadrons})/\sigma(e^+e^- \rightarrow \mu^+\mu^-) = N_c \sum Q_f^2$, tests both the number of colors (N_c) and active flavors (N_f) as a function of center of mass energy, shows that at energies above the bottom mass but below the top that $N_c = 3$ and $N_f = 5$. Decay of neutral pions to two photons is a direct measure of the square of the number of colors; the theoretical prediction was in remarkable agreement with data. Four jet measurements identified directly the triple gluon vertex and found that the gauge group is SU(3) instead of SO(3) or perhaps U(1)₃ [40, 41]. Similarly the running of the coupling agrees well for $N_c = 3$. By then, quantum chromodynamics (QCD) has established itself as the adequate theory to describe the strong nuclear force between fermionic quarks and bosonic gluons [48].

1.3 QCD Phase Diagram

Today, quantum chromodynamics becomes an example of triumph of success for the quantum field theory. Asymptotic freedom enabling us to define the theory completely in terms of the fundamental microscopic degrees of freedom - quarks and gluons - yet the theory portray ample range of phenomena from the mass spectrum of hadrons to deep-inelastic scattering processes. As such, QCD should also possess well defined thermodynamic characteristics. The only independent intrinsic scale in this theory is the dynamically generated confinement scale $\Lambda_{\text{QCD}} \sim 1 \text{ fm}^{-1}$ [48, 49, 50]. At extreme temperature T and/or baryo-chemical potential μ_B , well above Λ_{QCD} , the theory can be studied analytically, due to the asymptotic freedom. Nonetheless, most interesting experimental region of parameters T and μ_B is that of order Λ_{QCD} .

1.3.1 QCD Lagrangian and running coupling

Schematically, QCD Lagrangian has the form,

$$\mathcal{L} = -\frac{1}{4}F_a^{\mu\nu}F_{\mu\nu}^a + \sum_f [i\bar{\psi}\gamma^\mu(\partial_\mu - ig\frac{\lambda_a}{2}A_\mu^a)\psi - m_f\psi\bar{\psi}] \quad (1.1)$$

with,

$$F_{\mu\nu}^a = \partial_\mu A_\nu^a - \partial_\nu A_\mu^a + gf_{bc}^a A_\mu^b A_\nu^c \quad (1.2)$$

here A_μ^a 's are the non-abelian Yangs Mills field ($a = 1, 2, \dots, 8$), and m_f is the 'bare' quark mass, f_{abc} is the structure constant of the group and ψ the quark spinors, g being the strong coupling. Running coupling constant

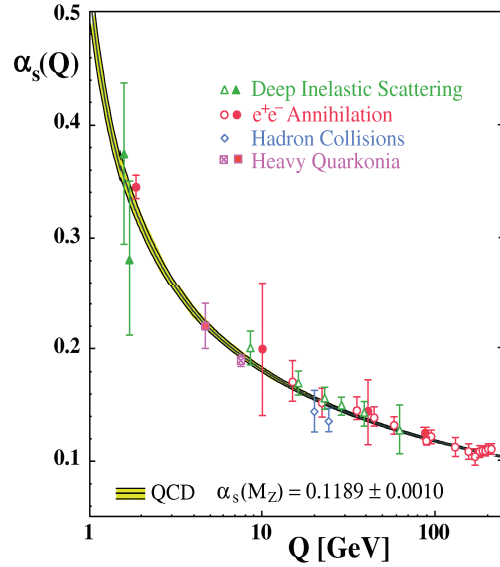


Figure 1.2: Running strong coupling constant.

reflect the change in dynamical strong physics, as the energy/momentum scale, at which physical processes occur, varies. As an example, an electron in short distance scale can appear to be composed of electron, positron and photons. The coupling constant has to be *renormalised* to incorporate the change as the scale of physical processes varies. QED coupling increase as the momentum scale is increased. In other words, effective electric charge becomes much larger at small distances. In QCD coupling constant, the change is reverse.

$$\alpha_s(q^2) = \frac{g^2}{4\pi} = \frac{\alpha_s(\Lambda_{\text{QCD}}^2)}{1 + \frac{\alpha_s(\Lambda_{\text{QCD}}^2)}{4\pi} \left(11 - \frac{2N_f}{3}\right) \ln \frac{Q^2}{\Lambda_{\text{QCD}}^2}} \quad (1.3)$$

where N_f is the number of flavors and $\Lambda_{\text{QCD}} \approx 200$ MeV. The coupling constant thus increases as the momentum scale Q decreases. Experimentally

measured values of α_s have been shown in Fig.[1.2]. Experimental measurements agree closely with QCD predictions.

1.3.2 Existence of a new state of matter

In the chiral limit, when lightest quarks, u and d , are taken to be massless, the Lagrangian of QCD acquires chiral symmetry $SU(2)_L \times SU(2)_R$, corresponding to $SU(2)$ flavor rotations of (u_L, d_L) and (u_R, d_R) doublets independently. The ground state of QCD breaks the chiral symmetry spontaneously locking independent $SU(2)_L$ and $SU(2)_R$ rotations into a single vector-like $SU(2)_V$ symmetry and generating 3 massless Goldstone pseudoscalar bosons – the pions. At sufficiently high temperature $T \gg \Lambda_{\text{QCD}}$, due to the asymptotic freedom of QCD, sort of free massless quark and gluon gas approximation should become applicable. In this regime chiral symmetry is not broken. Thus we must expect a transition from a chirally broken confined state to a chirally symmetric deconfined state at some temperature $T_c \sim \Lambda_{\text{QCD}}$ [51, 52]. The transition is akin to the Curie point in a ferromagnet, where the rotational $O(3)$ symmetry is restored by thermal fluctuations. Thermodynamic functions of QCD must be singular at the transition point, as always when the transition separates thermodynamic states of different global symmetry.

The possibility of a new state of nuclear matter was initially offered by Lee and Wick [53]. Both the statistical model of Hagedorn [54, 55] and the hadronic mean field approach of Walecka [56, 57, 58] predict a phase transition. From the QCD side, and before the advent of asymptotic freedom, Itoh was the first to suggest the possibility of deconfined quark matter [59].

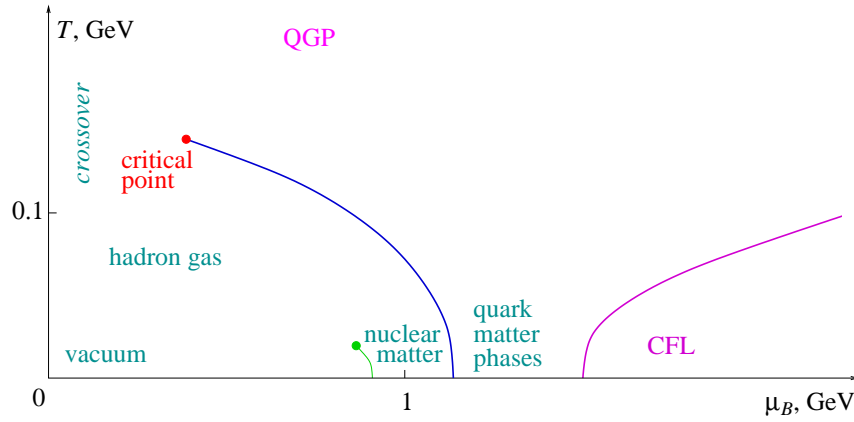


Figure 1.3: The contemporary view of the QCD phase diagram.

Collins and Perry [60] were the first to recognize the importance of asymptotic freedom, leading at large energies to a ‘quark soup’. Shuryak named it as ‘quark-gluon plasma’ (QGP) [61]. Simple dimensional analysis leads one to expect the temperature of such a QGP to be around $\Lambda_{\text{QCD}} \approx 200$ MeV, as this is a necessary momentum scale to resolve distances of order the nucleon and at the same time is the scale of normal nuclear energy densities of $1 \text{ GeV}/\text{fm}^3$. Frautschi found that Hagedorn’s bootstrap gives $T_c \approx 160$ MeV [55]. Current data for T_c from the lattice are in qualitative agreement with the previous results. The Wuppertal group found [62] chiral restoration at $151(3)(3)$ MeV and a crossover phase transition at $176(3)(4)$ MeV while the BNL/Bielefeld group found [63] $T_c = 192(7)(4)$. The point on the chiral phase transition line where the transition changes order is called tricritical point. The location of this point is one of the greatest challenge in the way to explore QCD phase. Studies suggest order of the transition at $\mu_B = 0$ is of the second order. Neither can it be claimed reliably (model or assumption independently) that the transition, if it begins as a second order at $\mu_B = 0$,

changes to first order. However, numerous model calculations show this is the case. When the up and down quark masses are set to their observed finite values, the second order transition line (where there was one) is replaced by a crossover. In the absence of the exact chiral symmetry (broken by quark masses) the transition from low to high temperature phases of QCD need not proceed through a singularity. Lattice simulations do indeed show that the transition is a crossover for $\mu_B = 0$.

1.4 Experimental Observables

As there are so many theoretical indications for a phase transition in QCD at low baryon chemical potential and at $T > T_c \simeq 160$ MeV, and since that unexplored phase would be a truly novel and interesting state of matter in which the ordinarily confined quarks and gluons—and not protons, neutrons, pions, etc.—are the pertinent degrees of freedom, one naturally asks how one might observe the creation of such conditions [64, 65]. The experimentally measured quantities associated with heavy-ion collisions naturally separate themselves into low momentum bulk observables, and high momentum jet observables according to their domain of viability.

1.4.1 Soft sector observables : Anisotropic flow

Heavy-ion collisions in ultra relativistic energy produce affluence of subatomic particles in all the directions in each collision event. In such collisions, flow refers to how energy, momentum, and number of these particles deluges in

all directions. The celebrated elliptic flow is a measure of how the flow is not uniform in all directions when viewed along the beam-line. It depicts the azimuthal momentum space anisotropy of emitted yield from non-central heavy-ion collisions in the plane transverse to the beam direction. It is designated as the second harmonic coefficient of the azimuthal Fourier decomposition of the momentum distribution. Being a radical observable elliptic flow directly reflects the initial spatial anisotropy, of the nuclear overlap zone in the transverse plane, directly translated into the observed momentum distribution of identified particles. Since the spatial anisotropy is largest at the beginning of the evolution, elliptic flow is especially sensitive to the early stages of system evolution. A measurement of elliptic flow thus provides access to the fundamental thermalization time scale and many more things in the early stages of a relativistic heavy-ion collision. Though original conception of the QGP was of a weakly interacting plasma of deconfined quarks and gluons. The course of hydrodynamics [66, 67, 68] to work well requires a strongly coupled quark gluon plasma, or sQGP, as named in [69, 70]. Strong evidence for a deconfined QGP could come from a robust result whereby hydrodynamics with a QGP equation of state (EOS) reproduces experimental data while hydro with a hadronic EOS does not. Since hydrodynamics mimic the evolution of the entire bulk there are a number of observables that can be compared to data. The simplest is the single particle spectra and their angular distribution with respect to the reaction plane. Fourier expansion of

the detected yield distribution,

$$dN(p_t, \phi) = dN(p_t) \left(1 + 2 \sum_n v_n(p_t) \cos(n\phi) \right), \quad (1.4)$$

where the normalization $dN(p_t)$ and v_2 , or azimuthal anisotropy, are the two most important moments for heavy ion collisions. Early results from RHIC and ideal hydrodynamics were quite promising: the v_2 of particle yields generated by hydro match quite well with data [71]. Elliptic flow is strong evidence for the existence of quark-gluon plasma, and has been described as one of the most important observations measured at the Relativistic Heavy Ion Collider (RHIC).

1.4.2 Hard sector observable : Jet quenching

A typical jet event at an ion-collider generally goes through three main stages of development. Firstly, an early time parton level hard scattering event produce a few energetic partons (quarks and gluons). Then, the development of shower in which each parton, via branching, broadens into a ‘jet’. Finally comes the hadronization stage in which the colored particles in the jet recombine into color-neutral mesons and baryons via fragmentation (at hard sector) and via coalescence (at soft sector). Quantitative understanding of all the three stages is required in order to expose the jet event completely. The exciting first evidence of jets came in early seventies [72, 73, 74, 75, 76]. Orders of magnitude more high p_t pions were observed than were expected from a low p_t extrapolation; the production spectrum had turned over from

exponential to power law. Soon afterward, two jet events were explicitly seen at e^+e^- colliders [38, 39]. While Bjorken was the first to suggest using jet suppression to learn about a QCD medium, the precision pQCD predictions of production rates [77, 78, 79, 80] held out the possibility for jet tomography: much like in medical applications such as a pet scan, a careful measurement of the jet quenching pattern would reveal information on the medium through which it travelled.

Stunning testimonials of elliptic flow and jet quenching coming from dedicated heavy-ion collider experiments *viz.*, STAR [81, 82, 83, 84, 85, 86, 87, 88, 89, 90, 91, 92], PHENIX [93, 94, 95, 96, 97, 98, 99, 100, 101, 102, 103, 104, 105], PHOBOS [106] and BRAHMS [107] of RHIC at BNL, ALICE [108, 109, 110, 111, 112] of LHC at CERN strongly articulated the fact that, the primordial hot soup of nuclear matter, produced in those experiments, indeed contains *partonic degrees of freedom* before freezing out to hadrons. Strong modification of internal architecture of the jet shower is generally governed by both elastic (associated with non-radiative scattering) and inelastic (associated with radiative scattering) processes. This modifications may either be in the form of energy degradation of the most energetic leading parton of the jet and broadening effects on the transverse momentum or be a change in in-jet gluon multiplicity leading to jet quenching. Observation of strong suppression of inclusive yields of high momentum hadrons and semi-inclusive rate of azimuthal back-to-back high momentum hadron pairs relative to p - p collisions, are the expectations from jet quenching. In order to estimate amount of jet quenching, we need to know the initial quark dis-

tributions from perturbative QCD, flavor energy loss, quark fragmentation into hadrons, H_Q , and H_Q decay into leptons (occasionally). A schematic outline is as follows,

$$\frac{Ed^3\sigma(e)}{dp^3} = \frac{E_i d^3\sigma(Q)}{dp_i^3} \otimes P(E_i \rightarrow E_f) \otimes D(Q \rightarrow H_Q) \otimes f(H_Q \rightarrow e),$$

where \otimes is a generic convolution. The electron decay spectrum, $f(H_Q \rightarrow e)$, includes the branching ratio to electrons. The change in the initial flavor spectra due to energy loss is denoted $P(E_i \rightarrow E_f)$.

The possibility of testing, *e.g.* deconfinement, depends heavily on the energy loss model and the mapping made between its input parameters and the physical medium. This mapping is a critical, although often overlooked, component of any model attempting tomography. Since the observed jet suppression cannot come from other sources, it must be due to final state energy loss. When energy loss is under theoretical control, then jet tomography is possible and the observed suppression pattern can be inverted to gain knowledge about the medium.

1.5 Chronicles of in-medium jet energy loss

1.5.1 Collisional energy loss

The story begins with James D. Bjorken's estimation of the energy loss for a high momentum fast parton, traversing through quark-gluon plasma, by way of elastic (traditionally known as collisional), $2 \rightarrow 2$, scatterings [113].

A parton travelling through a thermalized, deconfined quark-gluon plasma maintained at a fixed temperature T , has been considered taking into account only the t -channel diagrams. In this case $|\mathcal{M}_{2\rightarrow 2}|^2 \sim 1/t^2 \sim 1/(q^2 + \mu_i^2)^2$, where μ_i is the infrared cutoff which can be taken as Debye mass $\sim \mu_D \sim gT$. With some more additional kinematic constraints, this gives the first analytic formula for the energy loss per unit path length of a first parton jet,

$$\frac{dE}{dx} = \pi C_R \alpha_s^2 T^2 \left(1 + \frac{N_f}{6} \right) \log \frac{2\langle p \rangle T}{\mu_D^2}, \quad (1.5)$$

where C_R is the color Casimir of leading jet, $4/3$ for a quark or 3 for a gluon, N_f is the number of dynamic flavors in the medium, and $\langle p \rangle \approx 3T$ is the average momentum of the medium particles.

Thoma and Gyulassy [114] improved this estimation by incorporating the hard thermal loop (HTL) perturbation theory developed by Braaten and Pisarski [115, 116, 117]. The energy loss was found by deriving the linear response to the propagation jet as the source current by the induced fields in the dielectric medium. Braaten and Thoma [118, 119], expanding upon the earlier work of Svetitsky [120], evaluated the high momentum part of the dynamics using the vacuum matrix element and the low momentum piece with linear response separately and connected the soft and hard scales at a typical scale q^* which, to leading order, drops out of the problem as demonstrated later by P. Romatschke and M. Strickland [121].

Heavy flavor energy loss was addressed first by E. Braaten and M. H. Thoma [119]. These leading log results were compared to primary radiative

energy loss approximations and found to be small [122, 123], not surprising as this is a well known result from classical electrodynamics. However this turns out to be just a prejudice until the work by M. G. Mustafa [124] who demonstrated that with realistic kinematic limits at RHIC energies radiative and elastic losses are of the same order. This and the experimental evidence of surprisingly strong heavy quark quenching [89, 100] motivated to incorporate both radiative and collisional processes in jet quenching models and has generated a lots of interest in improving elastic calculations.

Some contemporary pragmatic developments in elastic loss include considerations of running coupling, finite formation time effects, and the importance of the higher moments of the distribution associated with path length fluctuations. A. Peshier had shown a large energy loss enhancement when the coupling was allowed to run [125]. Strong running coupling correction was further supported by J. Braun and H. J. Pirner [126]. S. Wicks however advocated that in the kinematic domain of RHIC and LHC this is actually a small effect [127]. It was needed to go beyond the calculations of asymptotic jets created in the infinite past. As a first attempt, S. Peigne, P. B. Gossiaux, and T. Gousset [128] claimed that finite formation time effects (the so called retardation effect) were large and persisted far beyond the expected single Debye length. A. Adil *et. al.* also consider the finite time formation problem in a classical linear response formalism by considering only the elastic pole contributions [129]. This was later confirmed through finite time energy loss calculations by P. B. Gossiaux *et. al.* [130]. Djordjevic again addressed the problem from a quantum mechanical point of view and removed the ‘unphys-

ical energy gain' [131]. Nevertheless, the effects of finite time and off shell parton creation in a finite size QCD medium seems to reduce energy loss as compared to earlier studies [132]. The issue is not settled yet and still under investigation.

Diffusion of charm quark in a quark-gluon plasma by way of fluctuation was first addressed by B. Svetitsky [120] way back, where he employed the Fokker-Planck equation. G. D. Moore and D. Teaney [133] thoroughly investigated the relativistic Langevin and Fokker-Planck equations in heavy ion collisions in order to estimate how much heavy quark thermalize in a heavy-ion collision. This work was applied to heavy quark energy loss with additional nonperturbative mesonic resonances by Rapp and van Hees [134]. However, for the pathlengths and densities at RHIC and LHC, the number of $2 \rightarrow 2$ collisions is of order a few, and the Gaussians resulting from these applications of the central limit theorem might be a crude approximation to the elastic energy loss distributions [127].

1.5.2 Radiative energy loss

Deriving nonabelian QCD radiative bremsstrahlung energy loss is certainly more involved. The formalisms created to tackle this problem can be roughly categorized into four groups ¹:

- (1) BDMPS-Z-ASW [141, 142, 143, 144, 153, 146, 154, 147, 148, 149, 150, 151, 152, 161, 162, 163, 164, 167, 181],
- (2) DGLV (GLV) [155, 156, 157, 158, 159, 160, 182, 190],

¹Abbreviations have been exposed later.

(3) WWOZ (Higher-Twist) [168, 169, 170, 171, 172, 180], and

(4) AMY [173, 174, 175, 177].

In early eighties F. A. Berends, R. Kleiss, P. De Causmaecker, R. Gastmans and T. T. Wu first studied some single bremsstrahlung processes in gauge theories [135]. Soon after, J. F. Gunion and G. Bertsch's [136] began this line of work by deriving the strong force field Feynman diagrams associated with the nuclear scattering at the regime of incoherent Bethe-Heitler radiation,

$$\frac{dN_g}{d\eta dk_{\perp}^2} = \frac{C_c \alpha_s}{\pi^2} \frac{q_{\perp}^2}{k_{\perp}^2 (k_{\perp} - q_{\perp})^2}, \quad (1.6)$$

where $k = (k^0, \vec{k}) = (\omega, k_{\parallel}, k_{\perp})$, and C_c are the color Casimir factors. However multiple coherent scattering over lengths/times shorter than the radiation formation time leads to interference that suppresses the emission of radiation; this is the well-known LPM effect in electromagnetism, named after Landau and Pomeranchuk [137] and Migdal [138]. Brodsky and Hoyer [139] began the work including these effects in QCD calculations initially to provide a bound on the energy loss of partons in nuclei, and it was continued by Gyulassy and Wang [140] to address multiple collisions and induced gluon bremsstrahlung in a thin plasma. Here they introduced the notion of a static color scattering center with a Yukawa-like screened potential and noted the importance of the unique nonabelian extension of the LPM effect in QCD, by which the radiation reinteracts with the medium. Baier, Dokshitzer, Mueller, Peigne, and Schiff (BDMPS) [141, 142, 143, 144] were the first to include this effect in an energy loss calculation. Unlike [140] which examined the thin plasma limit, like Landau and Pomeranchuk, BDMPS built up the

soft gluon radiation from single hard scatterings. BDMPS also examined the multiple soft scattering limit, similar to Migdal and Molière scattering [145]. Angular dependence of the radiative spectrum has been studied later by R. Baier *et. al.* [146, 147] and quenching studies in [148]. Meanwhile Zakharov independently developed an alternative formalism employing path integral methods to address coherent emission in QCD medium [149, 150, 151, 152], later it was shown to be equivalent to the BDMPS approach [153, 154], and eventually become BDMPS-Z formalism.

The thin plasma limit of Gyulassy and Wang extended the opacity expansion work of Gyulassy, Levai, and Vitev (GLV) [155, 156, 157, 158, 159, 160]. Their reaction operator approach allowed the derivation of a closed form solution of the resummed single inclusive gluon radiation distribution $dN_g/dxdk_{\perp}^2$ to all orders in opacity, L/λ .

At the same time, Urs Achim Wiedemann examined the dipole path integral, opacity expansion, and the multiple soft rescattering formalism of Zakharov and BDMPS limits [161, 162, 163, 164]. Wiedemann studied the relation between the BDMPS and Zakharov formalisms for medium-induced gluon radiation off hard quarks, and the radiation off very few scattering centers. Based on the non-abelian Furry approximation for the motion of hard partons in a spatially extended color field, Wiedemann managed derive a compact diagrammatic and explicitly color trivial expression for the n-th order term of the k_{\perp} -differential gluon radiation cross section in an expansion in the opacity of the medium.

The then emerging Wiedemann's formalism calculates parton energy loss

based on a path-integral formalism [165, 166]. The path-integral can be evaluated in two different approximations: (a) *Multiple soft scattering limit*: This is a saddle-point approximation of the path integral. For the case of infinite in-medium pathlength, the result coincides with the BDMPS expression for parton energy loss. For this reason, this limit is referenced sometimes as "BDMPS-limit". (b) *Opacity expansion*: This is an expansion of the integrand of the path integral in powers of (density times pathlength). The GLV $N = 1$ opacity result is in accordance with this formalism on the level of the Feynman diagrams and the analytic expression for the ω and k_{\perp} differential gluon energy distribution. Wiedemann and Salgado [167] also numerically investigated the BDMPS and GLV results, which resulted a code for calculating BDMPS energy loss 'quenching weights'.

Around the same time X. N. Wang, X. F. Guo, E. Wang, J. A. Osborne began the development of the *Higher-Twist* formalism [168, 169, 170, 171, 172]. The Higher-Twist scheme is all about evolving (changing) distributions of hadrons fragmenting from a jet due to the passage of it through a medium. One starts with a distribution of some detected hadrons (pions, kaons, protons etc.) and evolves it up in-vacuum or in-medium starting from some *final* lower virtuality up to some *initial* higher virtuality. Evolution in-vacuum is performed using the standard DGLAP evolution equations. There is no on-shell quark or gluon in this formalism. The final states always have to be on-shell hadrons. The in-medium evolution kernel describes the scattering of a hard initial quark with energy E and virtuality Q , off gluons in the medium and the induced emission of gluons with lower virtuality. The evolu-

tion charts the progress of the distributions from Q down to some lower yet perturbatively large scale. The evolution kernel does not contain effects of scattering off quark states or soft-elastic energy loss. The results presented do not contain the absorption of collinear partons or energy gain in the medium. The number of scatterings per radiation is assumed to be between 1 and 2. Solving the evolution equation, in essence, resums the effect of infinite emissions. Similar to GLV, the derivation builds up the energy loss from single hard scatterings but differs by making some alternative assumptions in their evaluation. Most important, the arbitrary potential in GLV, usually taken as Yukawa, is replaced by an arbitrary gluon distribution function. This obscures the relation between jet suppression patterns and physical medium quantities such as density and temperature.

Meanwhile then P. B. Arnold, G. D. Moore, and L. G. Yaffe (AMY) [173, 174, 175] developed a thermal field theoretic diagrammatic method for computation of energy loss in which leading-log and next-to-leading-log contributions are carefully tracked. Results are presented within a full leading-order evaluation of the shear viscosity, flavor diffusion constants, and electrical conductivity in high temperature QCD and QED. The presence of Coulomb logarithms associated with gauge interactions imply that the leading-order result for transport coefficients may themselves be expanded in an infinite series in powers of $1/\log(1/g)$. A next-to-leading-log approximation was found to approximate the full leading-order result quite well as long as the Debye mass is less than the temperature. Later S. Jeon and G. D. Moore [176, 177] found that the result is consistent with BDMPS. Ac-

counting correctly for the probabilistic nature of the energy loss, and making a leading-order accurate treatment of bremsstrahlung, they found that the suppression of the spectrum is nearly flat. A large advantage of this formalism is its simultaneous treatment of both gluon and photon bremsstrahlung, providing an added experimental consistency check. However their use of asymptotic states neglects the large interference effects from the initial production radiation, making comparison to data a bit uncertain.

1.5.3 Radiative loss of heavy flavor

M. G. Mustafa, D. Pal, D. K. Srivastava and M. Thoma made an early attempt to calculate the heavy quark energy loss in a QGP medium by using the Gunion and Bertsch formula of gluon emission for light quark scattering but just modifying the relevant kinematics for heavy quarks [178]. Later the soft gluon emission formula for heavy quarks in the high energy approximation was revisited by Dokshitzer and Kharzeev for the small angle limit. Soft gluon emission from a heavy quark was found to be suppressed in the forward direction compared to that from a light quark due to the mass effect (dead cone effect). The corresponding suppression factor was obtained as [179],

$$\mathcal{D}_{DK} = \left(1 + \frac{\theta_0^2}{\theta^2}\right)^{-2} \Big|_{\theta \ll 1}, \quad (1.7)$$

where $\theta_0 = M/E \ll 1$. With E being the energy of the heavy quark with mass, M and θ , the angle between the heavy quark and the radiated gluon. Motivated by these initiatives, which show just as in QED, in QCD a mas-

sive charge also radiates less - and for a consistent theoretical unified description of gluon, light quark, and heavy flavor suppression many working groups extend their works to include mass in the existing set of jet quenching formalisms. Zhang, Wang, and Wang [180] and Armesto, Salgado, and Wiedemann [181] included heavy quark mass effects in the WWGO-Z and BDMPS-Z-ASW formalisms. Djordjevic and Gyulassy included both the effects of a heavy quark jet and a gluon mass term in D-GLV [182].

Besides in-medium inelastic energy loss two other radiation effects have been studied: transition radiation and Ter-Mikayelian radiation reduction. Transition radiation occurs in classical electromagnetism when a relativistic charged particle propagates through an inhomogeneous medium, in particular the boundary between two spaces with different electrical properties [183, 184]. In heavy ion collisions just such a boundary forms between the deconfined QGP medium and the vacuum. M. Djordjevic [185] quantified the extra energy loss caused in this transition and detailed its regulation of infrared divergences ordinarily absorbed into DGLAP evolution.

The Ter-Mikayelian (TM) effect [186, 187] is a direct result of radiative quanta gaining mass in a plasma. As in beta decay, production of high momentum charged particles also has radiation associated with the process. For QCD this infrared divergent vacuum radiation is absorbed into fragmentation functions, but in-medium the finite gluon mass regulates and suppresses this radiation. Djordjevic and Gyulassy [188] calculated the QCD analog of the TM effect for single quark pairs.

Simon Wicks, William Horowitz, Magdalena Djordjevic and Miklos Gyu-

lassy (WHDG) extend the DGLV model to include both (1) elastic (2) inelastic parton energy losses and (3) jet path length fluctuations. The three effects combine to reduce the discrepancy between theory and the data without violating the global entropy bounds from multiplicity and elliptic flow data. Fluctuations of the geometric jet path lengths and the difference between the widths of fluctuations of elastic and inelastic energy loss play essential roles in the proposed model, eventually known as WHDG [189]. Recently M. Djordjevic and U. W. Heinz calculated radiative energy loss in a finite dynamical QCD medium [190]. Recent studies shown that developed theoretical formalism can robustly explain suppression data in ultra relativistic heavy ion collisions, which strongly suggests that pQCD in Quark-Gluon Plasma is able to provide a reasonable description of the underlying jet physics at LHC [191].

1.6 Essential features of jet models

1.6.1 Medium modeling in jet models

One of the main challenge in studying jet quenching is how to characterize the medium [192, 193, 194, 195, 196]. It is always important to clearly articulate, variations of different models that try to address jet quenching [197]. Various models uses various set of approximations. Broadly this can be classified in four different category,

1. *The medium as assemblage of static scattering centers*

Here the medium is modeled as a set of static colored scattering centers

with a specified density distribution along the trajectory of the projectile. A temporally decreasing density mimics the effects of an expanding medium. This class of model was pioneered by Baier, Dokshitzer, Mueller, Peigné and Schiff (BDMPS) [142, 143, 153] and independently by Zakharov [149, 151] as mentioned earlier. Gluon radiation is formulated in a path-integral that resums scatterings on multiple static colored scattering centers. Wiedemann [163] showed how this path-integral can be used to include interference effects between vacuum and medium-induced radiation in such a way that the k_{\perp} differential medium-induced gluon distribution can be achieved. Soft gluon approximation (Bjorken $x \ll 1$) was used in BDMPS derivation of the medium-induced gluon distribution [142, 143]. Later [153], the radiation spectrum is multiplied by an overall splitting function to take corrections for finite x into account. BDMPS-Z formalism use a saddle point approximation that amounts effectively to assuming that the projectile interacts with the medium via *multiple soft scattering* processes. The numerical results from the low- x , multiple soft scattering implementation of the BDMPS-Z formalism are based on the work by Armesto, Salgado and Wiedemann [163, 167, 181], abbreviated as ASW. In the totally coherent limit, in which the entire medium acts coherently towards gluon production, the multiple-soft scattering formalism results in a radiation spectrum that is a radiation term for gluon production with momentum transfer q_{\perp} convoluted with a Gaussian elastic scattering cross section $\propto \frac{1}{\hat{q}L} \exp[-q_{\perp}^2/\hat{q}L]$. Medium is

fully characterized in this limit by only the transport coefficient \hat{q} , the mean of the squared transverse momentum exchanged per unit path length.

2. *Characterizing via opacity expansion*

As mentioned earlier the *opacity expansion* pioneered by Gyulassy, Levai and Vitev [156, 158] (GLV) and independently by Wiedemann [163]. It also includes the interference between vacuum and medium-induced radiation and is based on a systematic expansion of the calculation in terms of the number of scatterings. The BDMPS–Z path-integral formalism can serve as a generating functional for the opacity expansion [163]. The opacity expansion formalism is another limit for the solution of the BDMPS-Z path integral. Behavior for higher opacities has been explored in [159]. The medium is characterized by two model parameters, the density of scattering centers ρ or mean free path λ , and a Debye screening mass μ_D used to regulate the infrared behavior of the single scattering cross section. In contrast to the multiple soft scattering approximation, this approach includes the power-law tail of the scattering cross section induced from QCD, leading to shorter formation times of the radiation compared to the multiple-soft scattering approximation.

3. *The medium as matrix elements of gauge field operators*

In this class of models, the multiple gluon exchanges between a partonic projectile and a spatially extended medium can be formulated in a field

theoretic way [170]. The higher-twist (HT) approach includes the interference between vacuum and medium-induced radiation. Properties of the medium enter the calculation in terms of higher-twist matrix elements. In practice the matrix elements are factorized in the PDFs and matrix elements describing the interaction between final state partons and the medium. This factorization is valid at leading order in the path length L in the medium.

4. *Thermally equilibrated, perturbative medium*

In thermal field-theory of parton energy loss in a weakly-coupled medium in perfect thermal equilibrium was developed by Arnold, Moore and Yaffe (AMY) [173, 174, 175]. The medium is formulated as a thermal equilibrium state in Hard Thermal Loop [115, 116, 117] improved finite temperature perturbation theory. As a consequence, all properties of the medium are specified fully by its temperature and baryon chemical potential. The calculation does not incorporate vacuum branching of the projectile parton. However, in principle, the perturbative description of the thermal medium applies only at very high temperature $T \gg T_c$.

As seen from the list above, different models of parton energy loss characterize the medium in terms of different model parameters. In the existing literature, the different approximations used for the medium in the various approaches have led to different ways to specify the medium properties. This lead to incompleteness in available energy loss model and also may lead to unphysical radiation in certain kinematic domains.

1.6.2 The unphysical ‘leakage radiation’

Sometimes in the present calculational framework the yield in the spectrum for $\omega > E$, *i.e.* above the kinematic boundary can be taken as a probability of total absorption of the parton, ‘death before arrival’. Simply ignoring the radiation spectrum beyond the kinematic limit leads to the unphysical result that in some cases the total radiation probability decreases with increasing density or path length, when the typical gluon energy is close to E . As an typical example, in GLV formalism the multigluon emissions were incorporated in [159] by *assuming* this Poissonian form of density distribution: $P(\epsilon|p_T) = \sum_n P_n(\epsilon|p_T)$, $P_1(x|p_T) = \exp(-\langle N_g(p_T) \rangle) dN_g/dx(x; p_T)$, and

$$P_{n+1}(\epsilon|p_T) = \frac{1}{n+1} \int dx P_n(x|p_T) \frac{dN_g}{dx}(\epsilon - x|p_T), \quad (1.8)$$

where the final momentum is expressed in terms of the initial momentum as $p_T^f = (1 - \epsilon)p_T^i$. This kind of poissonian convolution associated with the probability of leakage radiation, in which $P(\epsilon > 1; p_T)$ has nonzero weight which is not physical. For large regions of parameter space at RHIC and LHC this leakage is quite large due to kinematic constraints neglected in the Poisson approximation.

The situation is become worse for large-angle radiation. In the presently existing formalisms, the typical transverse momentum of the radiated gluon k_\perp depends on the typical transverse momentum exchanges q_\perp and the number of scatterings L/λ , but not on the gluon energy ω . As a result, there is always some radiation with ω smaller than the typical k_\perp and thus with a

large probability for radiation at $k_{\perp} \rightarrow \omega$. The quantitative impact of large angle radiation depends on the medium model (large q_{\perp} contributions in the medium cross section) and the choice of parameters. It was pointed out that the large-angle regime may be important for phenomenological applications. It has been argued that, most of the formalisms is based on the assumption of small transverse gluon momentum $|k_{\perp}| \ll \omega$ while one finds the main contribution to radiative energy loss for $|k_{\perp}| = O(\omega)$. Both features question the viability of all prevailing jet formalisms [164].

1.6.3 Kinematic approximations in jet models

All formalisms for energy loss of a high momentum parton through gluon radiations, have some common technical approximations. These approximations are implemented both at the level of *single emission kernel* calculations and at multiple gluon emission estimation schemes. Main kinematic approximations at the level of *single emission kernel*, are listed below (also see Refs. [198, 199, 200] for a comprehensive discussion):

- *Eikonal parton trajectory I* : Leading parton is having energy E (*i.e.* $p_z = E$ and $p_{\perp} = 0$, by definition to start with) is much larger than the transverse momentum exchanged gluon q_{\perp} with the medium, $E \gg q_{\perp}$, so that it does not give sufficient transverse kick to deflect the parton from straight trajectory along z axis. To relax this approximation it is therefore important to keep track of the terms of $\mathcal{O}(q_{\perp}/E)$ in the formalism.

- *Eikonal parton trajectory II* : Energy of the leading parton is sufficiently high, $E \gg k_{\perp}$ (k_{\perp} being transverse component of the emitted gluon) so that it does not get enough transverse kick also from emitted gluon. This ensures that the leading parton is in eikonal trajectory. However it does not fix any definite direction for gluon emission, which requires comparison of k_{\perp} with longitudinal component k_z or with energy ω of the emitted gluon. Therefore, it is important not to neglect terms of $\mathcal{O}(k_{\perp}/E)$ in the formalism to relax this approximation in the jet studies.
- *Soft gluon emission* : One often uses the additional approximation that the gluon energy is much smaller than the leading parton energy $\omega \ll E$. When x is the fraction of energy carried out by the emitted gluon, *i.e.*, $x = \omega/E$, this approximation ensures that $x \rightarrow 0$. When x is typical light cone variable, defined by the fraction of light cone (+)ve momentum carried out by the emitted gluon, *i.e.*, $x = k^+/p^+ = (k_{\perp}/\sqrt{s})e^{\eta}$, this approximation ensures $x \rightarrow 0$, only in the mid rapidity and backward rapidity regions ($-\infty \geq \eta \geq 0$) but not in the forward regions where η could be a large positive number.
- *Small angle/collinear gluon emission* : Energy of the emitted gluon ω is much larger than its transverse momentum k_{\perp} , $\omega \gg k_{\perp}$ and $\omega \simeq k_z$. For any $2 \rightarrow 3$ process, without loss of generality, one can take $k_{\perp} = \omega \sin \theta_g$ and $k_z = \omega \cos \theta_g$, where θ_g being the angle between direction of propagation of leading parton and direction of emitted gluon. This

particular approximation therefore implies $\theta_g \simeq 0$.

At this point it is worth mentioning that *soft gluon emission* approximation is a broader approximation as it automatically encompasses the *eikonal parton trajectory II* approximation, because energy w should always be more than the transverse momentum k_\perp for a massless emitted gluons. Other non-kinematic but worth mentioning approximations are the following,

- *Fixing the scale of running coupling* : In jet models usually coupling is taken to be 0.3. It is important to extract correct scales at which to evaluate the strong coupling involved in the energy loss calculations.
- *Double emission kernel* : So far only *single gluon emission kernel* have been introduced in the jet quenching models. Which is then been embedded in a multi gluon estimation schemes. There is a need go for *double gluon emission kernel* (*viz.* $Q q \rightarrow Q q g g$) calculation.

1.7 Stripping eikonal-collinear constrains

We have already articulated that QCD based analytical computations of quenching of jets have, so far, been clogged up with ‘soft-eikonal-collinear’ limits of parton kinematics. According to ‘soft-eikonal-collinear’ kinematic approximation, energy of the leading projectile parton E is taken to be quite large compared to the energy of the radiated gluon ω which, again, is supposed to be much larger than both the transverse momentum carried by the gluon k_{\perp} , as well as recoiling momentum (exchanged momentum) of scattering centre q_{\perp} ; and hence we can write,

$$E \gg \omega \gg k_{\perp}, q_{\perp} \gg m_{g,q} \gg \Lambda_{QCD} \quad (1.9)$$

The foundation analysis of radiative parton energy loss [140] are based on this ‘soft-eikonal-collinear’ approximations. Same legacy of this clutchy approximations is also being carried out by the next generation prevailing models of light/heavy flavor jet quenching studies. Extrapolating computations of parton energy loss, valid only in certain kinematic domain [given by (1.9)], to the full phenomenologically relevant kinematic range induces lots of unavoidable uncertainties. This may also lead to oversight of qualitatively new affair of medium radiation mechanisms for heavy flavor jet.

The main sprite of eikonality is propagation along straight trajectory. Once this approximation is stripped additional emission occur which is exclusively a phenomenon due to bending of jet by recoil effect and lies around the

direction of outgoing jet, one may reasonably identify it as QCD analogue of Quantum Electrodynamics (QED) synchrotron radiation. As discussed earlier one of the main challenges of contemporary jet study initiatives is to extend the theoretical framework for jet-medium interaction in hot-dense QCD ambience beyond soft and collinear approximations and reduce uncertainties intrinsic to the current theoretical studies.

In that march, this thesis work removes the eikonal and collinear approximation in single emission kernel calculation for various inelastic scattering processes which have immense importance in heavy ion collision physics. This allows to probe the cloud of gluon away from the forward direction. This endeavour removes the eikonal approximation and hence shows the advent of a treatment which allows the jet to bend with non-negligible recoil effect from the scattering in chromo-magnetic ambience enabling one to eventually treat the color synchrotron radiation of color charges.

1.8 Outline of Thesis

This thesis is organized as follows: In chapter 2 we generalize the most extensively used Gunion-Bertsch formula for the soft gluon emission derived within a perturbative QCD. We show that the corrections arising due to this generalisation is indeed very important for the phenomenology of the hot and dense matter produced in the heavy-ion collisions [201]. This generalization is sort of non-eikonal extension of eikonally approximated Gunion-Bertsch formula. In chapter 3 an attempt has been made to relax part of this ap-

proximation for $qq' \rightarrow qq'g$ processes and found a (15-20)% suppression in the differential cross-section for moderately hard jets because of the noneikonal effects. This may have consequence on the suppression of hadronic spectra at low transverse momenta [202]. Issues on heavy flavor have been addressed in Chapter 4. An improved generalized suppression factor for gluon emission off a heavy quark is derived within perturbative QCD, which is valid for the full range of rapidity of the radiated gluon and also has no restriction on the scaled mass of the quark with its energy [203]. In the appropriate limit it correctly reproduces the usual dead cone factor in the forward rapidity region. On the other hand, this improved suppression factor becomes close to unity in the backward direction. This indicates a small suppression of gluon emission in the backward region. In Chapter 5 we obtain the radiative energy loss of a heavy quark in a deconfined medium due to radiation of gluons off them using a recently derived generalized gluon emission spectrum. We find that the heavy flavour loses energy almost in a similar fashion like light quarks through this process. With this, we further analyze the nuclear modification factor for D-meson at LHC and RHIC energies [204]. In particular, the obtained result is found to be in close agreement with the most recent data from ALICE collaboration at 2.76 ATeV Pb-Pb collisions. We also discuss the nuclear modification factor due to the collisional energy loss. Furthermore, the result of non-photonic single electron from the decay of both D and B mesons is compared with the RHIC data at 200 AGeV Au-Au collisions, which is also in close agreement. Finally we have summarized in Chapter 6 mentioning some recent development in this line of research [205].

A few key calculations have been accommodated in Apendix.

Chapter 2

Gluon-Gluon Scattering

We have already discussed in the introduction that prime intention for any ultra-relativistic heavy-ion program is to study the behavior of nuclear or hadronic matter at extreme conditions like very high temperatures and energy densities. A particular goal lies in the identification of a new state of matter formed in such collisions, the quark-gluon plasma (QGP), where the quarks and gluons are liberated from the nucleons and move freely over an extended space-time region. Various measurements taken in CERN-SPS and BNL-RHIC do lead to wealth of information for the formation of QGP through the hadronic final states [206]. In the experiments at the CERN LHC, one indeed produced QGP during the first several fm/ c of the collisions and eventually substantiate the evidences already found in the past as well in the recent experiments. Some basic questions regarding the quark-gluon plasma one would like to discuss include the followings: What is the ‘equilibration time’ τ_0 from which the momentum distribution is equilibrated?

What is the ‘initial temperature’ value T_i at this moment? Is it well above the critical point T_c , so that one can use the perturbation theory? With which accuracy this concept makes sense, say how accurate is a thermodynamic relations between energy and entropy densities hold? What is the composition of the matter at this moment? What are the most unambiguous signals, which provide experimental estimates of these parameters?

Key questions of the plasma produced in such collisions include the dynamics of *equilibration and its time, initial temperature, energy-loss and jet quenching of high energetic partons, and elliptic flow of hadrons and its scaling with the number of valence quarks*. The Gunion-Bertsch formula for soft gluon emission has widely been used for various aspect of the heavy-ion phenomenology. To set the perspective we note that there are many papers in the literature based on the Gunion-Bertsch formula. We recall: the sequence of events in hot glue scenario [207], thermal equilibration and gluon chemical equilibration [208], parton matter viscosity [209], radiative energy-loss of high energy partons propagating through a thermalised QGP etc., where the Gunion-Bertsch formula has extensively been used. The original Gunion-Bertsch formula was derived by J. F. Gunion and G. Bertsch for gluon emission from quark-quark scattering [?] and later it was explicitly used to derive the soft gluon emission from gluon-gluon scattering. Recently a correction to the Gunion-Bertsch formula for soft gluon emission was obtained S. K. Das and J.-e Alam [210]. In present work we make an effort to generalise the Gunion-Bertsch formula for soft gluon emission from gluon-gluon scattering, *i.e.*, $gg \rightarrow ggg$ by relaxing the eikonal approximation and find a more impor-

tant correction than it is found in earlier studies. We also show that in the eikonal limit the generalization reduces to the Gunion-Bertsch formula. We further note that the results for similar inelastic processes can be obtained in a straightforward way by using our generalization.

2.1 Inelastic Gluon-Gluon Scattering ($gg \rightarrow ggg$)

For the process, $gg \rightarrow ggg$, there are 25 different Feynman diagrams. We note that k_1 and k_2 are momenta of the gluons in the entrance channel, k_3 and k_4 are those for exit channel gluons whereas k_5 is that of the emitted gluon. The invariant amplitude summed over all the final states and averaged over initial states for such process can elegantly be written as [135]:

$$\begin{aligned}
|\mathcal{M}_{gg \rightarrow ggg}|^2 &= \frac{1}{2} g^6 \frac{N_c^3}{N_c^2 - 1} \frac{\mathcal{N}}{\mathcal{D}} [(12345) + (12354) \\
&+ (12435) + (12453) + (12534) + (12543) \\
&+ (13245) + (13254) + (13525) + (13424) \\
&+ (14235) + (14325)] , \tag{2.1}
\end{aligned}$$

where N_c is the number of color, $g = \sqrt{4\pi\alpha_s}$ is the strong coupling,

$$\begin{aligned} \mathcal{N} = & (k_1 \cdot k_2)^4 + (k_1 \cdot k_3)^4 + (k_1 \cdot k_4)^4 + (k_1 \cdot k_5)^4 \\ & + (k_2 \cdot k_3)^4 + (k_2 \cdot k_4)^4 + (k_2 \cdot k_5)^4 + (k_3 \cdot k_4)^4 \\ & + (k_3 \cdot k_5)^4 + (k_4 \cdot k_5)^4, \end{aligned} \quad (2.2)$$

$$\begin{aligned} \mathcal{D} = & (k_1 \cdot k_2)(k_1 \cdot k_3)(k_1 \cdot k_4)(k_1 \cdot k_5)(k_2 \cdot k_3) \\ & (k_2 \cdot k_4)(k_2 \cdot k_5)(k_3 \cdot k_4)(k_3 \cdot k_5)(k_4 \cdot k_5), \end{aligned} \quad (2.3)$$

and

$$(ijklm) = (k_i \cdot k_j)(k_j \cdot k_k)(k_k \cdot k_l)(k_l \cdot k_m)(k_m \cdot k_i). \quad (2.4)$$

We now define the Mandelstam variables as

$$\begin{aligned} s &= (k_1 + k_2)^2, & t &= (k_1 - k_3)^2, & u &= (k_1 - k_4)^2, \\ s' &= (k_3 + k_4)^2, & t' &= (k_2 - k_4)^2, & u' &= (k_2 - k_3)^2, \end{aligned}$$

and

$$\begin{aligned}
k_1 \cdot k_2 &= \frac{s}{2}, & k_3 \cdot k_4 &= \frac{s'}{2}, & k_1 \cdot k_3 &= -\frac{t}{2}, \\
k_2 \cdot k_4 &= -\frac{t'}{2}, & k_1 \cdot k_4 &= -\frac{u}{2}, & k_2 \cdot k_3 &= -\frac{u'}{2}, \\
k_1 \cdot k_5 &= \frac{(s+t+u)}{2}, & k_2 \cdot k_5 &= \frac{(s+t'+u')}{2}, \\
k_3 \cdot k_5 &= \frac{(s+t'+u)}{2}, & k_4 \cdot k_5 &= \frac{(s+t+u')}{2},
\end{aligned} \tag{2.5}$$

with,

$$s + t + u + s' + t' + u' = 0.$$

Eq. (2.1) actually contains only twelve terms which are reduced from total 120 terms due to symmetry. Using (2.2), (2.3) and (2.4) the first two terms of (2.1) can be expressed as:

$$\begin{aligned}
&\frac{1}{2}g^6 \frac{N_c^3}{N_c^2 - 1} \frac{\mathcal{N}}{(k_1 \cdot k_3)(k_1 \cdot k_4)(k_2 \cdot k_4)(k_2 \cdot k_5)(k_3 \cdot k_5)} \\
&= \frac{1}{2}g^6 \left(\frac{N_c^3}{N_c^2 - 1} \right) \frac{8.4}{-tt'u(s+t'+u')(s+t'+u)},
\end{aligned} \tag{2.6}$$

and,

$$\begin{aligned}
&\frac{1}{2}g^6 \frac{N_c^3}{N_c^2 - 1} \frac{\mathcal{N}}{(k_1 \cdot k_3)(k_1 \cdot k_5)(k_2 \cdot k_4)(k_2 \cdot k_5)(k_3 \cdot k_4)} \\
&= \frac{1}{2}g^6 \left(\frac{N_c^3}{N_c^2 - 1} \right) \frac{8.4}{tt's'(s+t+u)(s+t'+u')},
\end{aligned} \tag{2.7}$$

After simplifying all the terms in this way, (2.1) can be written as

$$\begin{aligned}
|\mathcal{M}_{gg \rightarrow ggg}|^2 &= 16g^6 \frac{N_c^3}{N_c^2 - 1} \mathcal{N} \\
&\times \left[\frac{1}{s'(s+u+t)(s+u'+t')} \left(\frac{1}{tt'} + \frac{1}{uu'} \right) \right. \\
&\quad - \frac{1}{t'(s+u+t)(s+u+t')} \left(\frac{1}{ss'} + \frac{1}{uu'} \right) \\
&\quad - \frac{1}{u'(s+u+t)(s+u'+t)} \left(\frac{1}{tt'} + \frac{1}{ss'} \right) \\
&\quad + \frac{1}{s(s+u+t')(s+u'+t)} \left(\frac{1}{tt'} + \frac{1}{uu'} \right) \\
&\quad - \frac{1}{u(s+u'+t')(s+u+t')} \left(\frac{1}{tt'} + \frac{1}{ss'} \right) \\
&\quad \left. - \frac{1}{t(s+u'+t')(s+u'+t)} \left(\frac{1}{ss'} + \frac{1}{uu'} \right) \right] \quad (2.8)
\end{aligned}$$

and \mathcal{N} can also be obtained as

$$\begin{aligned}
\mathcal{N} &= \frac{1}{16}(s^4 + t^4 + u^4 + s'^4 + t'^4 + u'^4) \\
&\quad + \frac{1}{16} [(s+t+u)^4 + (s+t'+u')^4 + (s+t'+u)^4 \\
&\quad \quad + (s+t+u')^4]. \quad (2.9)
\end{aligned}$$

Now for a soft gluon emission ($k_5 \rightarrow 0$): $t' \rightarrow t$, $s' \rightarrow s$, $u' \rightarrow u$ and we can express the transverse component of the momentum of the emitted gluon in the centre of momentum frame of k_1 and k_2 as

$$\begin{aligned}
k_{\perp}^2 &= \frac{4(k_1 \cdot k_5)(k_2 \cdot k_5)}{s} = \frac{(s+t+u)(s+u'+t')}{s} \\
&= \frac{(s+t+u)^2}{s}. \quad (2.10)
\end{aligned}$$

Using (2.10) in (2.8) one can obtain a complete expression for the three-body matrix element in terms of the two-body matrix element and a infrared factor as

$$|\mathcal{M}_{gg \rightarrow ggg}|^2 = g^2 |\mathcal{M}_{gg \rightarrow gg}|^2 \frac{1}{k_{\perp}^2} \left[a_1 + a_2 \frac{t^4}{s^4} + a_3 \frac{k_{\perp}^4}{s^2} \right] \times \left[\left(a_4 + a_5 \frac{t}{s} + a_6 \frac{t^2}{s^2} \right) / \left(a_7 + a_8 \frac{t^2}{s^2} + a_9 \frac{t^3}{s^3} \right) \right], \quad (2.11)$$

where the full two-body matrix element is given as

$$|\mathcal{M}_{gg \rightarrow gg}|^2 = \frac{9}{2} g^4 \frac{s^2}{t^2} \left[a_7 + a_8 \frac{t^2}{s^2} + a_9 \frac{t^3}{s^3} \right], \quad (2.12)$$

and various coefficients are

$$\begin{aligned} a_1 &= 3 + 3 \frac{u^4}{s^4}, & a_2 &= 3, & a_3 &= 6, & a_4 &= 1 - \frac{s}{u}, \\ a_5 &= -1 - \frac{s^2}{u^2}, & a_6 &= \frac{s^2}{u^2} - \frac{s}{u}, & a_7 &= -\frac{u}{s}, & a_8 &= 3, \\ a_9 &= -\left(\frac{u}{s} + \frac{s^2}{u^2} \right). \end{aligned} \quad (2.13)$$

Furthermore, eliminating u using (2.10) and keeping terms upto $\mathcal{O}(1/k_{\perp}^2)$ and $\mathcal{O}(t^3/s^3)$ one can write (2.11) as

$$|\mathcal{M}_{gg \rightarrow ggg}|^2 = 12g^2 |\mathcal{M}_{gg \rightarrow gg}|_{GB}^2 \frac{1}{k_{\perp}^2} \left[1 + \frac{t}{2s} + \frac{5}{2} \frac{t^2}{s^2} - \frac{t^3}{s^3} + \mathcal{O}\left(\frac{t^4}{s^4}\right) \right], \quad (2.14)$$

where

$$|\mathcal{M}_{gg \rightarrow gg}|_{GB}^2 = \frac{9}{2} g^4 \frac{s^2}{t^2}. \quad (2.15)$$

The above equation (2.14) is a convergent series of t/s as can be seen below. It is now clearly decomposed in two factors: one is associated with the $2 \rightarrow 2$ process used by Gunion and Bertsch whereas the other one is the generalisation of the infrared factor for the emission of soft quanta. As we will see below, the first term in (2.14) will lead to the GB formula for the gluon multiplicity distribution in an appropriate limit where $t \sim q_{\perp}^2 \gg k_{\perp}^2$ (q_{\perp} is the transverse component of the momentum transfer). If the emitted gluon is much softer than others it can then be regulated by the Debye screening mass, m_D . On the other hand the second, the third and the fourth terms, respectively, would correspond to the correction terms over the GB term in the same spirit. We also note that the first term can also be obtained by just using the scalar QCD approximation in $2 \rightarrow 3$ process.

If one considers only a_1, a_4, a_6, a_7 in (2.11) and substitute $u = -s$, one will end up with the expression derived in S. K. Das and J.-e Alam [210] as

$$|\mathcal{M}_{gg \rightarrow ggg}|^2 = 12g^2 |\mathcal{M}_{gg \rightarrow gg}|_{GB}^2 \frac{1}{k_{\perp}^2} \left(1 + \frac{t^2}{s^2} \right), \quad (2.16)$$

which misses the leading order correction term of $\mathcal{O}(t/s)$ and also the right coefficient in the next order, $\mathcal{O}(t^2/s^2)$.

2.2 Gluon multiplicity distribution

Using (2.14) it is now straight forward to obtain the soft gluon multiplicity distribution in the mid-rapidity region as

$$\frac{dn_g}{d\eta dk_\perp^2} = \left[\frac{dn_g}{d\eta dk_\perp^2} \right]_{GB} \left(1 + \frac{(q_\perp^2 + m_D^2)}{2s} + \frac{5}{2} \frac{(q_\perp^2 + m_D^2)^2}{s^2} - \frac{(q_\perp^2 + m_D^2)^3}{s^3} \right), \quad (2.17)$$

where the GB formula can be obtained using (2.14) as

$$\left[\frac{dn_g}{d\eta dk_\perp^2} \right]_{GB} = \frac{C_A \alpha_s}{\pi^2} \frac{q_\perp^2}{k_\perp^2 [(k_\perp - q_\perp)^2 + m_D^2]}, \quad (2.18)$$

with the Casimir factor $C_A = 3$ and the Debye screening mass $m_D = gT$. We note that the first term in (2.17) would correspond to GB formula. It is also worth mentioning that this first term can be obtained by just using the scalar QCD approximation.

Now the average value of the momentum transfer squared can be obtained as

$$\langle q_\perp^2 \rangle = \left(\int_{m_D^2}^{s/4} dt \, t \frac{d\sigma}{dt} \right) / \left(\int_{m_D^2}^{s/4} dt \frac{d\sigma}{dt} \right), \quad (2.19)$$

where the maximum value of α_s is restricted by $s \geq 4m_D^2$ along with $s = \langle s \rangle = 18T^2$.

In Fig. 2.1 the ratio $R = \frac{dn_g}{d\eta dk_\perp^2} / \left. \frac{dn_g}{d\eta dk_\perp^2} \right|_{GB}$ is plotted with the center of momentum energy, \sqrt{s} of the gluon-gluon scattering for $T = 200$ MeV and

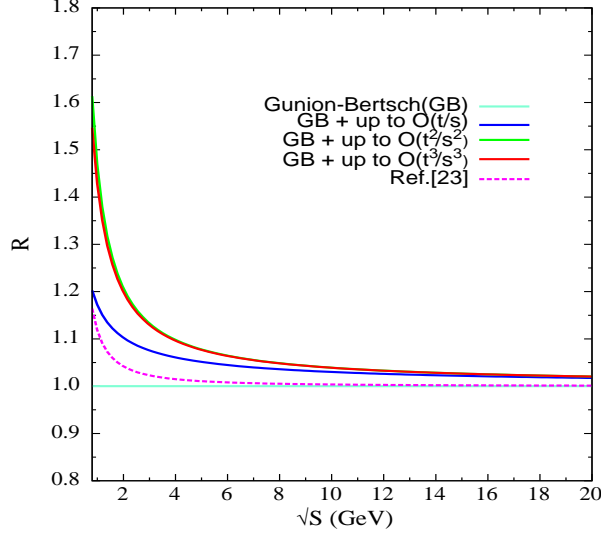


Figure 2.1: The ratio R as a function of \sqrt{s} at the center of momentum frame of gluon-gluon scattering at $T = 200$ MeV and $\alpha_s = 0.3$.

$\alpha_s = 0.3$. With these values the lower limit of $\sqrt{s} \sim 0.8\text{GeV}$ is restricted by the relation $s \geq 4m_D^2$. As can be seen from Fig. 2.1 that (2.17) is a convergent series in t/s and it also indicates a significant improvement compared to that of Ref. [210]. With the increase of \sqrt{s} the correction terms decrease and the ratio approaches the GB formula for very large value of \sqrt{s} . On the other hand the first and second order corrections are significant when $\sqrt{s} \leq 6$ GeV.

In Fig. 2.2 the ratio $R = \left. \frac{dn_g}{d\eta dk_\perp^2} / \frac{dn_g}{d\eta dk_\perp^2} \right|_{GB}$ is plotted as a function of the strong coupling α_s . We note that the maximum value of α_s is restricted by $s \geq 4m_D^2$. As can be seen the correction terms become important with the increase of α_s . At $\alpha_s = 0.3$, the correction up to $\mathcal{O}(t^3/s^3)$ is around 50% over the usual GB formula. We have also compared our results with that of

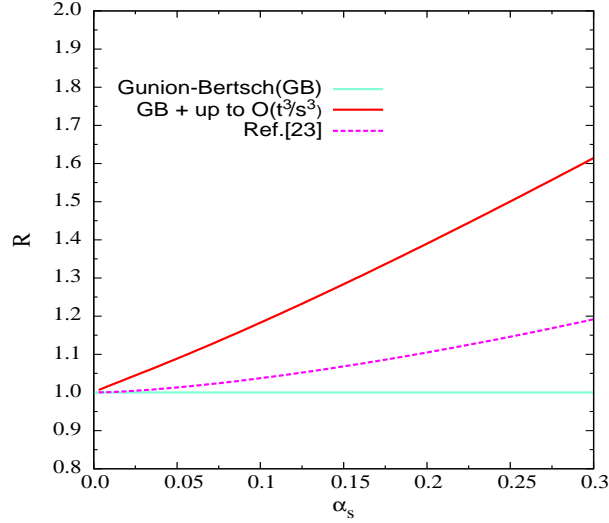


Figure 2.2: The ratio R as a function of strong coupling, α_s .

Ref. [210], which shows a significant improvement in the range of α_s displayed in Fig. 2.2.

Fig. 2.3 displays the ratio R as a function of T in the units of the critical temperature T_c . Here we have used the temperature dependent α_s with two momentum scale $Q = 2\pi T$ (red curve) and $4\pi T$ (green curve). We note that for the momentum scale $Q = 2\pi T$ the value of the coupling, $\alpha_s > 0.4$ for $T/T_c < 1.5$, which is really a very high for any practical purposes. On the other hand for $Q = 4\pi T$, the values of coupling lie in the domain $0.2 \leq \alpha_s \leq 0.35$ for the scaled temperature range, $1 \leq T/T_c \leq 6$. Nonetheless, the value of α_s and thus the lower bound of T/T_c would again be restricted by the relation $s \geq 4m_D^2$. As can be seen in Fig. 2.3, there is a sizable contribution ($\geq 40\%$) up to $\mathcal{O}(t^3/s^3)$ over the GB formula and a correction ($\geq 30\%$)

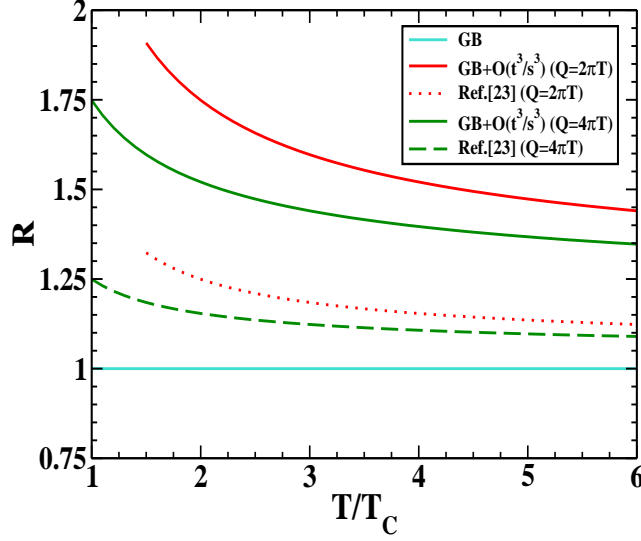


Figure 2.3: The ratio R up to $\mathcal{O}(t^3/s^3)$ is displayed as a function of T/T_c for temperature dependent α_s with two momentum scales $2\pi T$ (red curve) and $4\pi T$ (green curve). The corresponding results from Ref. [210] are represented by dotted (red) and dashed (green) curves.

compared to Ref. [210] in the temperature range $1 \leq T/T_C \leq 5$. This correction over the GB formula would be very important at the temperature domain relevant for the heavy-ion collisions.

2.3 Generalization to $2 \rightarrow n$, $n > 3$.

One of the most interesting development in perturbative QCD is the derivation of an exact expression, summing contribution of all diagrams to n -gluon processes for the *maximum helicity violation amplitude*. This is known as the

“Parke-Taylor formula” [211].

$$|M_n^{PT}|^2 = g_s^{2n-4} \frac{N_c^{n-2}}{N_c^2 - 1} \sum_{i>j} s_{ij}^4 \sum_{\text{P}} \frac{1}{s_{12}s_{23}\dots s_{n1}} \quad (2.20)$$

In the above $s_{ij} = (p_i + p_j)^2$, the summation P is over the $(n-1)!/2$ non-cyclic permutation of $(1\dots n)$. It looks like direct generalization of $n = 5$ case discussed above. Unfortunately, the exact result for other chiral amplitudes remains unknown. However, assuming that they are of the same magnitude as the “Parke-Taylor” one, one gets some estimate for the n-gluon matrix element. This was proposed first by Kunszt and Stirling who add the following factor in front of the “Parke-Taylor” formula

$$|M_n^{KS}|^2 = KS(n)|M_{PT}|^2, \quad \text{with} \quad KS(n) = \frac{2^n - 2(n+1)}{n(n-1)} \quad (2.21)$$

We have checked Eq.(2.21) against the exact results for $n = 4$ and $n = 5$, and found that in these cases one indeed needs the KS correction ($KS(4) = 1, KS(5) = 2$) to recover the analytical results correctly. For higher orders (2.21) does a very reasonable job, although it consistently overpredicts the cross section slightly. The true matrix element for $n \geq 5$ should therefore be within the range

$$2|M_n^{PT}|^2 \leq |M_n|^2 \leq |M_n^{KS}|^2. \quad (2.22)$$

2.4 Discussion

We have obtained a non-eikonal generalization of the Gunion-Bertsch formula for soft gluon emission in a process $gg \rightarrow ggg$. We found that the correction terms are important at various physical domains of temperature, coupling constant and the energy of gluon-gluon scattering. This generalization will be very apt for the phenomenology (*viz.*, hot glue scenario, chemical equilibration of gluons, partonic matter viscosity, radiative energy-loss of energetic partons and jet quenching) of heavy-ion collisions and would improve the present understanding on various phenomena in this area.

Chapter 3

Quark-Quark Scattering

Apart from gluon-gluon scattering another scattering process that have immense importance in the context of heavy-ion collision studies is the quark-quark scattering. This scattering process is greatly responsible for *jet quenching* phenomena, supposed to be the most prominent hard sector signature that favour the partonic degrees of freedom in the deconfined QCD matter. Tantalizing evidence of jet signature coming from dedicated heavy-ion experiments *viz.*, STAR and PHENIX@ RHIC-BNL [88, 97], ALICE @ LHC-CERN [110, 108] established the fact that, the primordial hot-soup of nuclear matter, produced in those experiments, indeed contain *partonic degrees of freedom* instead of *hadronic degrees of freedom*. Observation of strong suppression of inclusive yields of high momentum hadrons and semi-inclusive rate of azimuthal back-to-back high momentum hadron pairs relative to p - p collisions, are expectations from jet quenching. Both of them are extensively explored in collisions of Au - Au nuclei at $\sqrt{s} = 200$ A GeV in RHIC. ALICE,

the dedicated heavy-ion collider experiment at CERN, seems to appear as a factory of jets. Evidence for jet quenching has also been observed recently in $Pb-Pb$ collision at ALICE [110].

In this work we make an effort to relax the *eikonal parton trajectory I* (see 1.6.3) approximation in some extent for this radiative/inelastic process $qq' \rightarrow qq'g$. Investigation of all the matrix elements in $\mathcal{O}(\alpha_s^3)$ for the $2 \rightarrow 3$ radiative processes have been done keeping terms up to $\mathcal{O}(t/s)$. The first order in eikonal expansion, *i.e.*, $\mathcal{O}(t/s)$, is termed here as *noneikonal*, since the calculation is performed in Feynman gauge with Mandelstam variables instead of most extensively used light cone gauge with light cone variables¹. We have neglected terms of $\mathcal{O}(t^2/s^2)$ and higher orders. Nevertheless, we have used *soft gluon emission approximation* which automatically include *eikonal parton trajectory II* assumption.

3.1 Inelastic Quark-Quark Scattering ($qq' \rightarrow qq'g$)

The process $qq' \rightarrow qq'g$ (prime denotes different quark flavour) in $\mathcal{O}(\alpha_s^3)$ appears in five t channel Feynman diagrams, which are shown in the Fig. 3.1 (see also Fig. 3.2 for other details). Note that k_1 and k_2 are momenta of the different quark flavors in the entrance channel whereas k_3 and k_4 are those for exit channel and k_5 is that of the emitted gluon. Scattering angle between

¹After connecting t to q_\perp and s to E in the centre of momentum frame, term of $\mathcal{O}(t/s)$ ensures the relaxation of the approximation $E \gg q_\perp$ (*eikonal parton trajectory I*).

\mathbf{k}_1 and \mathbf{k}_3 is θ_q whereas θ_g is the angle between direction of emission of soft gluon $\hat{\mathbf{k}}_5$ and direction of *incoming* projectile quark $\hat{\mathbf{k}}_1$. We now again define the relevant Mandelstam variables for this $2 \rightarrow 3$ process as

$$\begin{aligned} s &= (k_1 + k_2)^2, & s' &= (k_3 + k_4)^2, \\ u &= (k_1 - k_4)^2, & u' &= (k_2 - k_3)^2, \\ t &= (k_1 - k_3)^2, & t' &= (k_2 - k_4)^2, \end{aligned} \quad (3.1)$$

with

$$s + t + u + s' + t' + u' = 0. \quad (3.2)$$

When the emitted gluon is soft ($k_5 \rightarrow 0$) compare to other external legs, one can assume : $t' \rightarrow t$, $s' \rightarrow s$, $u' \rightarrow u$ and we can express the transverse component of the momentum of the emitted gluon in the centre of momentum frame of k_1 and k_2 as

$$\begin{aligned} k_{\perp}^2 &= \frac{4(k_1 \cdot k_5)(k_2 \cdot k_5)}{s} \\ &= \frac{(s + t + u)(s + u' + t')}{s} \\ &= \frac{(s + t + u)^2}{s}. \end{aligned} \quad (3.3)$$

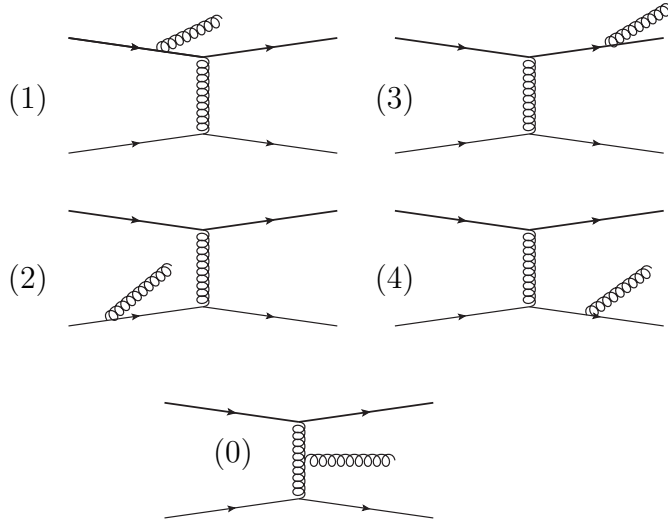


Figure 3.1: Five tree level Feynman diagrams for the process $qq' \rightarrow qq'g$. In each diagram the thick and thin lines signify the fact that projectile and target partons are of different flavour.

3.1.1 Hierarchy in momentum scales

The hierarchy among various scale of momentum, employed in the present work is stated as

$$\sqrt{s}, E > \sqrt{|t|}, q_{\perp} \gg w \geq k_{\perp} \geq m_D, \quad (3.4)$$

where m_D is the Debye screening mass acts as an infrared cut-off. We note that the above hierarchy relaxes the approximations $\sqrt{s}, E \gg \sqrt{|t|}, q_{\perp}$ (*Eikonal parton trajectories I*) and $w \gg k_{\perp}$ (*small angle/collinear gluon emission*).

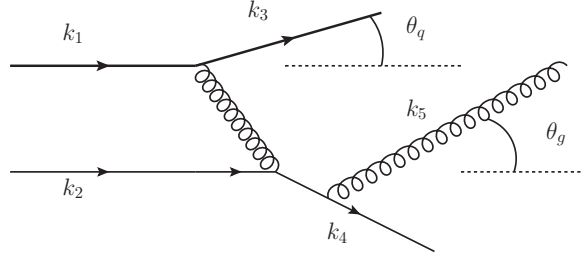


Figure 3.2: Non-zero angular deviation from eikonal trajectory. Angle between incoming and outgoing momentum of projectile is θ_q and direction of emission of gluon with that of incoming momentum of projectile parton is θ_g .

3.1.2 Matrix Elements, Amplitude and Cross-section

The gauge invariant amplitude summed over all the final states and averaged over initial states for the process, $qq' \rightarrow qq'g$, is

$$|\mathcal{M}_{qq' \rightarrow qq'g}|^2 = \sum_{i \geq j} \mathcal{M}_{ij}^2, \quad (3.5)$$

where i and j run from 0 to 4. We note that the index 0 represents the diagram where the soft gluon emits from the exchanged gluon line whereas the indices $m = 1, 2, 3, 4$ represent the diagrams where emission of the soft gluons are being from external fermion lines having momenta k_m (see Fig. 3.1). Equation (3.5) contains total fifteen terms in which there are five self interfering ‘genuine amplitudes’ for $i = j$ and ten cross interfering ‘interference amplitudes’ associated with gluon emissions involving two diagrams for $i \neq j$. Results are given below up to $\mathcal{O}(1/k_{\perp}^2)$ and $\mathcal{O}(t/s)$, for soft gluon emission.

Genuine amplitudes

By genuine amplitudes we are referring amplitudes that are coming from each diagrams by interfering with itself. In the Feynman gauge² all of them vanishes within *soft gluon emission* approximations and in $\mathcal{O}(1/k_\perp^2)$:

$$\mathcal{M}_{11}^2 = \mathcal{M}_{33}^2 = 0; \mathcal{M}_{22}^2 = \mathcal{M}_{44}^2 = 0; \mathcal{M}_{00}^2 = 0. \quad (3.6)$$

However, they may contribute in $\mathcal{O}(1)$, $\mathcal{O}(k_\perp^2)$, $\mathcal{O}(k_\perp^4)$ etc, and in $\mathcal{O}(t^2/s^2)$ and higher orders. All of them can safely be neglected in the soft emission limit as our aim is to go beyond the *eikonal approximation-I*, $E \gg q_\perp$.

Interference amplitudes

Within the approximations employed above the amplitudes corresponding to the matrix elements of $(1 \otimes 4)$ and $(2 \otimes 3)$ are identical in the leading order ($\mathcal{O}(1/k_\perp^2)$) as well in $\mathcal{O}(t/s)$ and given as

$$\mathcal{M}_{14}^2 = \mathcal{M}_{23}^2 = \frac{7}{8} \frac{128}{27} g^6 \frac{s^2}{t^2} \frac{1}{k_\perp^2} \left[1 + 2 \frac{t}{s} \right],$$

where $\mathcal{O}(t/s)$ is purely noneikonal (*i.e.*, the first order in eikonal approximation) in nature as noted earlier. Also the amplitudes for $(1 \otimes 2)$ and $(3 \otimes 4)$ are identical and the contribution is obtained in $\mathcal{O}(1/k_\perp^2)$ and $\mathcal{O}(t/s)$ as

$$\mathcal{M}_{12}^2 = \mathcal{M}_{34}^2 = \frac{1}{4} \frac{128}{27} g^6 \frac{s^2}{t^2} \frac{1}{k_\perp^2} \left[1 + \frac{t}{s} \right].$$

²In light cone gauge amplitudes coming from diagrams that involve gluon emission from target partons can only be neglected, others are not.

Both $(1 \otimes 3)$ and $(2 \otimes 4)$ are also identical within the employed hierarchy. However, they do not contribute in leading order but only in $\mathcal{O}(t/s)$. Hence, in Feynman gauge the contribution from the interference between *initial state* and *final state* radiations, is exclusively noneikonal in nature and given as

$$\mathcal{M}_{13}^2 = \mathcal{M}_{24}^2 = \frac{1}{4} \frac{128}{27} g^6 \frac{s^2}{t^2} \frac{1}{k_\perp^2} \left[\frac{1}{2} \frac{t}{s} \right],$$

Any diagram interfering with 0, *i.e.*, $(0 \otimes l)$ with $l = 1, 2, 3, 4$, does not contribute in $\mathcal{O}(1/k_\perp^2)$ but contributes in $(1/k_\perp \sqrt{t})$ and higher orders. In the limit $|\sqrt{t}| \sim q_\perp \gg w$, amplitudes of $\mathcal{O}(1/k_\perp \sqrt{t})$ are subleading, in comparison to $\mathcal{O}(1/k_\perp^2)$. Therefore, all of these (\mathcal{M}_{10}^2 , \mathcal{M}_{20}^2 , \mathcal{M}_{30}^2 and \mathcal{M}_{40}^2) do not contribute within the approximation used in this work.

The gauge invariant amplitude for the process, $qq' \rightarrow qq'g$, can now be obtained by summing all the subamplitudes as

$$|\mathcal{M}_{qq' \rightarrow qq'g}|^2 = 12g^2 |\mathcal{M}_{qq' \rightarrow qq'}|_{eknl}^2 \frac{1}{k_\perp^2} \left(1 + \frac{17t}{9s} \right), \quad (3.7)$$

where the two body amplitude is given as

$$|\mathcal{M}_{qq' \rightarrow qq'}|_{eknl}^2 = \frac{8}{9} g^4 \frac{s^2}{t^2}. \quad (3.8)$$

The three-body amplitude in (3.7) for the inelastic process, $qq' \rightarrow qq'g$, contains the two-body amplitude for the elastic process, an infrared factor for the emission of a soft gluon and a noneikonal correction factor. The expression in (3.7) will lead to the Gunion and Bertsch formula [136] for

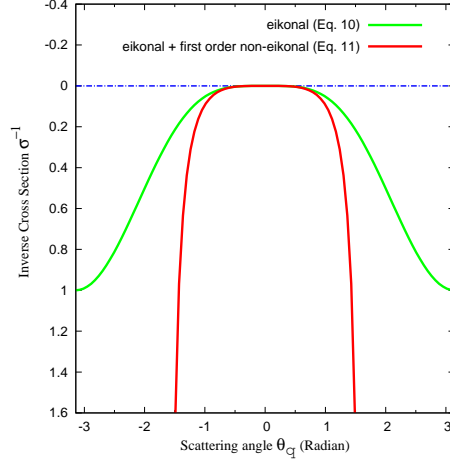


Figure 3.3: Inverse cross-section σ^{-1} vs. scattering angle θ .

the gluon multiplicity distribution in an appropriate limit $\frac{1}{k_{\perp}^2} \approx \frac{1}{k_{\perp}^2} \frac{q_{\perp}^2}{(k_{\perp} - q_{\perp})^2}$, where $|t| = q_{\perp}^2 \gg k_{\perp}^2$. If the emitted gluon is much softer than others it can then be regulated by the Debye screening mass, m_D . Terms within the parenthesis in (3.7) would correspond to noneikonal correction over the eikonal Gunion Bertsch formula. Eq. (3.7) is complete upto $\mathcal{O}(1/k_{\perp}^2)$ and $\mathcal{O}(t/s)$, for emission of a soft gluon in the process $qq' \rightarrow qq'g$. Similar investigation have been done earlier for the process $gg \rightarrow ggg$ [210, 201, 212].

Rutherford scattering beyond eikonal approximation

It is interesting to note how noneikonicity gives way to probe beyond Rutherford scattering limits. In the centre of momentum frame for a typical $2 \rightarrow 2$ (or even in case of $2 \rightarrow 3$ when fifth particle is ultra soft!) process

$$\frac{t}{s} = -\sin^2 \frac{\theta_q}{2} \quad (3.9)$$

The eikonal cross-section (σ_{eknl}) is directly connected to the *Rutherford scattering* scattering cross-section as

$$\sigma_{eknl} \propto \frac{s^2}{t^2} = \frac{1}{\sin^4(\theta_q/2)}. \quad (3.10)$$

When one relaxes the eikonal approximation then the cross-section can be written as

$$\sigma_{ne} \propto \frac{s^2}{t^2} \left(1 + \frac{17t}{9s}\right) = \frac{1}{\sin^4 \frac{\theta_q}{2}} \left(1 - \frac{17}{9} \sin^2 \frac{\theta_q}{2}\right), \quad (3.11)$$

which puts a restriction on the scattering angle, θ_q . In Fig.3.3 we have plotted inverse cross-section (σ^{-1}) for both eikonal and noneikonal case. Even though both behave identically with a similar plateau in the small angle scattering but noneikonal cross-section has a very sharp fall in comparison with the eikonal one for large angle scattering. As seen the noneikonal inverse matrix element is bounded by the scattering angle, $\theta_q = \pm 2 \sin^{-1}(3/\sqrt{17}) \simeq \pm 0.52\pi$, in centre of momentum frame, in contrary to that of eikonal one having a natural bound of $\pm\pi$. This indicates that the back scattering is forbidden for the case of $qq' \rightarrow qq'g$ when the emitted gluon is soft.

Cross-section in the first order in eikonal (*viz.*, noneikonal) approximation

The cross-section for the process $qq' \rightarrow qq'g$ can be obtained as

$$\sigma_{qq' \rightarrow qq'g} = \frac{1}{2s} \int \prod_{i=3}^5 \frac{d^3 k_i}{(2\pi)^3 2E_i} |\mathcal{M}_{qq' \rightarrow qq'g}| (2\pi)^4 \delta^4(k_1 + k_2 - k_3 + k_4 + k_5).$$

In the centre of momentum frame, $\mathbf{k}_1 + \mathbf{k}_2 = \mathbf{k}_3 + \mathbf{k}_4 + \mathbf{k}_5 = \mathbf{0}$, and one obtains

$$\begin{aligned} & \sigma_{qq' \rightarrow qq'g} \\ &= \frac{1}{2s} \int \frac{d^3 k_3}{(2\pi)^3 2E_3} \frac{1}{(2\pi)^3 2E_4} \frac{d^3 k_5}{(2\pi)^3 2E_5} |\mathcal{M}_{qq' \rightarrow qq'g}| (2\pi)^4 \delta(E_1 + E_2 - E_3 + E_4 + E_5) \\ &= \frac{1}{2s} \left[-\frac{1}{2} \frac{1}{(2\pi)^2} \int \frac{dq_{\perp}^2 dq_z}{E_3} \right] \frac{1}{(2\pi)^3 2E_4} \left[\frac{1}{4} \frac{1}{(2\pi)^2} \int \frac{dk_{\perp}^2 d\theta_g}{\sin \theta_g} \right] \\ & \quad \times 12g^2 \frac{8}{9} g^4 \frac{s^2}{t^2} \frac{1}{k_{\perp}^2} \left(1 + \frac{17t}{9s} \right) (2\pi)^4 \delta(E_1 + E_2 - E_3 + E_4 + \omega) \\ &= \frac{1}{2s} \left[-\frac{1}{2} \frac{1}{(2\pi)^2} \int \frac{dq_{\perp}^2}{E_1} \right] \frac{1}{(2\pi)^3 2E_1} \left[-\frac{1}{4} \frac{1}{(2\pi)^2} \int dk_{\perp}^2 d\eta \right] \\ & \quad \times 12g^2 \frac{8}{9} g^4 \frac{s^2}{(q_{\perp}^2)^2} \left(1 + \frac{q_{\perp}^2}{s} \right)^{-2} \frac{1}{k_{\perp}^2} \left(1 - \frac{17q_{\perp}^2}{9s} \right) (2\pi)^4, \quad (3.12) \end{aligned}$$

where we have used rapidity $\eta = -\ln[\tan(\theta_g/2)]$, $\mathbf{q} = \mathbf{k}_1 - \mathbf{k}_3$, $\mathbf{q}_{\perp} = \mathbf{q} \sin \theta_{\mathbf{q}}$.

The cross-section contains factors, having term like q_{\perp}^2/s , that are responsible for non-eikonal effects.

In thermal medium taking debye mass as infrared regulator, the differential cross-section can be expressed as

$$\frac{d \sigma^{qq' \rightarrow qq'g}}{dq_{\perp}^2 dk_{\perp}^2 d\eta} = 2C_A C_{qq'} \alpha^3 \frac{\Gamma_{ab}}{(q_{\perp}^2 + m_d^2)^2} \frac{1}{k_{\perp}^2 + m_d^2}, \quad (3.13)$$

where $C_A = 3$ and $C_{qq'} = 8/9$ are Casimir factors, and $\Gamma_{ab} = \zeta_a \zeta_b$, with

various factors are, explicitly, given as

$$\begin{aligned}\zeta_a &= \left(1 + \frac{q_\perp^2}{s}\right)^{-2}, \\ \zeta_b &= \left(1 - \frac{17}{9} \frac{q_\perp^2}{s}\right).\end{aligned}\tag{3.14}$$

The factor ζ_a comes from eikonal part of the matrix elements, and ζ_b is the noneikonal factor originated from noneikonal part of matrix elements. The differential cross-section for the process $qq' \rightarrow qq'g$ as given in Eq.(3.13) correctly reproduces the result of [213] in the limit $q_\perp^2 \gg k_\perp^2$ and in the eikonal limit, $\sqrt{s}, E \gg q_\perp^2$, as all the noneikonal factors, *viz.*, ζ_a and ζ_b become identically unity and so as Γ_{ab} .

3.2 Inelastic gluon-gluon fusion ($gg \rightarrow ggg$)

As discussed in Chapter (2) The three gluon production via gluon-gluon fusion $gg \rightarrow ggg$ is extremely important in the context of heavy-ion phenomenology. For a sequence of events: hot glue scenario of glasma field, thermal equilibration, gluon chemical equilibration in later time, parton matter viscosity, radiative energy-loss of high energy partons jet propagating through thermalised QGP, this process plays a crucial role. Matrix elements for the process $gg \rightarrow ggg$ have been computed up to $\mathcal{O}(t^3/s^3)$ in Chapter (2). Considering $\mathcal{O}(t/s)$ result it is now straightforward to evaluate the differential cross-section for this process in first order in eikonal approximation

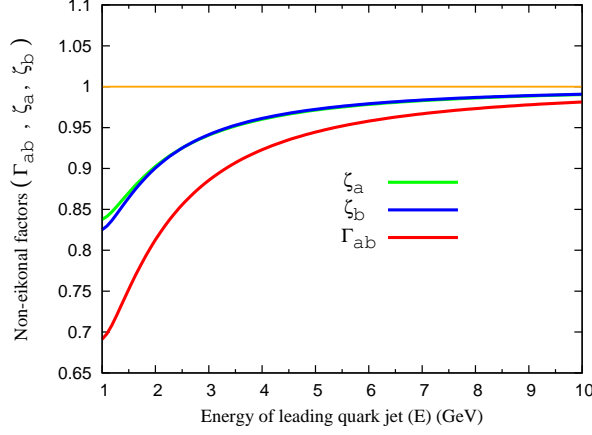


Figure 3.4: Typical estimation of noneikonal factors at $T = 300\text{MeV}$ with $\alpha = 0.3$ for the process $qq' \rightarrow qq'g$. First order noneikonal factors $\zeta_a = (1 + q_{\perp}^2/s)^{-2}$, $\zeta_b = (1 - 17q_{\perp}^2/9s)$, and the full contribution $\Gamma_{ab} = \zeta_a\zeta_b$.

as

$$\frac{d\sigma^{gg \rightarrow ggg}}{dq_{\perp}^2 dk_{\perp}^2 d\eta} = 2C_A C_{gg} \alpha^3 \frac{\Gamma_{ab}}{(q_{\perp}^2 + m_d^2)^2} \frac{1}{k_{\perp}^2 + m_d^2} \quad (3.15)$$

where $C_{gg} = 9/2$ and the factor, $\Gamma_{ab} = \zeta_a\zeta_b$, with its various components

$$\begin{aligned} \zeta_a &= \left(1 + \frac{q_{\perp}^2}{s}\right)^{-2}, \\ \zeta_b &= \left(1 - \frac{1}{2} \frac{q_{\perp}^2}{s}\right). \end{aligned} \quad (3.16)$$

The factor coming from eikonal part of matrix element ζ_a is same for both processes $qq' \rightarrow qq'g$ and $gg \rightarrow ggg$ whereas the noneikonal factor ζ_b is different. This noneikonal factor, obviously, does not put any restriction on the scattering angle ($\theta = \pm\pi$) for the process $gg \rightarrow ggg$, and allows it to go in full natural range $\pm\pi$ as compared to the process $qq' \rightarrow qq'g$.

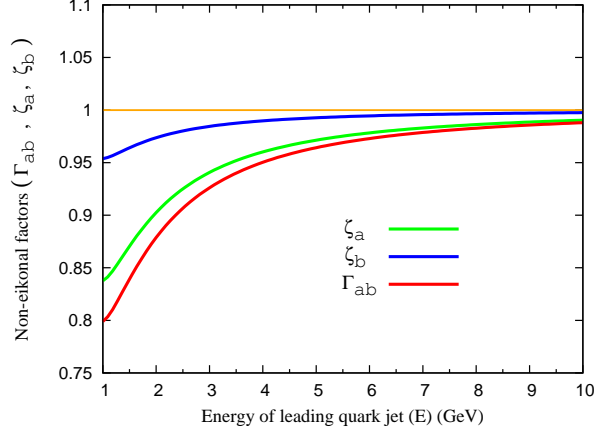


Figure 3.5: Typical estimation of noneikonal factors at $T = 300MeV$ with $\alpha = 0.3$ for the process $gg \rightarrow ggg$. First order noneikonal factors $\zeta_a = (1 + q_{\perp}^2/s)^{-2}$, $\zeta_b = (1 - q_{\perp}^2/2s)$ and the full contribution $\Gamma_{ab} = \zeta_a \zeta_b$.

Unlike $gg \rightarrow ggg$ where a Park-Taylor type formula [211] is available to compute the matrix element, the computation of matrix elements up to $\mathcal{O}(t/s)$ is quite cumbersome in case of $qg \rightarrow qgg$. Also in this work we have performed our study on inelastic quark-quark scattering but with different flavors. In case of same flavor $qq \rightarrow qqg$ things would be a more involved one. We leave them for future study.

3.3 Results and Discussion

For quantitative estimation of the noneikonal effects, we again need the average value of the momentum transfer squared which can be obtained [204]

as

$$\begin{aligned} \langle q_{\perp}^2 \rangle &\simeq \left(\int_{m_g^2}^{E^2} dq_{\perp}^2 q_{\perp}^2 \frac{d\sigma_{2 \rightarrow 3}}{dq_{\perp}^2} \right) / \left(\int_{m_g^2}^{E^2} dq_{\perp}^2 \frac{d\sigma_{2 \rightarrow 3}}{dq_{\perp}^2} \right) \\ &\simeq 2g^2 T^2 \ln(E/gT). \end{aligned} \quad (3.17)$$

In Fig.5.5 and Fig.3.5 the first order noneikonal factors: ζ_a , ζ_b and the full contribution Γ_{ab} for both processes $qq' \rightarrow qq'g$ and $gg \rightarrow ggg$, respectively, displayed. It can be seen that the noneikonal effects are $\sim (15 - 20)\%$ over eikonal one for moderately hard jets. However, the noneikonal effect gradually becomes mild for very high energetic jets. In the literature attempts have already been made to address the noneikonal propagation of partons for collision/elastic processes in a Monte-carlo approach by considering full $\mathcal{O}(\alpha_s^2)$ matrix elements for relevant $2 \rightarrow 2$ processes. Eikonal propagation approximation was found to be good on the 10% level. Present study also reveals that for radiative/inelastic process, *Eikonal parton trajectory I* approximation seems to be within (15 – 20)% level. This approximation should be crude only in soft and moderate momentum regimes.

There has always been a quest for large angle radiations. In the present study we do not assume small angle/collinear emission approximation either in the course of calculating matrix elements or in the calculations of kinematics. In most of the existing calculations in light cone gauge, the transverse momentum of the emitted gluon k_{\perp} depends on the exchanged transverse momentum q_{\perp} and on the number of scatterings L/λ (L is the length of the plasma and λ is the mean free path of the traversing parton) in a hot and

dense medium, but not on the gluon energy ω . As a consequence, ‘*there may be some anomalous radiation with ω smaller than the typical k_\perp* ’ [198]. In the present calculation the kinematic relation $k_\perp = \omega \sin \theta_g$ ensures no radiation with ω smaller than the typical k_\perp and one does not need to worry about q_\perp and L/λ .

The kinematic constraints, $E \gg \omega \gg k_\perp, q_\perp$ referred in the literature as soft eikonal approximation that neglects any change in parton trajectory due to multiple scatterings but assumes a straight line trajectory throughout. The diffusion of partons in a hot and dense medium can have an unavoidable link beyond the eikonal approximation and it is worth to relax eikonal approximation. In this work an attempt has been made to relax part of this approximation for some of the inelastic processes and their differential cross-sections in first order noneikonal approximation have been obtained. Primary estimation indicates 15–20% reduction in the cross section due to first order noneikonal effect for both the processes in the soft and intermediate parton energies. These cross-sections naturally reproduce eikonally approximated results in the eikonal limit, *i.e.*, $\sqrt{s}, E \gg q_\perp$. We also show that wide back scattering with scattering angle more than $\simeq \pm 0.52\pi$ is forbidden in case of $qq' \rightarrow qq'g$ when the emitted gluon is soft. This, however, is not the case for $gg \rightarrow ggg$. We intend quantitative estimation of this noneikonal effect in jet quenching and other consequences in heavy-ion collisions phenomenology. So far we have only addressed light flavors, we will be going to study heavy flavors and its mass suppression aspects in next.

Chapter 4

Heavy Flavor Bremsstrahlung

In order to probe characteristics of quark-gluon plasma medium, heavy quarks are believed to be very clean probes because they are brought to existence well before the formation of quark-gluon plasma. Heavy-quarks are able to follow-up the whole evolution of QGP. Heavy quarks interact with thermal light quarks /anti-quarks, and gluons through elastic and/or inelastic scattering. In this chapter an improved generalized suppression factor for gluon emission off a heavy quark is derived within perturbative QCD, which is valid for the full range of rapidity of the radiated gluon and also has no restriction on the scaled mass of the quark with its energy. In the appropriate limit it correctly reproduces the usual dead cone factor in the forward rapidity region. On the other hand, this improved suppression factor becomes close to unity in the backward direction. This indicates a smaller suppression compared to previous calculations, which should have an impact on the phenomenology of heavy quark energy loss in the hot and dense matter produced in ultra

relativistic heavy-ion collisions.

Some of the important features of the plasma produced in heavy-ion collisions include energy loss and jet quenching of high energetic partons, viz., light and heavy quarks. The Gunion-Bertsch (GB) formula for gluon emission from the processes $qq \rightarrow qqg$ has been widely used in different phenomenological studies of heavy ion collisions, in particular for radiative energy loss of high energy partons propagating through a thermalized QGP. The energy loss is presently a field of high interest in view of jet quenching of high energy partons, viz., both light and heavy quarks. Generally, one expects that jet quenching for heavy quarks should be weaker than that of light quarks. In contrast the non-photon data at RHIC reveal a similar suppression for heavy flavored hadrons compared to that of light hadrons.

An early attempt to calculate the heavy quark energy loss in a QGP medium was done in by using the GB formula of gluon emission for light quark scattering and just modifying the relevant kinematics for heavy quarks. Later the soft gluon emission formula for heavy quarks in the high energy approximation was renewed in for the small angle limit. Soft gluon emission from a heavy quark was found to be suppressed in the forward direction compared to that from a light quark due to the mass effect (dead cone effect). The corresponding suppression factor was obtained as,

$$\mathcal{D}_{DK} = \left(1 + \frac{\theta_0^2}{\theta^2}\right)^{-2} \Big|_{\theta \ll 1}, \quad (4.1)$$

where $\theta_0 = M/E \ll 1$. E is the energy of the heavy quark with mass, M

and θ , the angle between the heavy quark and the radiated gluon.

4.1 Spectrum without collinear approximation

In this work we make an attempt to revisit the issue and generalize the gluon emission off a heavy quark by relaxing the constraints imposed in earlier calculations on the emission angle of the radiated gluons and the scaled mass of the heavy quark with its energy. We have found a generalized expression of dead cone factor that is identical to (4.1) in appropriate limit and smoothly becomes unity (no suppression) in backward direction. This supports the point of [179] that main modification of the gluon radiation spectrum due to non-zero quark mass occurs at small angles (forward direction) and not in large angles (backward direction).

In Fig. 4.1 the five Feynman diagrams for the process $Qq \rightarrow Qqg$ are shown. According to the notation used in the figure, the Mandelstam variables are

$$s = (k_1 + k_2)^2, \quad s' = (k_3 + k_4)^2, \quad (4.2a)$$

$$u = (k_1 - k_4)^2, \quad u' = (k_2 - k_3)^2, \quad (4.2b)$$

$$t = (k_1 - k_3)^2, \quad t' = (k_2 - k_4)^2, \quad (4.2c)$$

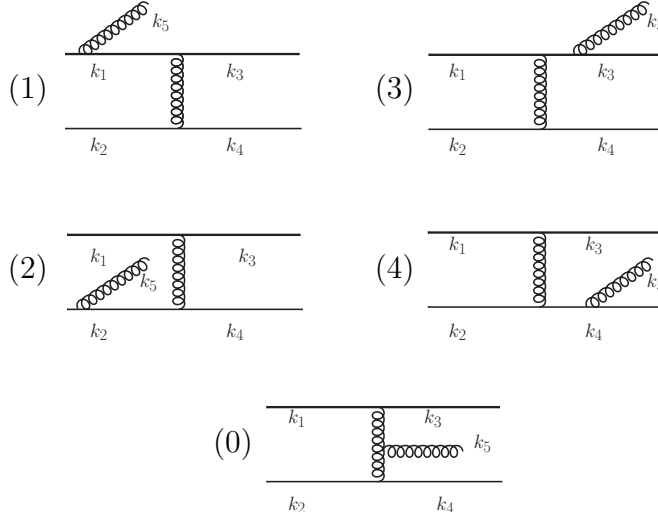


Figure 4.1: Five tree level Feynman diagrams for the process $Qq \rightarrow Qqg$. In each diagram the thick upper line represents the heavy quark (Q) whereas the thin lower line represents the background light quark.

with

$$s + t + u + s' + t' + u' = 4M^2 . \quad (4.3)$$

Soft gluon emission ($k_5 \rightarrow 0$) implies $t' \rightarrow t$, $s' \rightarrow s$, $u' \rightarrow u$. In the center of momentum frame we consider the case where the energy of the emitted gluon, ω is much smaller than the momentum transfer $\sqrt{|t|} \approx q_\perp$ from the projectile (heavy quark) to the target (light quark) which again is small compared to the energy of heavy quark E . This leads to the hierarchy

$$E \gg \sqrt{|t|} \gg \omega . \quad (4.4)$$

It is important to note that the scaled mass of the heavy quark with its

energy M/E and the gluon emission angle θ are free from any constrain.

The gauge invariant amplitude for the process $Qq \rightarrow Qqg$ can be written as the squared matrix elements from the diagrams of Fig. 4.1, including their interference terms,

$$|\mathcal{M}_{Qq \rightarrow Qqg}|^2 = \sum_{i \geq j} \mathcal{M}_{ij}^2, \quad (4.5)$$

where i and j run from 0 to 4 and $\mathcal{M}_{ij}^2 = \mathcal{M}_i \mathcal{M}_j^*$ with \mathcal{M}_i being the matrix element of diagram i (see Fig. 4.1).

With the hierarchy indicated in (4.4) the different matrix elements squared are obtained in the Feynman gauge as (see Appendix for details)

$$\begin{aligned} \mathcal{M}_{11}^2 &= \mathcal{M}_{33}^2 = \frac{128}{27} g^6 \frac{s^2}{t^2} \frac{1}{k_{\perp}^2} \left[\frac{M^2}{s} - 1 + \mathcal{J} \right] \mathcal{J}, \\ \mathcal{M}_{00}^2 &= \mathcal{M}_{22}^2 = \mathcal{M}_{44}^2 = 0, \\ \mathcal{M}_{13}^2 &= \frac{128}{27} g^6 \frac{s^2}{t^2} \frac{1}{k_{\perp}^2} \left[\frac{1}{4} \left(\frac{M^2}{s} - 1 + \mathcal{J} \right) \right] \mathcal{J}, \\ \mathcal{M}_{14}^2 &= \mathcal{M}_{23}^2 = \frac{128}{27} g^6 \frac{s^2}{t^2} \frac{1}{k_{\perp}^2} \left[\frac{7}{8} \left(1 - \frac{M^2}{s} \right) \right] \mathcal{J}, \\ \mathcal{M}_{12}^2 &= \mathcal{M}_{34}^2 = \frac{128}{27} g^6 \frac{s^2}{t^2} \frac{1}{k_{\perp}^2} \left[\frac{1}{4} \left(1 - \frac{M^2}{s} \right) \right] \mathcal{J}, \\ \mathcal{M}_{24}^2 &= \mathcal{M}_{10}^2 = \mathcal{M}_{20}^2 = \mathcal{M}_{30}^2 = \mathcal{M}_{40}^2 = 0, \end{aligned} \quad (4.6)$$

with

$$\mathcal{J} = 1 - \left[\left(\frac{s}{M^2} - 1 \right) \sin^2(\theta/2) + 1 \right]^{-1}, \quad (4.7)$$

and $k_{\perp} = \omega \sin \theta$, the transverse momentum of the emitted gluon.

The gauge invariant amplitude for the process $Qq \rightarrow Qqg$ can now be

obtained by summing all the sub-amplitudes (4.6),

$$\begin{aligned}
|\mathcal{M}_{Qq \rightarrow Qqg}|^2 &= 12g^2 |\mathcal{M}_{Qq \rightarrow Qq}|^2 \frac{1}{k_{\perp}^2} \frac{\mathcal{J}^2}{\left(1 - \frac{M^2}{s}\right)^2} \\
&= 12g^2 |\mathcal{M}_{Qq \rightarrow Qq}|^2 \frac{1}{k_{\perp}^2} \left(1 + \frac{M^2}{s \tan^2(\frac{\theta}{2})}\right)^{-2} \\
&= 12g^2 |\mathcal{M}_{Qq \rightarrow Qq}|^2 \frac{1}{k_{\perp}^2} \left(1 + \frac{M^2}{s} e^{2\eta}\right)^{-2}, \quad (4.8)
\end{aligned}$$

where $\eta = -\ln[\tan(\theta/2)]$, the rapidity of the emitted massless gluon. The two body amplitude is given by

$$|\mathcal{M}_{Qq \rightarrow Qq}|^2 = \frac{8}{9} g^4 \frac{s^2}{t^2} \left(1 - \frac{M^2}{s}\right)^2. \quad (4.9)$$

Equation (4.8), which is the main result of the present work, carries a generalized suppression factor, \mathcal{D} as

$$\mathcal{D} = \left(1 + \frac{M^2}{s \tan^2(\frac{\theta}{2})}\right)^{-2}. \quad (4.10)$$

This improved suppression factor is valid in the full range of θ (or rapidity of the emitted gluon) (i.e., $-\pi < \theta < +\pi$) and in the full range of M/\sqrt{s} (i.e., $0 < M/\sqrt{s} < 1$) as compared to Ref. [179]. As a note, the relation between the center of mass energy \sqrt{s} and the energy of the heavy quark E reads

$$s = 2E^2 + 2E\sqrt{E^2 - M^2} - M^2. \quad (4.11)$$

Below we discuss our results in more detail. First we consider two limits:

1. *Gunion-Bertsch limit*: For $M = 0$, (4.8) reduces to the well known result of Gunion and Bertsch [136] as

$$\begin{aligned}
|\mathcal{M}_{qq' \rightarrow qq'g}|^2 &= 12g^2 |\mathcal{M}_{qq' \rightarrow qq'}|^2 \frac{1}{k_\perp^2} \\
&\simeq 12g^2 |\mathcal{M}_{qq' \rightarrow qq'}|^2 \frac{1}{k_\perp^2} \frac{q_\perp^2}{(q_\perp - k_\perp)^2} \\
&= |\mathcal{M}_{qq' \rightarrow qq'g}|_{\text{GB}}^2,
\end{aligned} \tag{4.12}$$

where we have used (4.4) that implies $q_\perp \gg k_\perp$.

2. *Dokshitzer and Kharzeev's result*: In the limit $M \ll \sqrt{s}$ and $\theta \ll 1$, it is $\sqrt{s} \simeq 2E$ and $\tan(\theta/2) \simeq \theta/2$ and (4.8) reduces to

$$\begin{aligned}
|\mathcal{M}_{Qq \rightarrow Qqg}|^2 &= 12g^2 |\mathcal{M}_{Qq \rightarrow Qq}|^2 \frac{1}{k_\perp^2} \left(1 + \frac{M^2}{E^2 \theta^2}\right)^{-2} \\
&\simeq 12g^2 |\mathcal{M}_{Qq \rightarrow Qq}|^2 \frac{1}{k_\perp^2} \left(1 + \frac{\theta_0^2}{\theta^2}\right)^{-2},
\end{aligned} \tag{4.13}$$

where $\theta_0 = M/E$. This expression is precisely the result derived in Ref. [179].

4.2 Gluon multiplicity distribution

For convenience, we define \mathcal{R} as the ratio of the squared matrix element of the $2 \rightarrow 3$ to that of the $2 \rightarrow 2$ processes,

$$\mathcal{R} = \frac{|\mathcal{M}_{Qq \rightarrow Qqg}|^2}{|\mathcal{M}_{Qq \rightarrow Qq}|^2} = 3g^2 \frac{1}{\omega^2} \left(\frac{e^\eta + e^{-\eta}}{1 + \frac{M^2}{s} e^{2\eta}} \right)^2. \tag{4.14}$$

We note that this ratio, \mathcal{R} is related to the gluon emission multiplicity distribution as $dn_g/d\eta dk_\perp^2 = \mathcal{R}/16\pi^3$. For the massless case, $\mathcal{R}^{M \rightarrow 0}$ is symmetric in rapidity. In contrast, a finite mass of the quark renders \mathcal{R} to be asymmetric in rapidity. To explore this in more detail we consider the following rapidity regions:

1. *Forward rapidity* ($\eta \gg 0$): In this case (4.14) reduces to

$$\mathcal{R}_{\eta \gg 0} \rightarrow 3g^2 \frac{1}{\omega^2} \frac{s^2}{M^4} e^{-2\eta}. \quad (4.15)$$

Clearly, in this region of rapidity the gluon emission is exponentially suppressed, which indicates the presence of the dead cone in the forward direction if $M \neq 0$.

2. *Mid-rapidity* ($\eta \sim 0$): At mid-rapidity \mathcal{R} depends only weakly on η as

$$\mathcal{R}_{\eta \sim 0} \rightarrow 12g^2 \frac{1}{\omega^2} \left(1 + \frac{M^2}{s}\right)^{-2} \left[1 - 4\eta \frac{M^2}{s + M^2}\right]. \quad (4.16)$$

3. *Backward rapidity* ($\eta \ll 0$): Here (4.14) becomes

$$\mathcal{R}_{\eta \ll 0} \rightarrow 3g^2 \frac{1}{\omega^2} e^{-2\eta} = \mathcal{R}_{\eta \ll 0}^{M \rightarrow 0}. \quad (4.17)$$

In this region the gluon emission does not depend on the mass and is, therefore, the same for heavy as well as light quarks. This is an important aspect for gluon emission off a heavy quark.

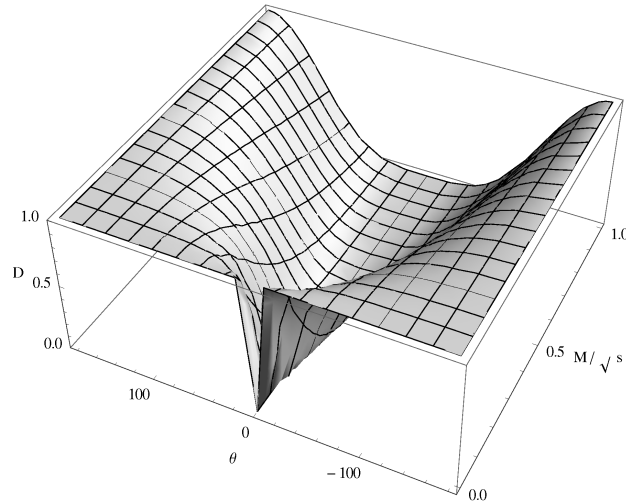


Figure 4.2: The suppression factor \mathcal{D} from (4.10) as a function of θ and M/\sqrt{s} .

We also note the dominant process (i.e., $Qg \rightarrow Qgg$) where a gluon acts as a target. Within the hierarchy (4.4) it differs from $Qq \rightarrow Qqg$ only by a color Casimir factor $C_A/C_F = 9/4$ as

$$|\mathcal{M}_{Qg \rightarrow Qgg}|^2 = \frac{C_A}{C_F} |\mathcal{M}_{Qq \rightarrow Qqg}|^2, \quad (4.18)$$

since the two body part is given as

$$|\mathcal{M}_{Qg \rightarrow Qg}|^2 = \frac{C_A}{C_F} |\mathcal{M}_{Qq \rightarrow Qq}|^2, \quad (4.19)$$

and the other factors are the same for both processes in the considered approximations. Therefore, the factors \mathcal{D} and \mathcal{R} remain unchanged.

In Fig. 4.2 the suppression factor \mathcal{D} [cf. Eq. (4.10)] is plotted as a function of θ and M/\sqrt{s} . Around $\theta \ll 1$ we observe a canyon for small M/\sqrt{s} and

a valley for large M/\sqrt{s} , which clearly indicate a presence of a dead cone in the forward direction with respect to the propagating heavy quark. The spread of the dead cone increases as M/\sqrt{s} increases. In the backward region, $\theta \sim \pm\pi$, the suppression factor saturates to unity. This suggests that the quark mass plays only a role in the forward direction when the energy of the quark becomes of the order of its mass.

The possibility of this large angle scattering might be important for heavy-ion phenomenology in the context of the non-photon electron data at RHIC and LHC. Furthermore, it might also have an impact on the description of the forward-backward asymmetry of dijets and the seen energy deposition at large angles in respect to the leading jet.

Figure 4.3 compares our result for the generalized suppression factor \mathcal{D} in (4.10) as a function of the emission angle θ for charm and bottom at two different energy ($E=5$ GeV and $E=10$ GeV). Among four typical cases 5 GeV bottom shows maximal suppression and 10 GeV charm quark shows least suppressions as scaled mass of the heavy quark with its energy is highest for the former and lowest for the later. For large emission angles the suppression factor, \mathcal{D} approaches to unity. This indicates that the backward emission is as strong as for light quarks.

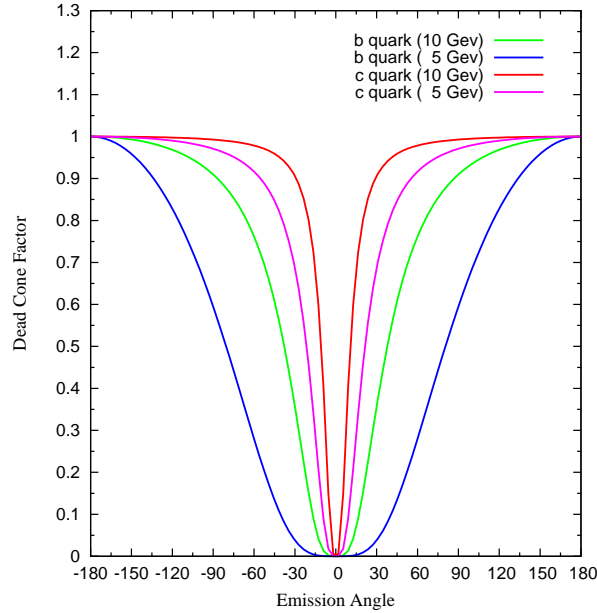


Figure 4.3: The suppression factor \mathcal{D} from (4.10) as a function of θ for charm and bottom at two different energy ($E= 5$ GeV and $E= 10$ GeV).

4.3 Discussion

Though its true that softer part of the heavy flavor spectrum gets thermalized owing to its interaction with bath particles, the high frequency hard part contain considerable bulk of energy which influences the experimental observables like nuclear suppression factor (R_{AA}), azimuthal asymmetry (v_2) etc. In this work we derived a compact expression that contains a generalized suppression factor for gluon emission off a heavy quark through the scattering with a light parton. In the appropriate limit this expression reduces to the usually known dead cone factor. Our analysis shows that there is a suppression of soft gluon emission due to the mass of the heavy quark in the forward direction. On the other hand, the present findings also indicate that

a heavy quark emits a soft gluon almost similar to that of a light quark in the backward rapidity region. The effects of gluon radiation by charm quarks on the transport coefficients *e.g.* drag, longitudinal and transverse diffusion and shear viscosity have been studied recently utilizing this new form of dead cone factor by S. Mazumder, T. Bhattacharyya and J. -eAlam [214]. In next we will see that this result indeed have have important consequences for a better understanding of heavy flavor energy loss in heavy- ion collisions.

Chapter 5

Energy loss of Heavy Quark

In this chapter we estimate the radiative energy loss of heavy flavours which is crucial in order to understand the properties of nuclear or hadronic matter at extreme conditions. Various diagnostic measurements taken at CERN Super Proton Synchrotron (SPS) in the past and at BNL Relativistic Heavy Ion Collider (RHIC) in the recent past have provided strong hints for the formation of QGP within a first few fm/ c of the collisions through the manifestation of hadronic final states. New data from heavy-ion experiments at CERN Large Hadron Collider (LHC) have further indicated the formation of such a state of matter.

One of the important features of the plasma produced in heavy-ion collisions is suppressed production of high energy hadrons compared to the case of pp collisions, called jet quenching. As discussed several times the term ‘jet quenching’, generally, ascribes to the modification of an energetic parton due to its interaction with the coloured medium while passing through it.

The basic idea is that the scales of hard (high- p_{\perp}) processes and the medium interactions in the context of heavy-ion collisions, are very distinct in accordance with the uncertainty principle. This provides the fact that the high- p_{\perp} parton production in $A - A$ collisions can be computed using perturbative QCD (pQCD), which is quite close to the vacuum rate scaled for binary $N - N$ collisions in an $A - A$ collision. The effect of medium is then treated as a final state interaction which is taken into account through the modification of the outgoing parton fragmentation pattern due to parton-medium interactions.

The heavy-ion program at BNL RHIC has clearly revealed that the phenomenon of jet quenching is mainly caused due to the energy loss of the initial hard parton via collisional and radiative processes, prior to hadronisation. The indication for jet quenching in heavy-ion program at CERN LHC has also been observed recently. The energy loss encountered by an energetic-parton in a QCD medium reveals the dynamical properties of that medium and presently is a field of high interest in view of jet quenching of high energy partons; both light and heavy quarks. Naively, one imagines that the amount of quenching for heavy flavours jet should be smaller than that of light flavours due to the large mass of heavy quarks. However, the single electron data at RHIC exhibit almost a similar suppression for heavy flavored hadrons compared to that for light hadrons.

As mentioned in the introduction a first attempt to estimate the radiative energy loss of heavy flavours in a QGP medium was made by using the Gunion Bertsch formula of gluon emission for light quark scattering and

appropriately modifying the relevant kinematics for heavy quarks. Later the GB-like formula for heavy quarks was reconsidered in Ref. [179] by introducing the mass in the matrix element but only within the small angle approximation. Due to this mass effect, a suppression, known as ‘dead cone’ effect, in the soft gluon emission off a heavy quark was predicted in comparison to that from a light quark. This resulted in a reduction of heavy quark energy loss induced by the medium [179], which is limited only to the forward direction. However, such a gluon radiation spectrum with a dead cone factor, only applicable to the forward direction, was also used in the literature uniformly for the full range of the emission angle (*i.e.*, both forward and backward direction) of gluon to calculate the heavy quark energy loss in the medium. This can lead to a unphysical result at large angle radiation, as discussed as well as shown in Ref. [203]. Further attempts were also made in the literature to improve the calculation of heavy quark energy loss with various ingredients as well as restrictions. In some cases the energy loss for charm quark was found to be different than the light quark. The subject of heavy quark energy loss is not yet a settled issue and requires more detailed analysis.

In a very recent work [203] (discussed in last Chapter) the probability of gluon emission off a heavy quark has been generalised by relaxing some of the constraints, *e.g.*, the gluon emission angle and the scaled mass of the heavy quark with its energy, which were imposed in earlier calculations [179]. It resulted in a very compact and elegant expression for the gluon radiation

spectrum off a heavy quark (*e.g.*, $Qq \rightarrow Qqg$) as [203]

$$\frac{dn_g}{d\eta dk_\perp^2} = \frac{C_A \alpha_s}{\pi} \frac{1}{k_\perp^2} \mathcal{D}, \quad (5.1)$$

where the transverse momentum of the emitted massless gluon is related to its energy by $k_\perp = \omega \sin \theta$, and the rapidity, $\eta = -\ln[\tan(\theta/2)]$, is related to the emission angle, and the generalised dead cone is given by

$$\mathcal{D} = \left(1 + \frac{M^2}{s} e^{2\eta}\right)^{-2} = \left(1 + \frac{M^2}{s \tan^2(\frac{\theta}{2})}\right)^{-2}. \quad (5.2)$$

Now, the Mandelstam variable s is given as, $s = 2E^2 + 2E\sqrt{E^2 - M^2} - M^2$, with E and M , respectively, the energy and mass of the heavy quark. C_A is the Casimir factor for adjoint representation and α_s is the strong coupling constant. In the small angle limit, $\theta \ll \theta_0 (= M/E) \ll 1$, the dead cone in (2) reduces to that in Ref. [179] as $(1 + \theta_0^2/\theta^2)^{-2}$ whereas for massless case it becomes unity and (5.1) reduces to the GB formula. The gluon spectrum for the process, $Qg \rightarrow Qgg$, can also be found in Ref. [203]. We also note that the gluon emission spectrum in (5.1) is obtained in Feynman gauge. The same result is also obtained using light-cone gauge.

The scaled gluon emission spectrum off a heavy quark with that of light quark) is displayed in Fig. 5.1 in the full domain of gluon emission angle, θ , off a heavy quark for the scaled mass $m = \frac{M}{\sqrt{s}} = 0.3$. This actually represents a two dimensional view of the scaled gluon emission probability off a heavy quark with that of a light quark as given in (5.1). We consider the direction of propagation of a heavy quark is from left to right along the horizontal

axis and collide with medium partons at the origin of a circle of unit radius. This simulation has been performed by throwing points at random directions within the full domain of θ but with a probabilistic weight $\mathcal{D}(\theta)$, which would then correspond to a point randomly on the selected θ -line as a ‘*red plus*’ inside the circle of unit radius. The shade with red pluses represents the soft gluon emission zone whereas the conical white zone in the forward direction indicates a dead cone for gluon emission due to the mass effect. It reveals a forward-backward asymmetry which encompasses the fact that the gluon emission off a heavy quark is as strong as that of light quark at the large angles (backward direction) whereas it is suppressed due to nonzero quark mass at the small angles (forward direction). However, if the energy of the heavy quark is large compared to its mass, the effect of dead cone diminishes, both heavy and light quark are expected to lose energy almost similarly. This result can have important consequences for a better understanding of heavy flavour energy loss in the context of heavy-ion collisions at RHIC and LHC. In this work we intend to use the gluon radiation spectrum in Ref. [203] to obtain the heavy flavour energy loss and attempt to understand the suppression of heavy flavoured hadrons in heavy-ion collisions.

Among the interactions that a charged particle undergoes, as it traverses a dense matter, inelastic (i.e. radiative) scattering is undoubtedly the most important and interesting one. A number of different energy loss models has also been formulated in the literature as mentioned in introduction. The basic differences among the different models are the various constraints (*e.g.*, kinematic cuts, large angle radiation etc.) implemented to make the calcu-

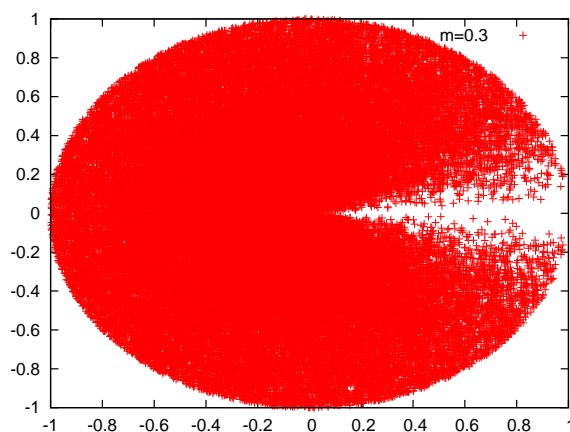


Figure 5.1: A Monte Carlo simulation for the suppression factor in (5.2) (see text for details).

lations manageable.

5.1 Radiative Energy Loss

In this section we define the rate of radiative energy loss of a parton with energy E , due to inelastic scatterings with the medium partons in a very canonical way as

$$\frac{dE}{dx} = \frac{\langle \omega \rangle}{\langle \lambda \rangle}, \quad (5.3)$$

where $\langle \omega \rangle$ and $\langle \lambda \rangle$ are the mean energy of emitted gluons and the mean free path of the traversing quark, respectively.

Among the set of variables $[k_{\perp}, \eta, \omega]$ in (5.1) any two together are sufficient to completely describe an emitted gluon. For convenience we now change the variable duo from $[k_{\perp}, \eta]$ to $[\omega, \eta]$ as

$$\frac{dn_g}{d\eta dk_{\perp}} \Rightarrow \frac{dn_g}{d\eta d\omega}. \quad (5.4)$$

It is now easy to find mean energy of the emitted soft gluons from the spectrum as

$$\begin{aligned} \langle \omega \rangle &= \left(\int \frac{dn_g}{d\eta d\omega} \omega \, d\eta d\omega \right) / \left(\int \frac{dn_g}{d\eta d\omega} \, d\eta d\omega \right) \\ &= \left(\int d\omega \int \mathcal{D} d\eta \right) / \left(\int \frac{1}{\omega} d\omega \int \mathcal{D} d\eta \right). \end{aligned} \quad (5.5)$$

Other important quantity in (5.3) is the mean free path $\langle \lambda \rangle$, which is the average distance covered by the traversing quark between two successive collision, *followed by a soft gluon radiation*. The magnitude of mean free

path depends on the characteristics of the system in which the energetic particle is traversing, and it is defined as

$$\langle \lambda \rangle = 1/(\sigma_{2 \rightarrow 3} \rho_{\text{qgp}}), \quad (5.6)$$

where $\sigma_{2 \rightarrow 3} \rho_{\text{qgp}} = \rho_q \sigma_{Qq(\bar{q}) \rightarrow Qq(\bar{q})g} + \rho_g \sigma_{Qg \rightarrow Qgg}$, $\sigma_{2 \rightarrow 3}$ is the cross section of relevant $2 \rightarrow 3$ processes and ρ_{qgp} is the density of QGP medium which acts as a background containing target partons, for the high energetic projectile quark. We also note that for heavy flavor the Landau-Pomeranchuk-Migdal (LPM) interference correction may be marginal, which we would estimate below based on the formation time of the emitted gluon along with the kinematical restrictions. Now, we recall the total cross section for $2 \rightarrow 3$ processes as given in Ref. [213] as

$$\begin{aligned} \sigma_{2 \rightarrow 3} &= 2 C_A \alpha_s^3 \int \frac{1}{(q_\perp^2)^2} dq_\perp^2 \int \frac{1}{k_\perp^2} dk_\perp^2 \int \mathcal{D} d\eta \\ &= 4 C_A \alpha_s^3 \int \frac{1}{(q_\perp^2)^2} dq_\perp^2 \int \frac{1}{\omega} d\omega \int \mathcal{D} d\eta, \end{aligned} \quad (5.7)$$

where q_\perp is the transverse momentum of the exchanged gluon. Combining (5.6) and (5.7) the energy loss in (5.3) can be written as

$$\begin{aligned} \frac{dE}{dx} &= 12 \alpha_s^3 \rho_{\text{qgp}} \int_{q_\perp^2|_{\min}}^{q_\perp^2|_{\max}} \frac{1}{(q_\perp^2)^2} dq_\perp^2 \\ &\quad \int_{\omega_{\min}}^{\omega_{\max}} d\omega 2 \int_{\eta_{\min}}^{\eta_{\max}} \mathcal{D} d\eta, \end{aligned} \quad (5.8)$$

where a factor of 2 has been introduced in η integral to cover both upper

and lower hemisphere. We note that for $\mathcal{D} = 1$, (5.8) becomes equivalent to the massless case. Unlike the consequence of Landau-Pomeranchuk-Migdal (LPM) interference correction as L^2 (see E), in this study where LPM effect is marginal dependence is linear in L .

5.1.1 Hierarchy and momentum cuts

At this point it is important to note that the hierarchy employed in obtaining (5.1) reads as

$$\sqrt{s}, E \gg \sqrt{|t|} \sim q_{\perp} \gg \omega > k_{\perp} \gg m_D, \quad (5.9)$$

where s, u, t are the usual Mandelstam variables and m_D is the Debye screening mass of the thermal gluons. Based on the above hierarchy we obtain the kinematic cuts explicitly on energy-momentum constraints and large angle radiation. The infra-red cut-off has been used as

$$q_{\perp}^2|_{min} \simeq \omega_{min}^2 \simeq k_{\perp}^2|_{min} \simeq m_D^2 = 4\pi\alpha_s T^2. \quad (5.10)$$

For ultraviolet cut-off on intermediate gluons, we have used,

$$q_{\perp}^2|_{max} = \frac{3}{2}ET - \frac{M^2}{4} + \frac{M^4}{48ET\beta_0} \log \left[\frac{M^2 + 6ET(1 + \beta_0)}{M^2 + 6ET(1 - \beta_0)} \right], \quad (5.11)$$

where $\beta_0 = (1 - M^2/E^2)^{1/2}$ and T is temperature of thermal background. The ultraviolet cut-off on energy for the emitted soft gluon has been taken

as average momentum of the intermediate gluon line as,

$$\omega_{max}^2 \simeq \langle q_{\perp}^2 \rangle . \quad (5.12)$$

5.1.2 Maximal rapidity integration :

The relation between ω and k_{\perp} , $\omega = k_{\perp} \cosh \eta$, can be used to obtain bound on η from top, which eventually excludes all collinear singularities for massless case. Finite cut on ω and k_{\perp} then leads to an inequality,

$$\cosh \eta > \omega_{max} / k_{\perp}|_{min} , \quad (5.13)$$

from which one can easily obtain the bound on η as

$$|\eta| < \log \left(\frac{\sqrt{\langle q_{\perp}^2 \rangle}}{m_D} + \sqrt{\frac{\langle q_{\perp}^2 \rangle}{m_D^2} - 1} \right) . \quad (5.14)$$

We are now in position to discuss the LPM effect which is usually included through a step function $\theta(\tau_i - \tau_f)$ while evaluating the spectrum of the radiated gluon. It basically implies that the formation time of the gluon, $\tau_f = \langle \omega \rangle / \langle k_{\perp}^2 \rangle$ must be smaller than the interaction time $\tau_i \sim \Lambda_{\text{QCD}}^{-1} = 0.49/T_C$. This on the other hand imposes a restriction on the phase space of the emitted gluon as $\langle \omega \rangle > 2\Lambda_{\text{QCD}} \approx 4T_C \sim gT \sim \mu_D$, provided $\alpha_s \sim 0.3$, $T_C \sim 170$ MeV and the temperature of the plasma, $T \sim 350$ MeV. Thus, the hierarchy in Eq.(5.9) excludes the modification of the radiative energy loss due to the LPM interference correction through the infrared regulator, μ_D . Therefore,

the present formalism becomes akin to the Bethe-Heitler approximation, in which the scattering centers are well separated and the intensity of the induced radiation from different scatterings is additive.

5.2 Improved energy loss expression:

It is very straightforward to obtain the radiative energy-loss through the inelastic processes, *viz.*, $Qq(\bar{q}) \rightarrow Qq(\bar{q})g$ and $Qg \rightarrow Qgg$, for a heavy quark from (5.8), which reads as

$$\begin{aligned} \frac{dE}{dx} &= 24 \alpha_s^3 \left(\rho_q + \frac{9}{4} \rho_g \right) \frac{1}{\mu_g} (1 - \beta_1) \\ &\quad \left(\frac{1}{\sqrt{(1 - \beta_1)}} [\log(\beta_1)^{-1}]^{1/2} - 1 \right) \mathcal{F}(\delta), \end{aligned} \quad (5.15)$$

where

$$\begin{aligned} \mathcal{F}(\delta) &= 2\delta - \frac{1}{2} \log \left(\frac{1 + M^2 e^{2\delta}/s}{1 + M^2 e^{-2\delta}/s} \right) \\ &\quad - \frac{M^2 \cosh \delta/s}{1 + 2M^2 \cosh \delta/s + M^4/s^2}, \\ \delta &= \frac{1}{2} \log \left[\frac{\log \beta_1^{-1}}{(1 - \beta_1)} \left(1 + \sqrt{1 - \frac{(1 - \beta_1)^{1/2}}{[\log \beta_1^{-1}]^{1/2}}} \right)^2 \right], \\ s &= E^2 (1 + \beta_0)^2, \quad \beta_1 = \frac{g^2 T}{C E}, \\ C &= \frac{3}{2} - \frac{M^2}{4ET} \\ &\quad + \frac{M^4}{48E^2 T^2 \beta_0} \log \left[\frac{M^2 + 6ET(1 + \beta_0)}{M^2 + 6ET(1 - \beta_0)} \right]. \end{aligned} \quad (5.16)$$

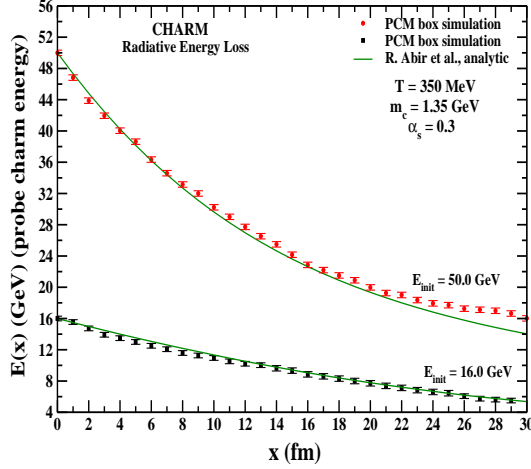


Figure 5.2: Energy of probe charm with distance traveled for radiative energy loss only [215].

Very recently this expression have been compared with to results from Parton Cascade Model for the evolution of charm quarks propagating through a thermal brick of QCD matter [215] and shows a remarkable agreement Fig. 5.2.

In conclusion, we have estimated the differential radiative energy-loss of heavy quarks propagating in a quark gluon plasma. Equation (5.15) together with (5.16) represents radiative energy loss of an energetic quark in a canonical way within the framework of perturbative QCD along with kinematical restrictions for an energetic parton and medium interaction. This, along with the collisional energy-loss acts as a strong force on heavy quarks, which pulls them to a stop. How it affect the observables of heavy flavors in its hard sector will be addressed next.

5.3 D Mesons at RHIC and LHC

5.3.1 Heavy quark production in pp collisions

At leading order pQCD, heavy quarks in pp collisions are mainly produced by fusion of gluons ($gg \rightarrow Q\bar{Q}$) or light quarks ($q\bar{q} \rightarrow Q\bar{Q}$) [216]. The cross-section for the production of heavy quarks from pp collisions at leading order can be expressed as [216, 217]:

$$\frac{d\sigma}{dy_1 dy_2 dp_T} = 2x_1 x_2 p_T \sum_{ij} \left[f_i^{(1)}(x_1, Q^2) f_j^{(2)}(x_2, Q^2) \hat{\sigma}_{ij} + f_j^{(1)}(x_1, Q^2) f_i^{(2)}(x_2, Q^2) \hat{\sigma}_{ij} \right] / (1 + \delta_{ij}), \quad (5.17)$$

where i and j are the interacting partons, $f_i^{(1)}$ and $f_j^{(2)}$ are the partonic structure functions and x_1 and x_2 are the fractional momenta of the interacting hadrons carried by the partons i and j . The short range subprocesses for the heavy quark production, $\hat{\sigma} = d\sigma/dt$ are defined as:

$$\frac{d\sigma}{dt} = \frac{1}{16\pi s^2} |\mathcal{M}|^2, \quad (5.18)$$

where $|\mathcal{M}|^2$ for the processes $gg \rightarrow Q\bar{Q}$ and $q\bar{q} \rightarrow Q\bar{Q}$ can be obtained from Ref.[216]. The running coupling constant α_s at leading order is

$$\alpha_s = \frac{12\pi}{(33 - 2N_f) \ln(Q^2/\Lambda^2)}, \quad (5.19)$$

where $N_f = 3$ is the number of active flavours and $\Lambda = \Lambda_{\text{QCD}}$. The p_T distribution of production of heavy quarks at leading order supplemented with a K-factor ≈ 2.5 is taken as the baseline for the calculation of the nuclear suppression factor, R_{AA} [221]. Effect of prefactor K is diluted during computation of nuclear modification factor due to its identical effects on both initial and final distributions profiles. Furthermore, the K-factor, if equal for c and b quarks, has not only a diluted effect but can actually be neglected in the ratios. The shadowing effect is considered using EKS98 parameterization [218] for nucleon structure functions and here we use the CTEQ4M [219] set for nucleon structure function. We use Peterson fragmentation function [220] with parameter $\epsilon_c = 0.06$ and $\epsilon_b = 0.006$ for fragmentation of c quarks into D mesons and b quarks into B mesons, respectively.

All the calculations are done assuming the mean intrinsic transverse momentum of the partons to be zero.

5.3.2 Initial Conditions and Evolution of the Medium

As the heavy quarks are expected to lose most of their energy during the earliest time after the formation of QGP, we can safely neglect the transverse expansion of the plasma while discussing the heavy quark energy loss.

We consider a heavy quark, which is being produced at a point (r, Φ) in a central collision and moves at an angle ϕ with respect to \hat{r} in the transverse plane. If R be the radius of the colliding nuclei, the path length covered by the heavy quark would vary from 0 to $2R$, before it exits the QGP. The distance covered by the heavy quark inside the plasma in a central collision,

L , is given by [221]:

$$L(\phi, r) = \sqrt{R^2 - r^2 \sin^2 \phi} - r \cos \phi. \quad (5.20)$$

We can estimate the average distance travelled by the heavy quarks in the plasma as:

$$\langle L \rangle = \frac{\int_0^R r dr \int_0^{2\pi} L(\phi, r) T_{AA}(r, b=0) d\phi}{\int_0^R r dr \int_0^{2\pi} T_{AA}(r, b=0) d\phi}, \quad (5.21)$$

where $T_{AA}(r, b=0)$ is the nuclear overlap function. We estimate $\langle L \rangle$ as 5.78 fm for central Au+Au collisions and 6.14 fm for central Pb+Pb collisions.

The temperature of the plasma at a time τ , assuming a chemically equilibrated plasma can be expressed as [189]

$$T(\tau) = \left(\frac{\pi^2}{1.202} \frac{\rho(\tau)}{(9N_f + 16)} \right)^{\frac{1}{3}}, \quad (5.22)$$

where the gluon density at time τ is given by [189]:

$$\rho_g(\tau) = \frac{1}{\pi R^2 \tau} \frac{dN_g}{dy}. \quad (5.23)$$

Here we consider only the gluon density as the heavy quarks lose most of their energy in interaction with gluons. We also add that the gluon multiplicity is taken as 3/2 times the number of charged hadrons and the initial temperature is obtained using (5.22), assuming an initial time.

We take $(\frac{dN_q}{dy}) \approx 1125$ for Au+Au collisions at 200 AGeV, ≈ 2855 for Pb+Pb collisions at 2.76 ATeV and ≈ 4050 for Pb+Pb collisions at 5.5 ATeV. We assume that the heavy quark having rapidity in the central region moves along the fluid of identical rapidity. This kind of approximation has been used earlier in literature.

We calculate the initial temperature of QGP formation T_0 at 200 ATeV as 400 MeV, at 2.76 ATeV as 525 MeV and at 5.5 ATeV as 590 MeV, assuming the initial time of QGP formation as $\tau_0 = 0.2 \text{ fm}/c$. The critical temperature T_c for the existence of QGP is taken as $\approx 170 \text{ MeV}$. The time, by which the plasma will reach the critical temperature, τ_c is found to be $\approx 2.627 \text{ fm}/c$ at 200 AGeV, $5.9038 \text{ fm}/c$ at 2.76 ATeV and $8.375 \text{ fm}/c$ at 5.5 ATeV, assuming Bjorken's cooling law, $T^3 \tau = \text{constant}$.

The average path length of the heavy quark inside the plasma is calculated as follows. The velocity v_T of a heavy quark can be expressed as p_\perp/m_T , where m_T is the transverse mass. Thus, the heavy quark would cross the plasma in a time $\tau_L = \langle L \rangle / v_T$. Now, if $\tau_c \geq \tau_L$, the heavy quark would remain inside the QGP during the entire period, τ_0 to τ_L . But if $\tau_c < \tau_L$, it would remain inside QGP only while covering the distance $v_T \times \tau_c$. Thus, we further approximate the expanding and cooling plasma with one at a temperature of T at $\tau = \langle L \rangle_{\text{eff}} / 2$, where $\langle L \rangle_{\text{eff}} = \min [\langle L \rangle, v_T \times \tau_c]$ (see Ref. [189]).

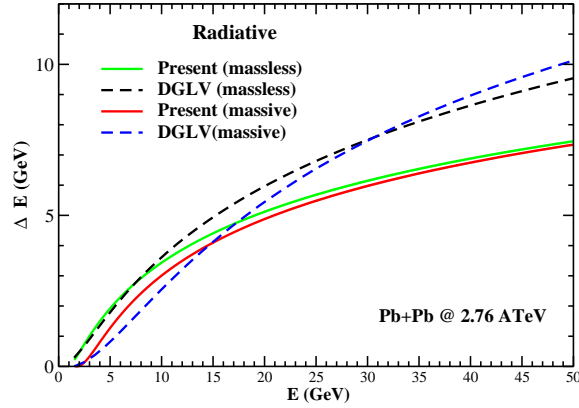


Figure 5.3: Comparison of average energy loss for light quark and charm quark with mass 1.5 GeV in a deconfined quark matter produced in Pb-Pb collision at 2.76 ATeV in the present and DGLV formalisms. For both cases the characteristics of the deconfined matter are treated in the same footing, *i.e.*, the strong coupling $\alpha_s = 0.3$ and the average path length, $\langle L \rangle \approx 6.14$ fm, traversed by an energetic quark in a deconfined medium produced in such collisions.

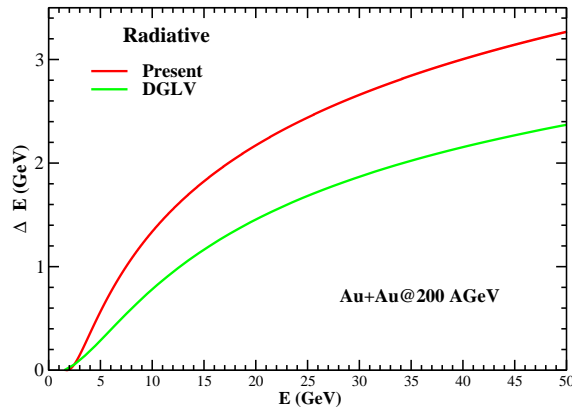


Figure 5.4: Same as Fig. 5.3 but only for charm quark in Au-Au collision at 200 AGeV with $\langle L \rangle = 5.78$ fm.

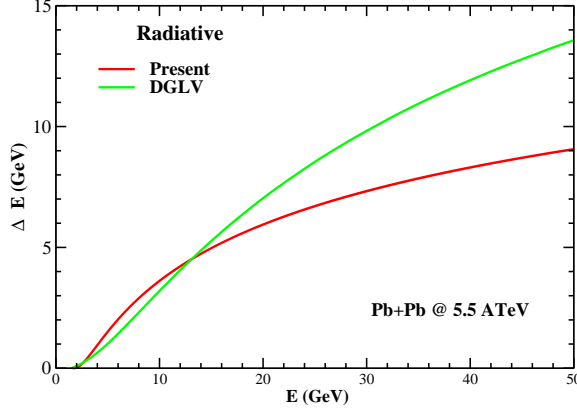


Figure 5.5: Same as Fig. 5.4 in Pb-Pb collision at 5.5 ATeV with $\langle L \rangle = 6.14$ fm.

5.4 Results and Discussion

In Fig. 5.3 a comparison of average radiative energy loss of an energetic quark traversing in a deconfined quark matter produced in Pb-Pb collision at 2.76A TeV in the present calculation with Djordjevic, Gyulassy, Levai and Vitev (DGLV) formalism. As can be seen both light and heavy quarks in the present formalism, within the gluon emission spectrum of $\mathcal{O}(\alpha_s)$ and $\mathcal{O}(1/k_\perp^2)$ as given in (5.1), lose energy in a similar fashion for $E \geq 10$ GeV since the effect of mass is small compared to the energy. However, it is slightly less than that of a light quark for $E \leq 10$ GeV, due to the dead cone suppression at small angles. In addition the results from the present calculation differ from that of DGLV one. These differences arise mainly because of the proper kinematic cuts for gluon emission as well as the method used to obtain energy loss. The various cuts in the present as well as in DGLV formalism are in

close proximity except the gluon emission in DGLV is constrained only to the forward emission angles, $\theta \leq \pi/2$, whereas in the present calculation the full range of θ is taken care off through the variable η as shown in (5.13) and (5.14).

In Figs.5.4, and 5.5 we have displayed average energy loss of a charm quark in a deconfined quark matter, respectively, at 200 AGeV Au-Au collision at RHIC and 5.5 ATeV Pb-Pb collision at LHC. We find that at RHIC energies the average energy loss of a charm quark in our formalism is higher than that of the DGLV formalism for the considered energy range, ($0 < E < 50$) GeV, of the charm quark. On the other hand Fig.5.5 is qualitatively similar to Fig.5.3 in terms of comparison of two formalism for heavy quark. As seen the average energy loss of charm quark is larger in the present formalism only in the domain, ($0 < E < 15$) GeV, of the charm quark and beyond which it is less compared to the DGLV formalism. The difference, in fact, increases as energy of the quark increases.

In Fig. 5.6 we display a comparison of collisional energy loss of charm quark as calculated by Peigne and Peshier (PP) in Ref. [125] for RHIC and LHC energies. As seen the collisional energy loss increases with the increase in centre of mass energy of the colliding ions.

In Fig. 5.7 the nuclear suppression factor, R_{AA} , for D meson is displayed considering both radiative and collisional energy loss and compared with the ALICE data at 2.76 ATeV. As can be seen the differences in radiative energy loss between the present and DGLV formalism discussed in Fig. 5.3 for 2.76 ATeV in Pb-Pb collisions is clearly reflected in Fig. 5.7. For the

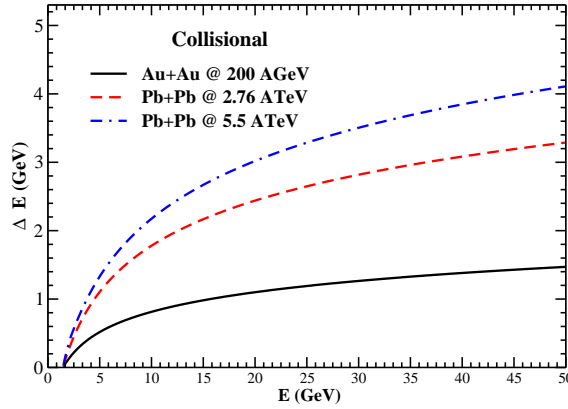


Figure 5.6: Collisional energy loss of charm quark in Pb-Pb collision at 2.76 ATeV and 5.5 ATeV at LHC, and 200 AGeV at RHIC energies.

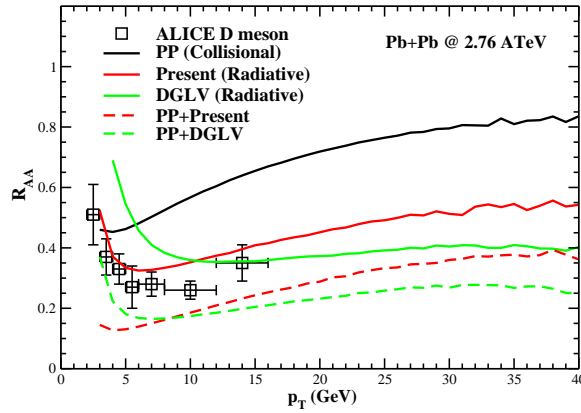


Figure 5.7: Nuclear modification factor R_{AA} for D mesons with both collisional and radiative energy loss in Pb-Pb collision at 2.76 ATeV. Only the systematic error bars are shown here.

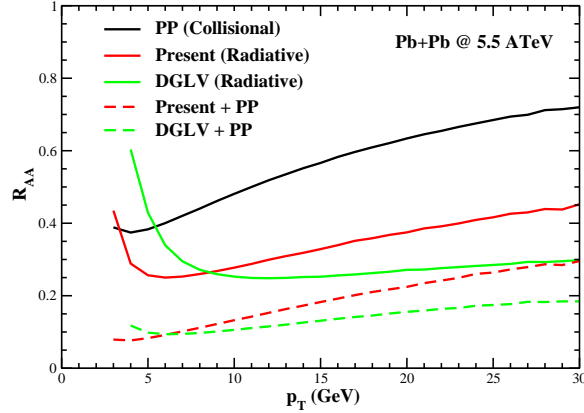


Figure 5.8: Nuclear modification factor, R_{AA} , for D mesons in Pb-Pb collision at 5.5 ATeV.

present calculation it is manifested in gradual increase of R_{AA} of D meson for transverse momentum, $p_{\perp} > 5$ GeV whereas in DGLV case it remains almost constant. The suppression factor obtained in the present formalism with radiative energy loss is in close agreement with the most recent data from ALICE collaboration at 2.76 ATeV. On the other hand the inclusion of the collision contribution is found to suppress R_{AA} further in both cases. As found the data suggest that the collisional contribution may be small. Nonetheless, more data in the high p_{\perp} domain is necessary to know the actual trend of the energy loss of charm quark and will finally constrain the various energy loss and jet quenching model in the literature. We also expect a similar rise in light hadrons for high p_{\perp} since both light and heavy quark lose energy in a similar fashion as shown in Fig. 5.3. However, we note that the ALICE data on R_{AA} for inclusive charge hadrons at 2.76 ATeV in Pb-Pb collision has also shown a similar increasing trend as p_{\perp} increases. It is

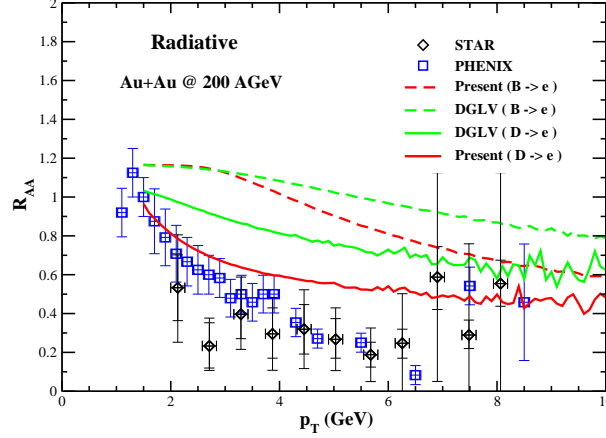


Figure 5.9: R_{AA} with only radiative energy loss for non-photonic single electron from the decay of individual D mesons and B mesons in Au-Au collision at 200 AGeV. Both systematic and statistical error bars are shown for STAR data whereas only systematic error bars are displayed for PHENIX data.

natural to believe that such data is completely dominated by the contribution from light hadrons. For completeness, we also display R_{AA} for LHC energy at 5.5 ATeV in Fig. 5.8.

In Fig. 5.9 the nuclear suppression factors for individual decay of D and B mesons to non-photonic single electron is displayed considering only the radiative energy loss for RHIC energy at 200 AGeV. As expected the contribution from the B decay is small compared to that of D decay. In Fig. 5.10 the total contribution of single electron from D and B decay is shown considering both radiative and collisional energy loss. It is found that the contributions of the collisional energy loss is important at RHIC energy. We also compare our results with that of DGLV. In Fig. 5.11, we give prediction for single electron result for LHC energy at 2.76 ATeV.

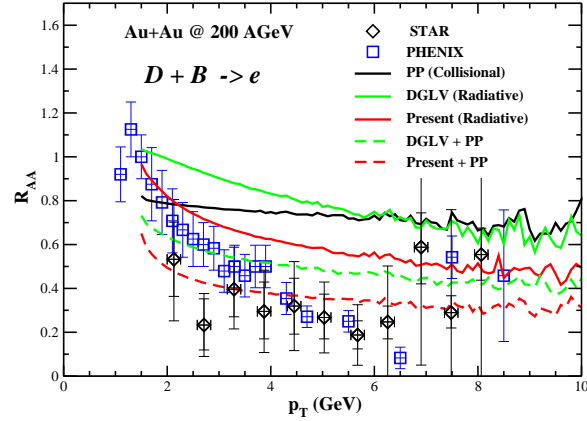


Figure 5.10: R_{AA} with collisional and radiative energy-loss for non-photonic single electron from the combined decay of both D and B mesons in Au-Au collision at 200 AGeV. Both systematic and statistical error bars are shown for STAR data whereas only systematic error bars are displayed for PHENIX data.

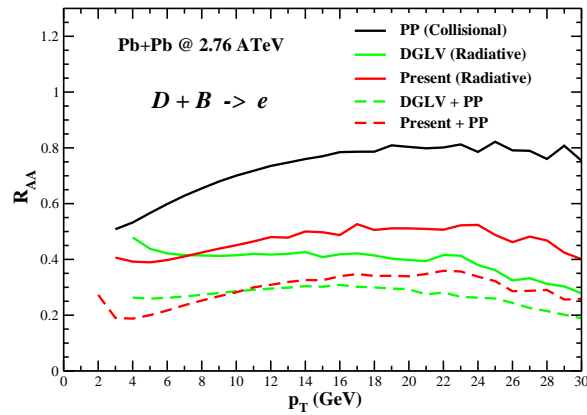


Figure 5.11: Same as Fig. 5.10 in Pb-Pb collision at 2.76 ATeV.

5.5 The endeavour

We obtain the radiative energy loss of a heavy quark akin to the Bethe-Heitler approximation by considering the most generalised gluon emission multiplicity expression derived very recently. This suggests that both energetic heavy and light quark lose energy due to gluon emission almost similarly and the mass plays a role only when the energy of the quark is of the order of it. The hierarchy used for simplifying the matrix element as well as for obtaining the gluon radiation spectrum imposes a restriction on the phase space of the emitted gluon in which the formation time is estimated to be less than the interaction time. This suggests that the LPM interference correction may be marginal. Further, we compare our results with the DGLV formalism and it is found to differ significantly. To compute the nuclear suppression factor for D -meson we consider both radiative and collision energy loss along with longitudinal expansion of the medium. The nuclear modification factor for D -meson with radiative energy loss obtained in the present formalism has an increasing trend at high p_{\perp} and found to agree closely with the very recent data from ALICE collaboration at 2.76 ATeV. When the collisional counter part is added independently, the further suppression is obtained in the nuclear modification factor. This suggest The non-photon single electron data at 200 AGeV RHIC energy requires contributions from collisional energy loss as well from B decay. However, it is necessary to obtain both radiative and collisional energy loss from the same formalism to minimize the various uncertainties, which is indeed a difficult task. Moreover, data at high p_{\perp} region with improved statistics are required to remove prejudice on different energy

loss and jet quenching models.

Chapter 6

Summary

Constituent *quark number scaling* of elliptic flow and *jet quenching* are supposed to be the most prominent signatures that favour the partonic degrees of freedom in the deconfined QCD matter. A jet is a narrow cone formed by assembly of hadrons and leptons, produced by fragmentation of highly energetic quarks and gluons, soon after impact of two hadrons/heavy-ions in ultra relativistic energies. However prior to hadronization *via* fragmentation, high momentum partons born in the initial stage of a heavy ion collisions (unlike hadron collisions), undergo series of interactions within the produced hot soup of deconfined matter. In these interactions, the energy of the high momentum partons is *reorganized* through collisional scatterings and *reduced* through medium induced gluon radiations, the latter being the dominant mechanism in this hot medium, the quark-gluon plasma. First evidence of parton energy loss has been observed at RHIC from the suppression of high

momentum particles by studying the nuclear modification factor and suppression of back-to-back correlations. This *jet tomography* is supposed to be the most prominent signatures that signify presence of the partonic degrees of freedom in the hot QCD matter.

In contemporary jet quenching models eikonal parton trajectory approximation constrains the leading parton of the jet to have energy E much larger than the transverse momentum of exchanged gluon q_{\perp} (with medium partons) as well as transverse momentum of the emitted gluon k_{\perp} *i.e.* $E \gg q_{\perp}, k_{\perp}$. The kinematic constraints $E \gg q_{\perp}, k_{\perp}$ referred in the literature as soft eikonal approximation neglects any change in parton trajectory due to multiple scatterings but assumes a straight line trajectory throughout. Hence it does not able to give sufficient transverse kick to deflect the parton from straight trajectory. In order to study *diffusion of jets* inside the hot matter it is crucial to overcome this approximation. In chapter 2, we have revisited the issue in Feynman gauge and make attempt to relax this approximation for the process $gg \rightarrow ggg$ [201]. We found that the correction terms are important at various physical domains of temperature, coupling constant and the energy of gluon-gluon scattering. This generalisation seems to be very apt for the phenomenology (*viz.* hot glue scenario, chemical equilibration of gluons, partonic matter viscosity, radiative energy-loss of energetic partons and jet quenching) of heavy-ion collisions and would improve the present understanding on various phenomena in this area. An attempt has been also been made to relax part of the eikonal approximation for the inelastic process $qq' \rightarrow qq'g$ in Chapter 3. For both $qq' \rightarrow qq'g$ and $gg \rightarrow ggg$ differential cross-sections

in first order noneikonal approximation have been obtained. Primary estimation indicates (15-20%) reduction in the cross section due to first order noneikonal effect for both the processes in the soft and intermediate parton energies [202]. These cross-sections naturally reproduce eikonally approximated results in the eikonal limit for soft emission, *i.e.*, $E \gg q_{\perp}, k_{\perp}$ and $q_{\perp} \gg k_{\perp}$. QGP produced at LHC where large virtuality scattering processes may be dominant one, seems to be less opaque to jets than predicted by constrained extrapolations from RHIC. There are however other views also, where another set of constrained extrapolations show considerable variation in the postdictions of RHIC-constrained scenarios with LHC data. Here this has been taken as a constraint and cause to disregard class of models which fail to predict/postdict correctly the uprising behaviour of nuclear modification factor rather than assigning it as a generic surprising feature of LHC data. Our results indicate some reductions in interaction strengths of jets due to non-eikonal effects, in soft and intermediate sector. In the soft sector when the problem is embedded into a hydrodynamically evolving density distribution this could lead to non-trivial effects. We also show that wide back scattering with scattering angle more than $\simeq 0.52\pi$ is forbidden in case of $qq' \rightarrow qq'g$ when the emitted gluon is soft. This, however, is not the case for $gg \rightarrow ggg$.

Small angle or collinear gluon emission approximation tells that energy ω of the emitted gluon is much larger than its transverse momentum k_{\perp} *i.e.* $\omega \gg k_{\perp}$. This connotes the fact that the angle between direction of propagation of leading parton and direction of emitted gluon is small, both

of them supposed to be collinear. In Chapter 4, We have recalled the process $qQ \rightarrow qQg$ in Feynman Gauge, where q and Q denote light and heavy quarks (*e.g.* charm) quark, respectively, instead of usually employed light-cone gauge in this context. We derived a compact expression that contains a generalized suppression factor for gluon emission off a heavy quark through the scattering with a light parton. This improved generalized suppression factor is derived within perturbative QCD and valid for the full range of rapidity of the radiated gluon *i.e.* free from *small angle/collinear* gluon emission approximation for soft gluon emissions [203]. In the appropriate limit this expression reduces to the usually known *dead cone factor*. Our analysis shows that even though there is a suppression of radiative soft gluon emission due to the mass of the heavy quark in the forward direction, it is almost tantamount in the backward regions. Consequently present findings indicate that a heavy quark emits a soft gluon almost similar to that of a light quark. This result seems to have important consequences for a better understanding of heavy flavor energy loss in heavy-ion collisions.

In Chapter 5, We obtained the radiative energy loss of a heavy quark akin to the Bethe-Heitler approximation by considering the most generalised gluon emission multiplicity expression derived [204]. It commends that both energetic heavy and light quark lose energy due to gluon emission almost similarly and the mass plays a role only when the energy of the quark is of the order of it. The hierarchy used for simplifying the matrix element as well as for obtaining the gluon radiation spectrum imposes a restriction on the phase space of the emitted gluon in which the formation time is estimated

to be less than the interaction time. This suggests that the LPM interference correction may be marginal. Further, we compare our results with the well know existing formalism and it is found to differ significantly. To compute the nuclear suppression factor for D-meson we consider both radiative and collision energy loss along with longitudinal expansion of the medium. The nuclear modification factor for D- meson with radiative energy loss obtained in the present formalism has an increasing trend at high transverse momentum and found to agree closely with the very recent data from ALICE collaboration at 2.76 ATeV [204].

The ALICE experiment in CERN have measured the *nuclear modification factor* R_{AA} of charmed mesons and heavy flavor mesons (in general) in semi-electronic channels at mid-rapidity regions. Measurements for R_{AA} have also been done for heavy flavored mesons in semi-muonic decay channels at forward rapidity regions. Fresh data from ALICE/LHC show features that appear to be in accordance with pQCD energy loss predictions : significant ascendancy of *nuclear modification factor* R_{AA} at LHC as a function of transverse momentum. This appears to be qualitatively different to the observed sluggish flatness at RHIC. Our results are in accordance with trends of R_{AA} both from RHIC as well as LHC. Since there is not a single adjustable parameters for us, the simultaneously good description of R_{AA} both at RHIC and at LHC in our model is rather encouraging. When the collisional counterpart is added independently, the further suppression is obtained in the nuclear modification factor. This suggest the non-photon single electron data at 200 AGeV RHIC energy might not requires contributions from collisional

energy loss as well from B decay. However, it is necessary to obtain both radiative and collisional energy loss from the same formalism to minimize the various uncertainties, which is indeed a difficult task. Moreover, data at high transverse momentum region with improved statistics are required to remove prejudice on different energy loss and jet quenching models.

The LHC data provide stringent tests of jet quenching theory complementary to those at RHIC, *via* the momentum dependence of heavy quark energy loss, which is predicted to be different in strongly and weakly coupled regimes of the QGP. The higher beam energy at LHC makes the rate of rare probes much higher than the RHIC. This opens a larger kinematic range for hadrons, photons and b quarks. Challenging theoretical advances, including higher-order jet calculations [201, 202, 203] and effective theories [222, 223, 224] that connect lattice simulations with transport processes, are needed to extract reliable values for the energy loss parameters and color screening length in the plasma from high precision data. Major numerical advances will be required to solve the transport equations describing rapid formation of an equilibration QGP. Such advances will not only elucidate the physics of QGP but also address intellectual challenges of strong coupling in many areas of physics.

Exploration of hot QCD matter has made enormous progress during the past decade. Experiments have discovered a new high-temperature phase, the strongly coupled QGP, which persists to the highest temperature probed. Surprising features of the QGP include near perfect fluidity and extreme opaqueness to all coloured probes. The rapid developments of theoretical

and experimental tools promises quantitative insights into the still mysterious properties of QGP during coming decade. These also have potential to enrich the study of other strongly coupled systems in nature and in the laboratory.

Appendix A

Collider Variables

Rapidity variables

In relativistic energy rapidity variable is defined as,

$$y = \frac{1}{2} \ln \frac{E + p_z}{E - p_z} \quad (\text{A.1})$$

$$= \frac{1}{2} \ln \frac{1 + p_z/E}{1 - p_z/E} = \tanh^{-1} \left(\frac{p_z}{E} \right) = \tanh^{-1}(\beta_L) \quad (\text{A.2})$$

Rapidity is more convenient to use than the longitudinal velocity ($\beta_L = p_z/E$). Rapidity has the advantage that they are additive under a longitudinal boost. A particle with rapidity y in a given inertial frame has rapidity $y + dy$ in a frame which moves relative to the first frame with rapidity dy in the $-z$ direction. One can see this from the addition formula of relativistic velocity β_1 and β_2 . The resultant velocity,

$$\beta = \frac{\beta_1 + \beta_2}{1 + \beta_1\beta_2} \quad (\text{A.3})$$

is also the addition formula for hyperbolic tangents,

$$\tanh(y_1 + y_2) = \frac{\tanh(y_1) + \tanh(y_2)}{1 + \tanh(y_1) \tanh(y_2)} \quad (\text{A.4})$$

In terms of rapidity variable, velocity and Lorentz factor can be written as,

$$\begin{aligned} \beta &= \tanh(y) \\ \gamma &= \cosh(y), \end{aligned}$$

and the transformation can be rewritten as,

$$\begin{pmatrix} t' \\ z' \end{pmatrix} = \begin{pmatrix} \cosh(y) & -\sinh(y) \\ -\sinh(y) & \cosh(y) \end{pmatrix} \begin{pmatrix} t \\ z \end{pmatrix} \quad (\text{A.5})$$

which is a hyperbolic rotation. Rapidity is the relativistic analog of non-relativistic velocity. In the non-relativistic limit, $p \ll m$ and Eq.A.1 can be written as,

$$\begin{aligned} y &= \frac{1}{2} \ln \frac{\sqrt{p^2 + m^2} + mv_z}{\sqrt{p^2 + m^2} - mv_z} = \frac{1}{2} \ln \frac{m + mv_z}{m - mv_z} \\ &= \frac{1}{2} [\ln(1 + v_z) - \ln(1 - v_z)] \approx v_z \end{aligned} \quad (\text{A.6})$$

In terms of the rapidity variables, particle 4-momenta can be parameterised as,

$$p^\mu = (E, p_x, p_y, p_z) = (m_T \cosh y, p_x, p_y, m_T \sinh y) \quad (\text{A.7})$$

with transverse mass (m_T),

$$m_T = \sqrt{m^2 + p_T^2} = \sqrt{m^2 + p_x^2 + p_y^2} \quad (\text{A.8})$$

Pseudo-rapidity Variable

For a particle emitted at an angle θ with respect to the beam axis, rapidity variable is,

$$\begin{aligned} y &= \frac{1}{2} \ln \frac{E + p_z}{E - p_z} \\ &= \frac{1}{2} \ln \frac{\sqrt{m^2 + p^2} + p \cos \theta}{\sqrt{m^2 + p^2} - p \cos \theta} \end{aligned} \quad (\text{A.9})$$

At very high energy, $p \gg m$, the mass can be neglected,

$$\begin{aligned} y &= \frac{1}{2} \ln \frac{p + p \cos \theta}{p - p \cos \theta} \\ &= -\ln \tan \theta/2 \equiv \eta \end{aligned} \quad (\text{A.10})$$

η is called pseudorapidity. Only angle θ determine the pseudorapidity. It is a convenient parameter for experimentalists when details of the particle, *e.g.* mass, momentum etc. are not known, but only the angle of emission is known (for example in emulsion experiments).

Light cone momentum:

For a particle with 4-momentum $p(p_0, p_\perp, p_z)$, forward and backward light cone variables are defined as,

$$p_+ = p_0 + p_z \quad (\text{A.11})$$

$$p_- = p_0 - p_z \quad (\text{A.12})$$

It is apparent that for a particle traveling along the beam axis, forward light cone momentum is higher than for a particle traveling opposite to the beam axis. An important property of the light cone is that in case of a boost, light cone momentum is multiplied by a constant factor. It can be seen when writing the momentum in terms of rapidity variable, $p^\mu = (m_T \cosh y, p_x, p_y, m_T \sinh y)$,

$$p_+ = m_T e^y \quad (\text{A.13})$$

$$p_- = m_T e^{-y} \quad (\text{A.14})$$

Invariant distribution:

Let us show d^3p/E is Lorentz invariant. The differential of Lorentz boost in longitudinal direction is,

$$\begin{aligned}
dp_z^* &= \gamma(dp_z - \beta dE) = \gamma\left(dp_z - \beta \frac{p_z dp_z}{E}\right), \\
&= \frac{dp_z}{E} \gamma(E - \beta p_z) = \frac{dp_z}{E} E^*
\end{aligned} \tag{A.15}$$

where we have used, $E^2 = m^2 + p_T^2 + p_z^2 \Rightarrow EdE = p_z dp_z$. Then dp_z/E is Lorentz invariant. Since p_T is Lorentz invariant, d^3p/E is also Lorentz invariant.

The Lorentz invariant differential yield is,

$$E \frac{d^3N}{d^3p} = E \frac{d^3N}{d^2p_T dp_z} = \frac{d^3N}{d^2p_T dy} \tag{A.16}$$

where the relation $dp_z/E = dy$ is used. Some times experimental results are given in terms of pseudorapidity. The transformation from (y, p_T) to (η, p_T) is the following,

$$\frac{dN}{d\eta dp_T} = \sqrt{1 - \frac{m^2}{m_T^2 \cosh^2 y}} \frac{dN}{dy dp_T} \tag{A.17}$$

Appendix B

Gluon Kinematics

We have observed that the four-vector dot product $k_1.k_5$ appeared in eq. C.1. Below, we list down all other such dot-products which eventually appear in other matrix amplitudes. With the choice of k_i in COM frame we get,

Computing $k_1.k_5$:

$$\begin{aligned}
k_1.k_5 &= E_1 k_\perp \text{cosec}\theta - k_{1z} k_\perp \cot\theta \\
&= \sqrt{k_{1z}^2 + m^2} k_\perp \text{cosec}\theta - k_{1z} k_\perp \cot\theta \\
&= k_{1z} k_\perp \left(\sqrt{1 + m^2/k_{1z}^2} \text{cosec}\theta - k_{1z} k_\perp \cot\theta \right) \\
&= \frac{s - m^2}{2\sqrt{s}} k_\perp \left(\sqrt{1 + \frac{4m^2/s}{(1 - m^2/s)^2}} \text{cosec}\theta - \cot\theta \right) \\
&\quad \left[\text{In COM frame, } k_{1z} = \frac{(s - m^2)}{2\sqrt{s}} \right] \\
&= \frac{s - m^2}{2\sqrt{s}} \omega \left(\sqrt{1 + \frac{4m^2/s}{(1 - m^2/s)^2}} - \cos\theta \right) \tag{B.1}
\end{aligned}$$

Computing $k_2.k_5$:

$$\begin{aligned}
 k_2.k_5 &= E_2 k_{\perp} \operatorname{cosec}\theta + k_{1z} k_{\perp} \cot\theta \\
 &= k_{1z} k_{\perp} \operatorname{cosec}\theta + k_{1z} k_{\perp} \cot\theta \\
 &= \frac{(s - m^2)}{2\sqrt{s}} k_{\perp} (\operatorname{cosec}\theta + \cot\theta) \\
 &= \frac{(s - m^2)}{2\sqrt{s}} \omega (1 + \cos\theta)
 \end{aligned} \tag{B.2}$$

In the eikonal limit, $k_1.k_5 \simeq k_3.k_5$ and $k_2.k_5 \simeq k_4.k_5$.

Appendix C

Matrix Elements

Below, we list the amplitudes corresponding to diagrams (1) – (5) (Fig.4.1).

$$\begin{aligned}
 -i\mathcal{M}_1 &= \bar{u}(k_3)(-ig\gamma^\mu t_{ij}^a) \frac{i(k_1^j - k_5^j + m)}{(k_1 - k_5)^2 - m^2} (-ig\gamma^\nu t_{jk}^b) u(k_1) \frac{-ig_{\mu\mu'}}{t} \bar{u}(k_4)(-ig\gamma^{\mu'} t_{ln}^a) u(k_2) \epsilon_\nu^* \\
 -i\mathcal{M}_2 &= \bar{u}(k_3)(-ig\gamma^\mu t_{ik}^a) u(k_1) \frac{-ig_{\mu\mu'}}{t} \bar{u}(k_4)(-ig\gamma^{\mu'} t_{lp}^a) \frac{i(k_2^p - k_5^p)}{(k_2 - k_5)^2} (-ig\gamma^\nu t_{pn}^b) u(k_2) \epsilon_\nu^* \\
 -i\mathcal{M}_3 &= \bar{u}(k_3)(-ig\gamma^\mu t_{ij}^b) \frac{i(k_3^j + k_5^j + m)}{(k_3 + k_5)^2 - m^2} (-ig\gamma^\mu t_{jk}^a) u(k_1) \frac{-ig_{\mu\mu'}}{t} \bar{u}(k_4)(-ig\gamma^{\mu'} t_{ln}^a) u(k_2) \epsilon_\nu^* \\
 -i\mathcal{M}_4 &= \bar{u}(k_3)(-ig\gamma^\mu t_{ik}^a) u(k_1) \frac{-ig_{\mu\mu'}}{t} \bar{u}(k_4)(-ig\gamma^\nu t_{lp}^b) \frac{i(k_4^p + k_5^p)}{(k_4 + k_5)^2} (-ig\gamma^{\mu'} t_{pn}^a) u(k_2) \epsilon_\nu^* \\
 -i\mathcal{M}_5 &= \bar{u}(k_3)(-ig\gamma^\rho t_{ik}^c) u(k_1) \frac{-ig_{\rho\rho'}}{t} g f_{cbd} \mathcal{V}^{\rho'\nu\lambda} \frac{-ig_{\lambda\lambda'}}{t} \bar{u}(k_4)(-ig\gamma^{\lambda'} t_{ln}^d) u(k_2) \epsilon_\nu^*
 \end{aligned}$$

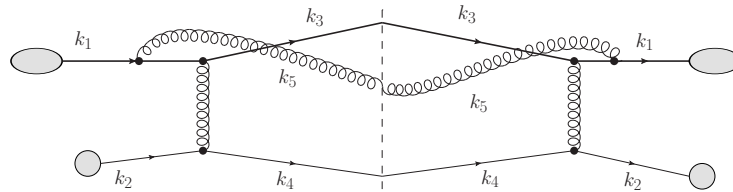
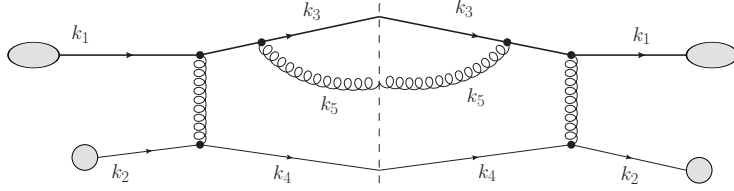
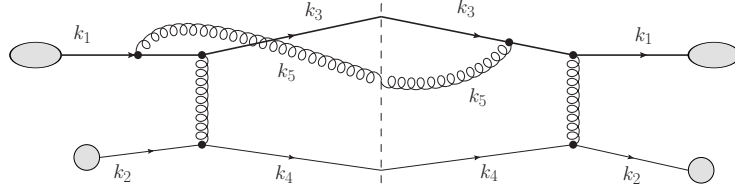


Figure C.1: $\mathcal{M}_1 \otimes \mathcal{M}_1^\dagger$

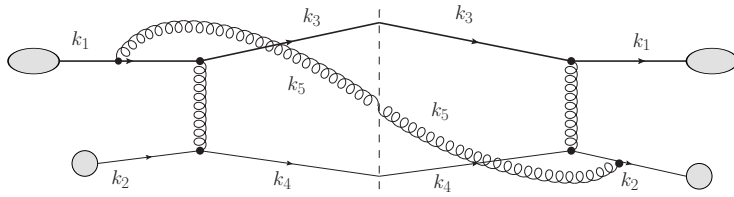
$$\begin{aligned}
\mathcal{M}_1 \otimes \mathcal{M}_1^\dagger &\approx -g^6 \frac{8}{3 \times 36} \frac{1}{t^2} \frac{1}{(2k_1 \cdot k_5)^2} (64M_Q^6 - 128M_Q^4 s + 64M_Q^2 s^2) \\
&= -g^6 \frac{8}{3 \times 36} \frac{s^2}{t^2} \frac{64M_Q^2}{(2k_1 \cdot k_5)^2} \left(1 - \frac{M_Q^2}{s}\right)^2 \\
&= \frac{128}{27} g^6 \frac{s^2}{t^2} \frac{1}{k_\perp^2} \left(\frac{-M_Q^2}{s \tan^2 \frac{\theta}{2}}\right) \left(\frac{1 - \frac{M_Q^2}{s}}{1 + \frac{M_Q^2}{s \tan^2 \frac{\theta}{2}}}\right)^2 \\
&= \frac{128}{27} g^6 \frac{s^2}{t^2} \frac{1}{k_\perp^2} \left(-1 - \frac{M_Q^2}{s \tan^2 \frac{\theta}{2}} + 1\right) \left(\frac{1 - \frac{M_Q^2}{s}}{1 + \frac{M_Q^2}{s \tan^2 \frac{\theta}{2}}}\right)^2 \\
&= \frac{128}{27} g^6 \frac{s^2}{t^2} \frac{1}{k_\perp^2} \left(\frac{M_Q^2}{s} - 1 + \frac{1 - \frac{M_Q^2}{s}}{1 + \frac{M_Q^2}{s \tan^2 \frac{\theta}{2}}}\right) \left(\frac{1 - \frac{M_Q^2}{s}}{1 + \frac{M_Q^2}{s \tan^2 \frac{\theta}{2}}}\right) \\
&= \frac{128}{27} g^6 \frac{s^2}{t^2} \frac{1}{k_\perp^2} (\Delta_M^2 - 1 + \mathcal{J}) \mathcal{J} \tag{C.1}
\end{aligned}$$

Figure C.2: $\mathcal{M}_3 \otimes \mathcal{M}_3^\dagger$

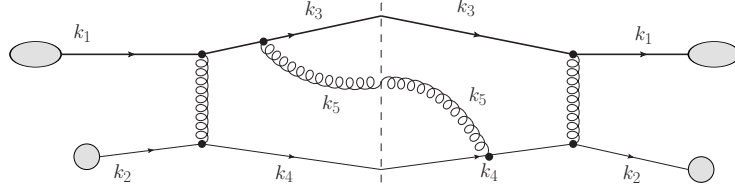
$$\begin{aligned}
\mathcal{M}_3 \otimes \mathcal{M}_3^\dagger &\approx -g^6 \frac{8}{3 \times 36} \frac{1}{t^2} \frac{1}{(2k_3 \cdot k_5)^2} (64M_Q^6 - 128M_Q^4 s + 64M_Q^2 s^2) \\
&= -g^6 \frac{8}{3 \times 36} \frac{s^2}{t^2} \frac{64M_Q^2}{(2k_3 \cdot k_5)^2} \left(1 - \frac{M_Q^2}{s}\right)^2 \\
&= \frac{128}{27} g^6 \frac{s^2}{t^2} \frac{1}{k_\perp^2} \left(\frac{-M_Q^2}{s \tan^2 \frac{\theta}{2}}\right) \left(\frac{1 - \frac{M_Q^2}{s}}{1 + \frac{M_Q^2}{s \tan^2 \frac{\theta}{2}}}\right)^2 \\
&= \frac{128}{27} g^6 \frac{s^2}{t^2} \frac{1}{k_\perp^2} \left(-1 - \frac{M_Q^2}{s \tan^2 \frac{\theta}{2}} + 1\right) \left(\frac{1 - \frac{M_Q^2}{s}}{1 + \frac{M_Q^2}{s \tan^2 \frac{\theta}{2}}}\right)^2 \\
&= \frac{128}{27} g^6 \frac{s^2}{t^2} \frac{1}{k_\perp^2} \left(\frac{M_Q^2}{s} - 1 + \frac{1 - \frac{M_Q^2}{s}}{1 + \frac{M_Q^2}{s \tan^2 \frac{\theta}{2}}}\right) \left(\frac{1 - \frac{M_Q^2}{s}}{1 + \frac{M_Q^2}{s \tan^2 \frac{\theta}{2}}}\right) \\
&= \frac{128}{27} g^6 \frac{s^2}{t^2} \frac{1}{k_\perp^2} (\Delta_M^2 - 1 + \mathcal{J}) \mathcal{J} \tag{C.2}
\end{aligned}$$

Figure C.3: $\mathcal{M}_1 \otimes \mathcal{M}_3^\dagger$

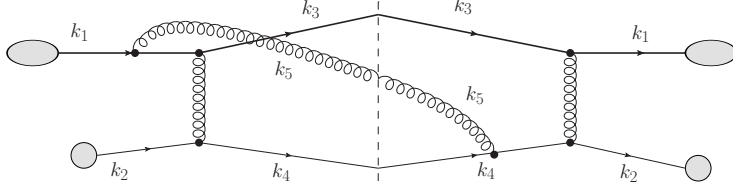
$$\begin{aligned}
\mathcal{M}_1 \otimes \mathcal{M}_3^\dagger &\approx -g^6 \frac{1}{3 \times 36} \frac{1}{t^2} \frac{(64M_Q^6 - 128M_Q^4 s + 64M_Q^2 s^2)}{(4k_1 \cdot k_5 k_3 \cdot k_5)} \\
&= -g^6 \frac{1}{3 \times 36} \frac{s^2}{t^2} \frac{64M_Q^2}{(4k_1 \cdot k_5 k_3 \cdot k_5)} \left(1 - \frac{M_Q^2}{s}\right)^2 \\
&= \frac{128}{27} g^6 \frac{s^2}{t^2} \frac{1}{k_\perp^2} \frac{1}{8} \left(\frac{-M_Q^2}{s \tan^2 \frac{\theta}{2}}\right) \left(\frac{1 - \frac{M_Q^2}{s}}{1 + \frac{M_Q^2}{s \tan^2 \frac{\theta}{2}}}\right)^2 \\
&= \frac{128}{27} g^6 \frac{s^2}{t^2} \frac{1}{k_\perp^2} \frac{1}{8} \left(-1 - \frac{M_Q^2}{s \tan^2 \frac{\theta}{2}} + 1\right) \left(\frac{1 - \frac{M_Q^2}{s}}{1 + \frac{M_Q^2}{s \tan^2 \frac{\theta}{2}}}\right)^2 \\
&= \frac{128}{27} g^6 \frac{s^2}{t^2} \frac{1}{k_\perp^2} \frac{1}{8} \left(\frac{M_Q^2}{s} - 1 + \frac{1 - \frac{M_Q^2}{s}}{1 + \frac{M_Q^2}{s \tan^2 \frac{\theta}{2}}}\right) \left(\frac{1 - \frac{M_Q^2}{s}}{1 + \frac{M_Q^2}{s \tan^2 \frac{\theta}{2}}}\right) \\
&= \frac{128}{27} g^6 \frac{s^2}{t^2} \frac{1}{k_\perp^2} \frac{1}{8} (\Delta_M^2 - 1 + \mathcal{J}) \mathcal{J} \tag{C.3}
\end{aligned}$$

Figure C.4: $\mathcal{M}_1 \otimes \mathcal{M}_2^\dagger$

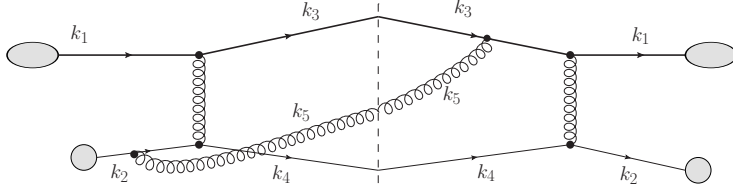
$$\begin{aligned}
\mathcal{M}_1 \otimes \mathcal{M}_2^\dagger &\approx g^6 \frac{2}{3 \times 36} \frac{1}{t^2} \frac{1}{(4k_1 \cdot k_5 k_2 \cdot k_5)} (32s^3 - 96M_Q^2 s^2 + 96M_Q^4 s - 32m^6) \\
&= g^6 \frac{2}{3 \times 36} \frac{s^2}{t^2} \frac{32s}{(4k_1 \cdot k_5 k_2 \cdot k_5)} \left(1 - \frac{M_Q^2}{s}\right)^3 \\
&= \frac{128}{27} g^6 \frac{s^2}{t^2} \frac{1}{k_\perp^2} \frac{1}{8} \left(1 - \frac{M_Q^2}{s}\right)^2 \left(1 + \frac{M_Q^2}{s \tan^2 \frac{\theta}{2}}\right)^{-1} \\
&= \frac{128}{27} g^6 \frac{s^2}{t^2} \frac{1}{k_\perp^2} \frac{1}{8} (1 - \Delta_M^2) \mathcal{J}
\end{aligned} \tag{C.4}$$

Figure C.5: $\mathcal{M}_3 \otimes \mathcal{M}_4^\dagger$

$$\begin{aligned}
\mathcal{M}_3 \otimes \mathcal{M}_4^\dagger &\approx g^6 \frac{2}{3 \times 36} \frac{1}{t^2} \frac{1}{(4k_3 \cdot k_5 k_4 \cdot k_5)} (32s^3 - 96M_Q^2 s^2 + 96M_Q^4 s) \\
&= g^6 \frac{2}{3 \times 36} \frac{s^2}{t^2} \frac{32s}{(4k_3 \cdot k_5 k_4 \cdot k_5)} \left(1 - \frac{M_Q^2}{s}\right)^3 \\
&= \frac{128}{27} g^6 \frac{s^2}{t^2} \frac{1}{k_\perp^2} \frac{1}{8} \left(1 - \frac{M_Q^2}{s}\right)^2 \left(1 + \frac{M_Q^2}{s \tan^2 \frac{\theta}{2}}\right)^{-1} \\
&= \frac{128}{27} g^6 \frac{s^2}{t^2} \frac{1}{k_\perp^2} \frac{1}{8} (1 - \Delta_M^2) \mathcal{J}
\end{aligned} \tag{C.5}$$

Figure C.6: $\mathcal{M}_1 \otimes \mathcal{M}_4^\dagger$

$$\begin{aligned}
 \mathcal{M}_1 \otimes \mathcal{M}_4^\dagger &\approx g^6 \frac{7}{3 \times 36} \frac{1}{t^2} \frac{1}{(4k_1 \cdot k_5 k_4 \cdot k_5)} (-32M_Q^6 + 96M_Q^4 s - 96M_Q^2 s^2 + 32s^3) \\
 &= g^6 \frac{7}{3 \times 36} \frac{s^2}{t^2} \frac{32s}{4k_1 \cdot k_5 k_4 \cdot k_5} \left(1 - \frac{M_Q^2}{s}\right)^3 \\
 &= \frac{128}{27} g^6 \frac{s^2}{t^2} \frac{1}{k_\perp^2} \frac{7}{16} \left(1 - \frac{M_Q^2}{s}\right)^2 \left(1 + \frac{M_Q^2}{s \tan^2 \frac{\theta}{2}}\right)^{-1} \\
 &= \frac{128}{27} g^6 \frac{s^2}{t^2} \frac{1}{k_\perp^2} \frac{7}{16} (1 - \Delta_M^2) \mathcal{J} \tag{C.6}
 \end{aligned}$$

Figure C.7: $\mathcal{M}_2 \otimes \mathcal{M}_3^\dagger$

$\mathcal{M}_2 \otimes \mathcal{M}_3^\dagger$

$$\begin{aligned}
\mathcal{M}_2 \otimes \mathcal{M}_3^\dagger &\approx g^6 \frac{7}{3 \times 36} \frac{1}{t^2} \frac{1}{(4k_2 \cdot k_5 k_3 \cdot k_5)} (-32M_Q^6 + 96M_Q^4 s - 96M_Q^2 s^2 + 32s^3) \\
&= g^6 \frac{7}{3 \times 36} \frac{s^2}{t^2} \frac{32s}{(4k_2 \cdot k_5 k_3 \cdot k_5)} \left(1 - \frac{M_Q^2}{s}\right)^3 \\
&= \frac{128}{27} g^6 \frac{s^2}{t^2} \frac{1}{k_\perp^2} \frac{7}{16} \left(1 - \frac{M_Q^2}{s}\right)^2 \left(1 + \frac{M_Q^2}{s \tan^2 \frac{\theta}{2}}\right)^{-1} \\
&= \frac{128}{27} g^6 \frac{s^2}{t^2} \frac{1}{k_\perp^2} \frac{7}{16} (1 - \Delta_M^2) \mathcal{J}
\end{aligned} \tag{C.7}$$

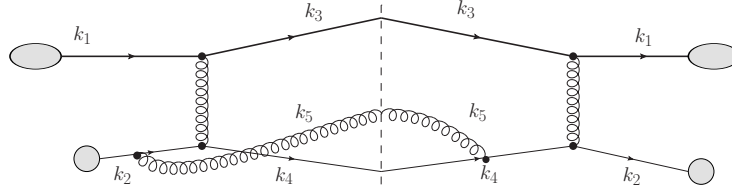


Figure C.8: $\mathcal{M}_2 \otimes \mathcal{M}_4^\dagger$

$$\begin{aligned}
\mathcal{M}_2 \otimes \mathcal{M}_4^\dagger &\approx g^6 \frac{1}{3 \times 36} \frac{1}{t^2} \frac{1}{4k_2 \cdot k_5 k_4 \cdot k_5} [0] \\
&= g^6 \frac{1}{3 \times 36} \frac{32s^2 t}{t^2} \frac{1}{4k_2 \cdot k_5 k_4 \cdot k_5} \left[\left(1 - \frac{M_Q^2}{s}\right)^2 + \frac{t^2}{2s^2} + \frac{t}{s} \right] \\
&= \frac{128}{27} g^6 \frac{s^2}{t^2} \frac{1}{k_\perp^2} \frac{1}{16} \tan^2 \frac{\theta}{2} \left[\frac{t}{s} \left(1 + \frac{\frac{t}{s} \left(1 + \frac{t}{2s}\right)}{\left(1 - \frac{M_Q^2}{s}\right)^2}\right) \right] \frac{1}{\mathcal{F}_{45}}
\end{aligned} \tag{C.8}$$

Unlike others, \mathcal{M}_{24} contains only $\mathcal{O}(t/s)$ (and higher orders) terms. That is reason why it was neglected in the earlier eikonal calculation.

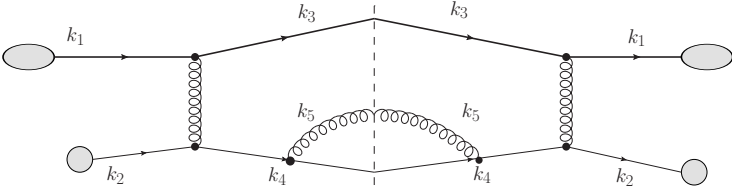


Figure C.9: $\mathcal{M}_4 \otimes \mathcal{M}_4^\dagger$

$\mathcal{M}_4 \otimes \mathcal{M}_4^\dagger$ \mathcal{M}_{44} can be completely neglected in the soft limit.

Appendix D

Color Factors

$$\begin{aligned}
\mathcal{C}_{11} &= t_{ij}^a t_{jk}^b t_{ln}^a \{t_{ij}^a t_{jk}^b t_{ln}^a\}^\dagger \\
&= (t^a t^b)_{ik} t_{ln}^a \{(t^a t^b)_{ik} t_{ln}^a\}^\dagger \\
&= \chi_k^\dagger t^a t^b \chi_i \underbrace{\chi_n^\dagger t^a \chi_l \chi_l^\dagger t^{a'}}_{\chi_n \chi_i^\dagger t^b t^{a'}} \chi_n \chi_i^\dagger t^b t^{a'} \chi_k \\
&= \text{Tr}(t^a t^{a'}) \text{Tr}(t^a t^b t^b t^{a'}) \\
&= \frac{4}{3} \mathcal{I} \text{Tr}(t^a t^{a'}) \text{Tr}(t^a t^{a'}) \quad \left[t^b t^b = \frac{4}{3} \mathcal{I} \text{ (}\mathcal{I} \text{: Identity matrix)} \right] \\
&= \frac{4}{3} \mathcal{I} \frac{1}{2} \delta^{aa'} \frac{1}{2} \delta^{aa'} \\
&= \frac{8}{3}
\end{aligned} \tag{D.1}$$

where χ_i, χ_j, χ_k are the quark color states denoted by three mutually orthogonal vectors: (1,0,0) or (0,1,0) or (0,0,1).

Other color factors can be found out in a similar way.

Appendix E

L^2 Dependence

Here we have investigated the WHDG and HT LPM factor to show how L^2 dependence popping up.

$$\begin{aligned}
\Delta_{\text{WHDG}} &= \int dz \left[1 - \cos \left(\frac{(\mathbf{k} - \mathbf{q})^2 + \beta^2}{2xE} z \right) \right] \rho(z) \\
&= \int dz \sin^2 \left(\frac{(\mathbf{k} - \mathbf{q})^2 + \beta^2}{4xE} z \right) \rho(z) \\
&= \int dz \left[1 - \cos \left(\frac{(\mathbf{k} - \mathbf{q})^2 + \beta^2}{2xE} z \right) \right] 2e^{-2z/L} \theta(z) / L \\
&= \int_0^\infty dz 2e^{2z/L} / L - \int_0^\infty dz \cos \left(\frac{(\mathbf{k} - \mathbf{q})^2 + \beta^2}{2xE} z \right) 2e^{-2z/L} / L \\
&= 1 - \frac{2}{L} \int_0^\infty dz e^{-2z/L} \cos \left(\frac{(\mathbf{k} - \mathbf{q})^2 + \beta^2}{2xE} z \right) \\
&= 1 - \frac{2}{L} \left[\frac{2/L}{4/L^2 + \left(\frac{(\mathbf{k} - \mathbf{q})^2 + \beta^2}{2xE} \right)^2} \right] \\
&= 1 - 4 \left[4 + \left(\frac{(\mathbf{k} - \mathbf{q})^2 + \beta^2}{2xE} \right)^2 L^2 \right]^{-1} \\
&= 1 - \left[1 + \frac{1}{4} \left(\frac{(\mathbf{k} - \mathbf{q})^2 + \beta^2}{2xE} \right)^2 L^2 \right]^{-1} \\
&\simeq \frac{1}{4} \left(\frac{(\mathbf{k} - \mathbf{q})^2 + \beta^2}{2xE} \right)^2 L^2 \tag{E.1}
\end{aligned}$$

Assumption :

1. $(\mathbf{k} - \mathbf{q})^2 + \beta^2 \ll 2xE/L$ where $\beta^2 = m_g^2 + x^2M_q^2$.

$$\frac{dN_g}{dxdk_{\perp}^2 dt} = \frac{2}{\pi} \alpha_s \frac{\hat{q}}{k_{\perp}^4} P(x) \left(\frac{k_{\perp}^2}{k_{\perp}^2 + x^2M^2} \right)^4 \sin^2 \left(\frac{t - t_i}{2\tau_f} \right), \quad (\text{E.2})$$

where,

$$\begin{aligned} \hat{q} &= \int dq_{\perp}^2 \frac{d\sigma}{dq_{\perp}^2} q_{\perp}^2 \\ \tau_f &= 2Ex(1-x)/(k_{\perp}^2 + x^2M^2) \\ x &= \omega/E \\ P(x) &\sim 1/x. \end{aligned} \quad (\text{E.3})$$

with k_{\perp} is the transverse momentum of the radiated gluon, and x is the ratio between the gluon energy and the heavy quark energy. In addition, α_s is the strong coupling constant, $P(x)$ is the splitting function of the gluon and \hat{q} is the gluon transport coefficient. The gluon formation time τ_f is defined as $\tau_f = 2Ex(1-x)/(k_{\perp}^2 + x^2M^2)$, with E and M being the energy and mass of heavy quarks, and τ_i being the initial time.

Assumption :

1. $k_{\perp}^2 \gg q_{\perp}^2$.

$$\begin{aligned}
\Delta_{\text{ASW-SH}} &= \int dz \left[1 - \cos \left(\frac{(\mathbf{k} - \mathbf{q})^2 + x^2 M_q^2}{2\omega} z \right) \right] \rho(z) \\
&= \int dz \left[1 - \cos \left(\frac{(\mathbf{k} - \mathbf{q})^2 + x^2 M_q^2}{2\omega} z \right) \right] \theta(z) \theta(L - z) / L \\
&= \int_0^L dz \left[1 - \cos \left(\frac{(\mathbf{k} - \mathbf{q})^2 + x^2 M_q^2}{2\omega} z \right) \right] / L \\
&= \frac{2}{L} \int_0^L dz \sin^2 \left(\frac{(\mathbf{k} - \mathbf{q})^2 + x^2 M_q^2}{4\omega} z \right) \\
&= 1 - \sin \left[\frac{(\mathbf{k} - \mathbf{q})^2 + x^2 M_q^2}{2\omega} L \right] / \left[\frac{(\mathbf{k} - \mathbf{q})^2 + x^2 M_q^2}{2\omega} L \right] \\
&\simeq \frac{1}{3!} \left(\frac{(\mathbf{k} - \mathbf{q})^2 + x^2 M_q^2}{2\omega} \right)^2 L^2 \tag{E.4}
\end{aligned}$$

Assumption :

1. $(\mathbf{k} - \mathbf{q})^2 + x^2 M_q^2 \ll 2\omega/L$.

Bibliography

- [1] M. Riordan and W. A. Zajc, “The first few microseconds,” *Sci. Am.* 294N5, 24 (2006) [Spektrum Wiss. 2006 N11, **36** (2006)].
- [2] D. N. Spergel *et al.* [WMAP Collaboration], “Wilkinson Microwave Anisotropy Probe (WMAP) three year results: implications for cosmology,” *Astrophys. J. Suppl.* **170**, 377 (2007) [astro-ph/0603449].
- [3] E. Komatsu *et al.* [WMAP Collaboration], “Five-Year Wilkinson Microwave Anisotropy Probe (WMAP) Observations: Cosmological Interpretation,” *Astrophys. J. Suppl.* **180**, 330 (2009) [arXiv:0803.0547 [astro-ph]].
- [4] D. Larson, J. Dunkley, G. Hinshaw, E. Komatsu, M. R. Nolta, C. L. Bennett, B. Gold and M. Halpern *et al.*, “Seven-Year Wilkinson Microwave Anisotropy Probe (WMAP) Observations: Power Spectra and WMAP-Derived Parameters,” *Astrophys. J. Suppl.* **192**, 16 (2011) [arXiv:1001.4635 [astro-ph.CO]].
- [5] G. Aad *et al.* [ATLAS Collaboration], “Observation of a new particle in the search for the Standard Model Higgs boson with the ATLAS

- detector at the LHC,” Phys. Lett. B **716**, 1 (2012) [arXiv:1207.7214 [hep-ex]].
- [6] S. Chatrchyan *et al.* [CMS Collaboration], “Observation of a new boson at a mass of 125 GeV with the CMS experiment at the LHC,” Phys. Lett. B **716**, 30 (2012) [arXiv:1207.7235 [hep-ex]].
- [7] T. Ludlam and L. McLerran, “What have we learned from the Relativistic Heavy Ion Collider?,” Phys. Today **56N10**, 48 (2003).
- [8] J. J. Thomson, “Cathode rays,” Phil. Mag. **44**, 293 (1897).
- [9] E. Rutherford, “The scattering of alpha and beta particles by matter and the structure of the atom,” Phil. Mag. **21**, 669 (1911).
- [10] E. Rutherford, “Physics at the British Association,” Nature **106**, 357 (1920).
- [11] J. Chadwick, “Possible Existence of a Neutron,” Nature **129**, 312 (1932).
- [12] H. Yukawa, “On the interaction of elementary particles,” Proc. Phys. Math. Soc. Jap. **17**, 48 (1935).
- [13] C. M. G. Lattes, H. Muirhead, G. P. S. Occhialini and C. F. Powell, “Processes Involving Charged Mesons,” Nature **159**, 694 (1947).
- [14] C. M. G. Lattes, G. P. S. Occhialini and C. F. Powell, “Observations on the Tracks of Slow Mesons in Photographic Emulsions. 1,” Nature **160**, 453 (1947).

-
- [15] G. D. Rochester and C. C. Butler, "Evidence for the Existence of New Unstable Elementary Particles," *Nature* **160**, 855 (1947).
- [16] M. Gell-Mann, "Isotopic Spin and New Unstable Particles," *Phys. Rev.* **92**, 833 (1953).
- [17] M. Gell-Mann, "The Interpretation of the New Particles as Displaced Charged Multiplets," *Nuovo Cimento* **4** Suppl. 2, 848 (1956).
- [18] T. Nakano and K. Nishijima, "Charge Independence for V particles," *Prog. Theor. Phys.* **10** **5**, 581 (1953).
- [19] M. Gell-Mann and Y. Ne'eman, "The Eightfold Way" Benjamin, 1964.
- [20] V. E. Barnes, P. L. Connolly, D. J. Crennell, B. B. Culwick, W. C. Delaney, W. B. Fowler, P. E. Hagerty and E. L. Hart *et al.*, "Observation of a Hyperon with Strangeness -3," *Phys. Rev. Lett.* **12**, 204 (1964).
- [21] M. Gell-Mann, "The story of quarks," *Int. J. Mod. Phys. A* **28**, 1330016 (2013).
- [22] J. D. Bjorken, "Asymptotic Sum Rules at Infinite Momentum," *Phys. Rev.* **179**, 1547 (1969).
- [23] C. G. Callan, Jr. and D. J. Gross, "High-energy electroproduction and the constitution of the electric current," *Phys. Rev. Lett.* **22**, 156 (1969).
- [24] E. D. Bloom, D. H. Coward, H. C. DeStaebler, J. Drees, G. Miller, L. W. Mo, R. E. Taylor and M. Breidenbach *et al.*, "High-Energy In-

- elastic e p Scattering at 6-Degrees and 10-Degrees,” Phys. Rev. Lett. **23**, 930 (1969).
- [25] M. Breidenbach, J. I. Friedman, H. W. Kendall, E. D. Bloom, D. H. Coward, H. C. DeStaebler, J. Drees and L. W. Mo *et al.*, “Observed Behavior of Highly Inelastic electron-Proton Scattering,” Phys. Rev. Lett. **23**, 935 (1969).
- [26] M. Y. Han and Y. Nambu, “Three Triplet Model with Double SU(3) Symmetry,” Phys. Rev. **139**, B1006 (1965).
- [27] R. P. Feynman, “Very high-energy collisions of hadrons,” Phys. Rev. Lett. **23**, 1415 (1969).
- [28] J. B. Kogut and L. Susskind, “The Parton picture of elementary particles,” Phys. Rept. **8**, 75 (1973).
- [29] J. D. Bjorken and E. A. Paschos, “Inelastic Electron Proton and gamma Proton Scattering, and the Structure of the Nucleon,” Phys. Rev. **185**, 1975 (1969).
- [30] J. Kuti and V. F. Weisskopf, “Inelastic lepton - nucleon scattering and lepton pair production in the relativistic quark parton model,” Phys. Rev. D **4**, 3418 (1971).
- [31] C. -N. Yang and R. L. Mills, “Conservation of Isotopic Spin and Isotopic Gauge Invariance,” Phys. Rev. **96**, 191 (1954).

-
- [32] L. D. Faddeev and V. N. Popov, “Feynman Diagrams for the Yang-Mills Field,” *Phys. Lett. B* **25**, 29 (1967).
- [33] G. ’t Hooft, “Renormalization of Massless Yang-Mills Fields,” *Nucl. Phys. B* **33**, 173 (1971).
- [34] D. J. Gross and F. Wilczek, “Ultraviolet Behavior of Nonabelian Gauge Theories,” *Phys. Rev. Lett.* **30**, 1343 (1973).
- [35] D. J. Gross and F. Wilczek, “Asymptotically Free Gauge Theories. 1,” *Phys. Rev. D* **8**, 3633 (1973).
- [36] D. J. Gross and F. Wilczek, “Asymptotically Free Gauge Theories. 2,” *Phys. Rev. D* **9**, 980 (1974).
- [37] H. D. Politzer, “Reliable Perturbative Results for Strong Interactions?,” *Phys. Rev. Lett.* **30**, 1346 (1973).
- [38] G. Hanson, G. S. Abrams, A. Boyarski, M. Breidenbach, F. Bulos, W. Chinowsky, G. J. Feldman and C. E. Friedberg *et al.*, “Evidence for Jet Structure in Hadron Production by $e^+ e^-$ Annihilation,” *Phys. Rev. Lett.* **35**, 1609 (1975).
- [39] R. Brandelik *et al.* [TASSO Collaboration], “Evidence for Planar Events in $e^+ e^-$ Annihilation at High-Energies,” *Phys. Lett. B* **86**, 243 (1979).
- [40] P. Abreu *et al.* [DELPHI Collaboration], “Experimental study of the triple gluon vertex,” *Phys. Lett. B* **255**, 466 (1991).

-
- [41] D. Decamp *et al.* [ALEPH Collaboration], “Evidence for the triple gluon vertex from measurements of the QCD color factors in Z decay into four jets,” *Phys. Lett. B* **284**, 151 (1992).
- [42] H. Georgi and H. D. Politzer, “Electroproduction scaling in an asymptotically free theory of strong interactions,” *Phys. Rev. D* **9**, 416 (1974).
- [43] Y. Watanabe, L. N. Hand, S. Herb, A. Russell, C. Chang, K. W. Chen, D. J. Fox and A. Kotlewski *et al.*, “Test of Scale Invariance in Ratios of Muon Scattering Cross-Sections at 150-GeV and 56-GeV,” *Phys. Rev. Lett.* **35**, 898 (1975).
- [44] C. Chang, K. W. Chen, D. J. Fox, A. Kotlewski, P. F. Kunz, L. N. Hand, S. Herb and A. Russell *et al.*, “Observed Deviations from Scale Invariance in High-Energy Muon Scattering,” *Phys. Rev. Lett.* **35**, 901 (1975).
- [45] P. Aurenche, M. Fontannaz, J. -P. Guillet, E. Pilon and M. Werlen, “A New critical study of photon production in hadronic collisions,” *Phys. Rev. D* **73**, 094007 (2006) [hep-ph/0602133].
- [46] S. Kluth, “Tests of Quantum Chromo Dynamics at e+ e- Colliders,” *Rept. Prog. Phys.* **69**, 1771 (2006) [hep-ex/0603011].
- [47] K. G. Wilson, “Confinement of Quarks,” *Phys. Rev. D* **10**, 2445 (1974).
- [48] W. J. Marciano and H. Pagels, “Quantum Chromodynamics: A Review,” *Phys. Rept.* **36**, 137 (1978).

-
- [49] S. R. Coleman and D. J. Gross, “Price of asymptotic freedom,” *Phys. Rev. Lett.* **31**, 851 (1973).
- [50] S. Weinberg, “Nonabelian Gauge Theories of the Strong Interactions,” *Phys. Rev. Lett.* **31**, 494 (1973).
- [51] F. Karsch, E. Laermann and A. Peikert, “Quark mass and flavor dependence of the QCD phase transition,” *Nucl. Phys. B* **605**, 579 (2001) [hep-lat/0012023].
- [52] O. Kaczmarek and F. Zantow, “Static quark anti-quark interactions in zero and finite temperature QCD. I. Heavy quark free energies, running coupling and quarkonium binding,” *Phys. Rev. D* **71**, 114510 (2005) [hep-lat/0503017].
- [53] T. D. Lee and G. C. Wick, “Vacuum Stability and Vacuum Excitation in a Spin 0 Field Theory,” *Phys. Rev. D* **9**, 2291 (1974).
- [54] R. Hagedorn, “Statistical thermodynamics of strong interactions at high-energies,” *Nuovo Cim. Suppl.* **3**, 147 (1965).
- [55] S. C. Frautschi, “Statistical bootstrap model of hadrons,” *Phys. Rev. D* **3**, 2821 (1971).
- [56] J. D. Walecka, “A Theory of highly condensed matter,” *Annals Phys.* **83**, 491 (1974).

-
- [57] S. A. Chin and J. D. Walecka, “An Equation of State for Nuclear and Higher-Density Matter Based on a Relativistic Mean-Field Theory,” *Phys. Lett. B* **52**, 24 (1974).
- [58] G. Baym and C. Pethick, “Neutron Stars,” *Ann. Rev. Nucl. Part. Sci.* **25**, 27 (1975).
- [59] N. Itoh, “Hydrostatic Equilibrium of Hypothetical Quark Stars,” *Prog. Theor. Phys.* **44**, 291 (1970).
- [60] J. C. Collins and M. J. Perry, “Superdense Matter: Neutrons Or Asymptotically Free Quarks?,” *Phys. Rev. Lett.* **34**, 1353 (1975).
- [61] E. V. Shuryak, “Quantum Chromodynamics and the Theory of Superdense Matter,” *Phys. Rept.* **61**, 71 (1980).
- [62] Y. Aoki, Z. Fodor, S. D. Katz and K. K. Szabo, “The QCD transition temperature: Results with physical masses in the continuum limit,” *Phys. Lett. B* **643**, 46 (2006) [hep-lat/0609068].
- [63] M. Cheng, N. H. Christ, S. Datta, J. van der Heide, C. Jung, F. Karsch, O. Kaczmarek and E. Laermann *et al.*, “The QCD equation of state with almost physical quark masses,” *Phys. Rev. D* **77**, 014511 (2008) [arXiv:0710.0354 [hep-lat]].
- [64] B. B. Back, M. D. Baker, M. Ballintijn, D. S. Barton, B. Becker, R. R. Betts, A. A. Bickley and R. Bindel *et al.*, “The PHOBOS perspective on discoveries at RHIC,” *Nucl. Phys. A* **757**, 28 (2005) [nucl-ex/0410022].

-
- [65] M. A. Lisa, S. Pratt, R. Soltz and U. Wiedemann, “Femtoscopy in relativistic heavy ion collisions,” *Ann. Rev. Nucl. Part. Sci.* **55**, 357 (2005) [nucl-ex/0505014].
- [66] P. F. Kolb and U. W. Heinz, “Hydrodynamic description of ultrarelativistic heavy ion collisions,” In *Hwa, R.C. (ed.) et al.: Quark gluon plasma* 634-714 [nucl-th/0305084].
- [67] P. Huovinen and P. V. Ruuskanen, “Hydrodynamic Models for Heavy Ion Collisions,” *Ann. Rev. Nucl. Part. Sci.* **56**, 163 (2006) [nucl-th/0605008].
- [68] T. Hirano, N. van der Kolk and A. Bilandzic, “Hydrodynamics and Flow,” *Lect. Notes Phys.* **785**, 139 (2010) [arXiv:0808.2684 [nucl-th]].
- [69] M. Gyulassy, “The QGP discovered at RHIC,” nucl-th/0403032.
- [70] M. Gyulassy and L. McLerran, “New forms of QCD matter discovered at RHIC,” *Nucl. Phys. A* **750**, 30 (2005) [nucl-th/0405013].
- [71] P. Huovinen, P. F. Kolb, U. W. Heinz, P. V. Ruuskanen and S. A. Voloshin, “Radial and elliptic flow at RHIC: Further predictions,” *Phys. Lett. B* **503**, 58 (2001) [hep-ph/0101136].
- [72] M. Jacob and S. Nussinov, “Pion production in high-energy proton anti-proton annihilation,” FERMILAB-PUB-72-067-T.
- [73] M. Jacob, R. Slansky and C. C. Wu, “Systematics of single particle spectra in proton proton collisions,” FERMILAB-PUB-72-062-T.

-
- [74] F. W. Busser, L. Camilleri, L. di Lella, G. Gladding, A. Placci, B. G. Pope, A. M. Smith and J. K. Yoh *et al.*, “Observation of π^0 mesons with large transverse momentum in high-energy proton proton collisions,” *Phys. Lett. B* **46**, 471 (1973).
- [75] B. Alper *et al.* [British-Scandinavian ISR Collaboration], “Production of high transverse momentum particles in p p collisions in the central region at the CERN ISR,” *Phys. Lett. B* **44**, 521 (1973).
- [76] M. Banner, J. L. Hamel, J. P. Pansart, A. V. Stirling, J. Teiger, H. Zacccone, J. Zsembery and G. Bassompierre *et al.*, “Large transverse momentum particle production at 90 degrees in proton-p proton collisions at the ISR,” *Phys. Lett. B* **44**, 537 (1973).
- [77] F. Aversa, P. Chiappetta, M. Greco and J. P. Guillet, “QCD Corrections to Parton-Parton Scattering Processes,” *Nucl. Phys. B* **327**, 105 (1989).
- [78] S. S. Adler *et al.* [PHENIX Collaboration], “Mid-rapidity neutral pion production in proton proton collisions at $\sqrt{s} = 200$ -GeV,” *Phys. Rev. Lett.* **91**, 241803 (2003) [hep-ex/0304038].
- [79] B. Jager, A. Schafer, M. Stratmann and W. Vogelsang, “Next-to-leading order QCD corrections to high p(T) pion production in longitudinally polarized pp collisions,” *Phys. Rev. D* **67**, 054005 (2003) [hep-ph/0211007].

-
- [80] D. de Florian, “Next-to-leading order QCD corrections to one hadron production in polarized pp collisions at RHIC,” *Phys. Rev. D* **67**, 054004 (2003) [hep-ph/0210442].
- [81] K. H. Ackermann *et al.* [STAR Collaboration], “Elliptic flow in Au + Au collisions at 130 GeV,” *Phys. Rev. Lett.* **86**, 402 (2001) [nucl-ex/0009011].
- [82] C. Adler *et al.* [STAR Collaboration], “Identified particle elliptic flow in Au + Au collisions at 130 GeV,” *Phys. Rev. Lett.* **87**, 182301 (2001) [nucl-ex/0107003].
- [83] C. Adler *et al.* [STAR Collaboration], “Azimuthal anisotropy and correlations in the hard scattering regime at RHIC,” *Phys. Rev. Lett.* **90**, 032301 (2003) [nucl-ex/0206006].
- [84] C. Adler *et al.* [STAR Collaboration], “Disappearance of back-to-back high p_T hadron correlations in central Au+Au collisions at 200 GeV,” *Phys. Rev. Lett.* **90**, 082302 (2003) [nucl-ex/0210033].
- [85] J. Adams *et al.* [STAR Collaboration], “Transverse momentum and collision energy dependence of high $p(T)$ hadron suppression in Au+Au collisions at ultrarelativistic energies,” *Phys. Rev. Lett.* **91**, 172302 (2003) [nucl-ex/0305015].
- [86] J. Adams *et al.* [STAR Collaboration], “Azimuthally sensitive HBT in Au + Au collisions at $\sqrt{s} = 200$ GeV,” *Phys. Rev. Lett.* **93**, 012301 (2004) [nucl-ex/0312009].

-
- [87] J. Adams *et al.* [STAR Collaboration], “Azimuthal anisotropy in Au+Au collisions at 200 GeV,” *Phys. Rev. C* **72**, 014904 (2005) [nucl-ex/0409033].
- [88] J. Adams *et al.* [STAR Collaboration], “Experimental and theoretical challenges in the search for the quark gluon plasma: The STAR Collaboration’s critical assessment of the evidence from RHIC collisions,” *Nucl. Phys. A* **757**, 102 (2005) [nucl-ex/0501009].
- [89] J. Bielcik [STAR Collaboration], “Centrality dependence of heavy flavor production from single electron measurement in $s(\text{NN})^{1/2} = 200\text{-GeV}$ Au + Au collisions,” *Nucl. Phys. A* **774**, 697 (2006) [nucl-ex/0511005].
- [90] B. I. Abelev *et al.* [STAR Collaboration], “Identified baryon and meson distributions at large transverse momenta from Au+Au collisions at 200 GeV,” *Phys. Rev. Lett.* **97**, 152301 (2006) [nucl-ex/0606003].
- [91] B. I. Abelev *et al.* [STAR Collaboration], “Erratum: Transverse momentum and centrality dependence of high-pt non-photonic electron suppression in Au+Au collisions at 200 GeV,” *Phys. Rev. Lett.* **98**, 192301 (2007) [Erratum-*ibid.* **106**, 159902 (2011)] [nucl-ex/0607012].
- [92] J. Adams *et al.* [STAR Collaboration], “Direct observation of dijets in central Au+Au collisions at 200-GeV,” *Phys. Rev. Lett.* **97**, 162301 (2006) [nucl-ex/0604018].

-
- [93] K. Adcox *et al.* [PHENIX Collaboration], “Centrality dependence of charged particle multiplicity in Au - Au collisions at $\sqrt{s(NN)}^{**}(1/2) = 130\text{-GeV}$,” *Phys. Rev. Lett.* **86**, 3500 (2001) [nucl-ex/0012008].
- [94] S. S. Adler *et al.* [PHENIX Collaboration], “Elliptic flow of identified hadrons in Au+Au collisions at $\sqrt{s(NN)}^{**}(1/2) = 200\text{-GeV}$,” *Phys. Rev. Lett.* **91**, 182301 (2003) [nucl-ex/0305013].
- [95] S. S. Adler *et al.* [PHENIX Collaboration], “High p_T charged hadron suppression in Au + Au collisions at $\sqrt{s_{NN}} = 200\text{ GeV}$,” *Phys. Rev. C* **69**, 034910 (2004) [nucl-ex/0308006].
- [96] S. S. Adler *et al.* [PHENIX Collaboration], “Bose-Einstein correlations of charged pion pairs in Au + Au collisions at $\sqrt{s(NN)}^{**}(1/2) = 200\text{-GeV}$,” *Phys. Rev. Lett.* **93**, 152302 (2004) [nucl-ex/0401003].
- [97] K. Adcox *et al.* [PHENIX Collaboration], “Formation of dense partonic matter in relativistic nucleus-nucleus collisions at RHIC: Experimental evaluation by the PHENIX collaboration,” *Nucl. Phys. A* **757**, 184 (2005) [nucl-ex/0410003].
- [98] S. S. Adler *et al.* [PHENIX Collaboration], “Centrality dependence of direct photon production in $\sqrt{s(NN)}^{**}(1/2) = 200\text{-GeV}$ Au + Au collisions,” *Phys. Rev. Lett.* **94**, 232301 (2005) [nucl-ex/0503003].
- [99] S. S. Adler *et al.* [PHENIX Collaboration], “Dense-Medium Modifications to Jet-Induced Hadron Pair Distributions in Au+Au Collisions at 200 GeV,” *Phys. Rev. Lett.* **97**, 052301 (2006) [nucl-ex/0507004].

-
- [100] S. S. Adler *et al.* [PHENIX Collaboration], “Nuclear modification of electron spectra and implications for heavy quark energy loss in Au+Au collisions at $\sqrt{s(NN)}^{1/2} = 200$ -GeV,” *Phys. Rev. Lett.* **96**, 032301 (2006) [nucl-ex/0510047].
- [101] S. S. Adler *et al.* [PHENIX Collaboration], “Common suppression pattern of eta and pi0 mesons at high transverse momentum in Au+Au collisions at 200 GeV,” *Phys. Rev. Lett.* **96**, 202301 (2006) [nucl-ex/0601037].
- [102] A. Adare *et al.* [PHENIX Collaboration], “Scaling properties of azimuthal anisotropy in Au+Au and Cu+Cu collisions at 200 GeV,” *Phys. Rev. Lett.* **98**, 162301 (2007) [nucl-ex/0608033].
- [103] A. Adare *et al.* [PHENIX Collaboration], “Energy Loss and Flow of Heavy Quarks in Au+Au Collisions at 200 GeV,” *Phys. Rev. Lett.* **98**, 172301 (2007) [nucl-ex/0611018].
- [104] A. Adare *et al.* [PHENIX Collaboration], “System Size and Energy Dependence of Jet-Induced Hadron Pair Correlation Shapes in Cu+Cu and Au+Au Collisions at 200 and 62.4 GeV,” *Phys. Rev. Lett.* **98**, 232302 (2007) [nucl-ex/0611019].
- [105] A. Adare *et al.* [PHENIX Collaboration], “Quantitative Constraints on the Opacity of Hot Partonic Matter from Semi-Inclusive Single High Transverse Momentum Pion Suppression in Au+Au collisions at $\sqrt{s} = 200$ GeV,” *Phys. Rev. C* **77**, 064907 (2008) [arXiv:0801.1665 [nucl-ex]].

-
- [106] B. B. Back *et al.* [PHOBOS Collaboration], “Energy dependence of particle multiplicities in central Au+Au collisions,” *Phys. Rev. Lett.* **88**, 022302 (2002) [nucl-ex/0108009].
- [107] I. Arsene *et al.* [BRAHMS Collaboration], “Quark gluon plasma and color glass condensate at RHIC? The Perspective from the BRAHMS experiment,” *Nucl. Phys. A* **757**, 1 (2005) [nucl-ex/0410020].
- [108] KAamodt *et al.* [ALICE Collaboration], “Elliptic flow of charged particles in Pb-Pb collisions at 2.76 TeV,” *Phys. Rev. Lett.* **105**, 252302 (2010) [arXiv:1011.3914 [nucl-ex]].
- [109] KAamodt *et al.* [ALICE Collaboration], “Charged-particle multiplicity density at mid-rapidity in central Pb-Pb collisions at $\sqrt{s_{NN}} = 2.76$ TeV,” *Phys. Rev. Lett.* **105**, 252301 (2010) [arXiv:1011.3916 [nucl-ex]].
- [110] K. Aamodt *et al.* [ALICE Collaboration], “Suppression of Charged Particle Production at Large Transverse Momentum in Central Pb-Pb Collisions at $\sqrt{s_{NN}} = 2.76$ TeV,” *Phys. Lett. B* **696**, 30 (2011) [arXiv:1012.1004 [nucl-ex]].
- [111] K. Aamodt *et al.* [ALICE Collaboration], “Centrality dependence of the charged-particle multiplicity density at mid-rapidity in Pb-Pb collisions at $\sqrt{s_{NN}} = 2.76$ TeV,” *Phys. Rev. Lett.* **106**, 032301 (2011) [arXiv:1012.1657 [nucl-ex]].
- [112] K. Aamodt *et al.* [ALICE Collaboration], “Higher harmonic anisotropic flow measurements of charged particles in Pb-Pb colli-

- sions at $\sqrt{s_{NN}}=2.76$ TeV,” Phys. Rev. Lett. **107**, 032301 (2011) [arXiv:1105.3865 [nucl-ex]].
- [113] J. D. Bjorken, “Energy Loss of Energetic Partons in Quark - Gluon Plasma: Possible Extinction of High $p(t)$ Jets in Hadron - Hadron Collisions,” FERMILAB-PUB-82-059-THY.
- [114] M. H. Thoma and M. Gyulassy, “Quark Damping and Energy Loss in the High Temperature QCD,” Nucl. Phys. B **351**, 491 (1991).
- [115] E. Braaten and R. D. Pisarski, “Resummation and Gauge Invariance of the Gluon Damping Rate in Hot QCD,” Phys. Rev. Lett. **64**, 1338 (1990).
- [116] E. Braaten and R. D. Pisarski, “Soft Amplitudes in Hot Gauge Theories: A General Analysis,” Nucl. Phys. B **337**, 569 (1990).
- [117] E. Braaten and R. D. Pisarski, “Deducing Hard Thermal Loops From Ward Identities,” Nucl. Phys. B **339**, 310 (1990).
- [118] E. Braaten and M. H. Thoma, “Energy loss of a heavy fermion in a hot plasma,” Phys. Rev. D **44**, 1298 (1991).
- [119] E. Braaten and M. H. Thoma, “Energy loss of a heavy quark in the quark - gluon plasma,” Phys. Rev. D **44**, 2625 (1991).
- [120] B. Svetitsky, “Diffusion of charmed quarks in the quark-gluon plasma,” Phys. Rev. D **37** (1988) 2484.

-
- [121] P. Romatschke and M. Strickland, “Collisional energy loss of a heavy quark in an anisotropic quark-gluon plasma,” *Phys. Rev. D* **71**, 125008 (2005) [hep-ph/0408275].
- [122] M. Gyulassy and M. Plumer, “Jet quenching as a probe of dense matter,” *Nucl. Phys. A* **527**, 641 (1991).
- [123] X. -N. Wang, M. Gyulassy and M. Plumer, “The LPM effect in QCD and radiative energy loss in a quark gluon plasma,” *Phys. Rev. D* **51**, 3436 (1995) [hep-ph/9408344].
- [124] M. G. Mustafa, “Energy loss of charm quarks in the quark-gluon plasma: Collisional versus radiative,” *Phys. Rev. C* **72**, 014905 (2005) [hep-ph/0412402].
- [125] A. Peshier, “The QCD collisional energy loss revised,” *Phys. Rev. Lett.* **97**, 212301 (2006) [hep-ph/0605294].
- [126] J. Braun and H. -J. Pirner, “Effects of the running of the QCD coupling on the energy loss in the quark-gluon plasma,” *Phys. Rev. D* **75**, 054031 (2007) [hep-ph/0610331].
- [127] S. Wicks, “Fluctuations with small numbers: Developing the perturbative paradigm for jet physics in the QGP at RHIC and LHC,” AAT-3333486, Ph.D. thesis, Columbia University (2008).
- [128] S. Peigne, P. -B. Gossiaux and T. Gousset, “Retardation effect for collisional energy loss of hard partons produced in a QGP,” *JHEP* **0604**, 011 (2006) [hep-ph/0509185].

-
- [129] A. Adil, M. Gyulassy, W. A. Horowitz and S. Wicks, “Collisional Energy Loss of Non Asymptotic Jets in a QGP,” *Phys. Rev. C* **75**, 044906 (2007) [nucl-th/0606010].
- [130] P. B. Gossiaux, J. Aichelin, C. Brandt, T. Gousset and S. Peigne, “Energy loss of a heavy quark produced in a finite-size quark-gluon plasma,” *J. Phys. G* **34**, S817 (2007) [hep-ph/0703095].
- [131] M. Djordjevic, “Collisional energy loss in a finite size QCD matter,” *Phys. Rev. C* **74**, 064907 (2006) [nucl-th/0603066].
- [132] A. Ayala, J. Magnin, L. M. Montano and E. Rojas, “Collisional parton energy loss in a finite size QCD medium revisited: Off mass-shell effects,” *Phys. Rev. C* **77**, 044904 (2008) [arXiv:0706.2377 [hep-ph]].
- [133] G. D. Moore and D. Teaney, “How much do heavy quarks thermalize in a heavy ion collision?,” *Phys. Rev. C* **71**, 064904 (2005) [hep-ph/0412346].
- [134] H. van Hees, V. Greco and R. Rapp, “Heavy-quark probes of the quark-gluon plasma at RHIC,” *Phys. Rev. C* **73**, 034913 (2006) [nucl-th/0508055].
- [135] F. A. Berends, R. Kleiss, P. De Causmaecker, R. Gastmans and T. T. Wu, “Single Bremsstrahlung Processes in Gauge Theories,” *Phys. Lett. B* **103**, 124 (1981).
- [136] J. F. Gunion and G. Bertsch, “Hadronization By Color Bremsstrahlung,” *Phys. Rev. D* **25**, 746 (1982).

-
- [137] L. D. Landau and I. Pomeranchuk, “Limits of applicability of the theory of bremsstrahlung electrons and pair production at high-energies,” Dokl. Akad. Nauk Ser. Fiz. **92**, 535 (1953).
- [138] A. B. Migdal, “Bremsstrahlung and pair production in condensed media at high-energies,” Phys. Rev. **103**, 1811 (1956).
- [139] S. J. Brodsky and P. Hoyer, “A Bound on the energy loss of partons in nuclei,” Phys. Lett. B **298**, 165 (1993) [hep-ph/9210262].
- [140] M. Gyulassy and X. -n. Wang, “Multiple collisions and induced gluon Bremsstrahlung in QCD,” Nucl. Phys. B **420**, 583 (1994) [nucl-th/9306003].
- [141] R. Baier, Y. L. Dokshitzer, A. H. Mueller, S. Peigne and D. Schiff, “The Landau-Pomeranchuk-Migdal effect in QED,” Nucl. Phys. B **478**, 577 (1996) [hep-ph/9604327].
- [142] R. Baier, Y. L. Dokshitzer, A. H. Mueller, S. Peigne and D. Schiff, “Radiative energy loss of high-energy quarks and gluons in a finite volume quark - gluon plasma,” Nucl. Phys. B **483**, 291 (1997) [hep-ph/9607355].
- [143] R. Baier, Y. L. Dokshitzer, A. H. Mueller, S. Peigne and D. Schiff, “Radiative energy loss and $p(T)$ broadening of high-energy partons in nuclei,” Nucl. Phys. B **484**, 265 (1997) [hep-ph/9608322].

-
- [144] R. Baier, Y. L. Dokshitzer, A. H. Mueller and D. Schiff, “Radiative energy loss of high-energy partons traversing an expanding QCD plasma,” *Phys. Rev. C* **58**, 1706 (1998) [hep-ph/9803473].
- [145] H. A. Bethe, “Moliere’s theory of multiple scattering,” *Phys. Rev.* **89**, 1256 (1953).
- [146] R. Baier, Y. L. Dokshitzer, A. H. Mueller and D. Schiff, “Angular dependence of the radiative gluon spectrum and the energy loss of hard jets in QCD media,” *Phys. Rev. C* **60**, 064902 (1999) [hep-ph/9907267].
- [147] R. Baier, Y. L. Dokshitzer, A. H. Mueller and D. Schiff, “On the angular dependence of the radiative gluon spectrum,” *Phys. Rev. C* **64**, 057902 (2001) [hep-ph/0105062].
- [148] R. Baier, Y. L. Dokshitzer, A. H. Mueller and D. Schiff, “Quenching of hadron spectra in media,” *JHEP* **0109**, 033 (2001) [hep-ph/0106347].
- [149] B. G. Zakharov, “Fully quantum treatment of the Landau-Pomeranchuk-Migdal effect in QED and QCD,” *JETP Lett.* **63**, 952 (1996) [hep-ph/9607440].
- [150] B. G. Zakharov, “Landau-Pomeranchuk-Migdal effect for finite size targets,” *Pisma Zh. Eksp. Teor. Fiz.* **64**, 737 (1996) [*JETP Lett.* **64**, 781 (1996)] [hep-ph/9612431].
- [151] B. G. Zakharov, “Radiative energy loss of high-energy quarks in finite size nuclear matter and quark - gluon plasma,” *JETP Lett.* **65**, 615 (1997) [hep-ph/9704255].

-
- [152] B. G. Zakharov, “Coherent final state interaction in jet production in nucleus-nucleus collisions,” *JETP Lett.* **76**, 201 (2002) [*Pisma Zh. Eksp. Teor. Fiz.* **76**, 236 (2002)] [hep-ph/0207206].
- [153] R. Baier, Y. L. Dokshitzer, A. H. Mueller and D. Schiff, “Medium induced radiative energy loss: Equivalence between the BDMPS and Zakharov formalisms,” *Nucl. Phys. B* **531**, 403 (1998) [hep-ph/9804212].
- [154] R. Baier, D. Schiff and B. G. Zakharov, “Energy loss in perturbative QCD,” *Ann. Rev. Nucl. Part. Sci.* **50**, 37 (2000) [hep-ph/0002198].
- [155] M. Gyulassy, P. Levai and I. Vitev, “Jet quenching in thin plasmas,” *Nucl. Phys. A* **661**, 637 (1999) [hep-ph/9907343].
- [156] M. Gyulassy, P. Levai and I. Vitev, “Jet quenching in thin quark gluon plasmas. 1. Formalism,” *Nucl. Phys. B* **571**, 197 (2000) [hep-ph/9907461].
- [157] M. Gyulassy, P. Levai and I. Vitev, “NonAbelian energy loss at finite opacity,” *Phys. Rev. Lett.* **85**, 5535 (2000) [nucl-th/0005032].
- [158] M. Gyulassy, P. Levai and I. Vitev, “Reaction operator approach to nonAbelian energy loss,” *Nucl. Phys. B* **594**, 371 (2001) [nucl-th/0006010].
- [159] M. Gyulassy, P. Levai and I. Vitev, “Jet tomography of Au+Au reactions including multigluon fluctuations,” *Phys. Lett. B* **538**, 282 (2002) [nucl-th/0112071].

-
- [160] M. Gyulassy, P. Levai and I. Vitev, “Reaction operator approach to multiple elastic scatterings,” *Phys. Rev. D* **66**, 014005 (2002) [nucl-th/0201078].
- [161] A. Kovner and U. A. Wiedemann, “Eikonal evolution and gluon radiation,” *Phys. Rev. D* **64**, 114002 (2001) [hep-ph/0106240].
- [162] U. A. Wiedemann, “Transverse dynamics of hard partons in nuclear media and the QCD dipole,” *Nucl. Phys. B* **582**, 409 (2000) [hep-ph/0003021].
- [163] U. A. Wiedemann, “Gluon radiation off hard quarks in a nuclear environment: Opacity expansion,” *Nucl. Phys. B* **588**, 303 (2000) [hep-ph/0005129].
- [164] U. A. Wiedemann, “Jet quenching versus jet enhancement: A Quantitative study of the BDMPS-Z gluon radiation spectrum,” *Nucl. Phys. A* **690**, 731 (2001) [hep-ph/0008241].
- [165] N. Armesto, C. A. Salgado and U. A. Wiedemann, “Measuring the collective flow with jets,” *Phys. Rev. Lett.* **93**, 242301 (2004), [hep-ph/0405301];
- [166] C. A. Salgado and U. A. Wiedemann, “Medium modification of jet shapes and jet multiplicities,” *Phys. Rev. Lett.* **93**, 042301 (2004), [hep-ph/0310079];
- [167] C. A. Salgado and U. A. Wiedemann, “Calculating quenching weights,” *Phys. Rev. D* **68**, 014008 (2003) [hep-ph/0302184].

-
- [168] X. -N. Wang, “Dynamical screening and radiative parton energy loss in a quark gluon plasma,” *Phys. Lett. B* **485**, 157 (2000) [nucl-th/0003033].
- [169] X. -f. Guo and X. -N. Wang, “Multiple scattering, parton energy loss and modified fragmentation functions in deeply inelastic e A scattering,” *Phys. Rev. Lett.* **85**, 3591 (2000) [hep-ph/0005044].
- [170] X. -N. Wang and X. -f. Guo, “Multiple parton scattering in nuclei: Parton energy loss,” *Nucl. Phys. A* **696**, 788 (2001) [hep-ph/0102230].
- [171] E. Wang and X. -N. Wang, “Parton energy loss with detailed balance,” *Phys. Rev. Lett.* **87**, 142301 (2001) [nucl-th/0106043].
- [172] J. A. Osborne, E. Wang and X. -N. Wang, “Evolution of parton fragmentation functions at finite temperature,” *Phys. Rev. D* **67**, 094022 (2003) [hep-ph/0212131].
- [173] P. B. Arnold, G. D. Moore and L. G. Yaffe, “Transport coefficients in high temperature gauge theories. 1. Leading log results,” *JHEP* **0011**, 001 (2000) [hep-ph/0010177].
- [174] P. B. Arnold, G. D. Moore and L. G. Yaffe, “Transport coefficients in high temperature gauge theories. 2. Beyond leading log,” *JHEP* **0305**, 051 (2003) [hep-ph/0302165].
- [175] P. B. Arnold, G. D. Moore and L. G. Yaffe, “Photon and gluon emission in relativistic plasmas,” *JHEP* **0206**, 030 (2002) [hep-ph/0204343].

-
- [176] S. Jeon and G. D. Moore, “Energy loss of leading partons in a thermal QCD medium,” *Phys. Rev. C* **71**, 034901 (2005) [hep-ph/0309332].
- [177] S. Turbide, C. Gale, S. Jeon and G. D. Moore, “Energy loss of leading hadrons and direct photon production in evolving quark-gluon plasma,” *Phys. Rev. C* **72**, 014906 (2005) [hep-ph/0502248].
- [178] M. G. Mustafa, D. Pal, D. K. Srivastava and M. Thoma, “Radiative energy loss of heavy quarks in a quark gluon plasma,” *Phys. Lett. B* **428**, 234 (1998) [nucl-th/9711059].
- [179] Y. L. Dokshitzer and D. E. Kharzeev, “Heavy quark colorimetry of QCD matter,” *Phys. Lett. B* **519**, 199 (2001) [hep-ph/0106202].
- [180] B. -W. Zhang, E. Wang and X. -N. Wang, “Heavy quark energy loss in nuclear medium,” *Phys. Rev. Lett.* **93**, 072301 (2004) [nucl-th/0309040].
- [181] N. Armesto, C. A. Salgado and U. A. Wiedemann, “Medium induced gluon radiation off massive quarks fills the dead cone,” *Phys. Rev. D* **69**, 114003 (2004) [hep-ph/0312106].
- [182] M. Djordjevic and M. Gyulassy, “Heavy quark radiative energy loss in QCD matter,” *Nucl. Phys. A* **733**, 265 (2004) [nucl-th/0310076].
- [183] V. N. Baier and V. M. Katkov, “Quantum theory of transition radiation and transition pair creation,” *Phys. Lett. A* **252**, 263 (1999) [hep-ph/9811302].

-
- [184] D. Schildknecht and B. G. Zakharov, “Transition radiation in quantum regime as a diffractive phenomenon,” hep-ph/0501241.
- [185] M. Djordjevic, “Transition radiation in QCD matter,” Phys. Rev. C **73**, 044912 (2006) [nucl-th/0512089].
- [186] M. L. Ter-Mikayelian, Dokl. Akad. Nauk SSSR **94**, 1033 (1954).
- [187] M. L. Ter-Mikayelian, *High-Energy Electromagnetic Processes in Condensed Media* (John Wiley & Sons, 1972).
- [188] M. Djordjevic and M. Gyulassy, “The Ter-Mikayelian effect on QCD radiative energy loss,” Phys. Rev. C **68**, 034914 (2003) [nucl-th/0305062].
- [189] S. Wicks, W. Horowitz, M. Djordjevic and M. Gyulassy, “Elastic, inelastic, and path length fluctuations in jet tomography,” Nucl. Phys. A **784**, 426 (2007) [nucl-th/0512076].
- [190] M. Djordjevic and U. W. Heinz, “Radiative energy loss in a finite dynamical QCD medium,” Phys. Rev. Lett. **101**, 022302 (2008) [arXiv:0802.1230 [nucl-th]].
- [191] M. Djordjevic and M. Djordjevic, “LHC jet suppression of light and heavy flavor observables,” arXiv:1307.4098 [hep-ph].
- [192] D. d’Enterria, “Jet quenching,” arXiv:0902.2011 [nucl-ex].
- [193] D. d’Enterria, “Jet quenching in QCD matter: From RHIC to LHC,” Nucl. Phys. A **827**, 356C (2009) [arXiv:0902.2488 [nucl-ex]].

-
- [194] U. A. Wiedemann, “Jet Quenching in Heavy Ion Collisions,” arXiv:0908.2306 [hep-ph].
- [195] M. Spousta, “Jet Quenching at LHC,” Mod. Phys. Lett. A **28**, 1330017 (2013) [arXiv:1305.6400 [hep-ex]].
- [196] A. Majumder and M. Van Leeuwen, “The Theory and Phenomenology of Perturbative QCD Based Jet Quenching,” Prog. Part. Nucl. Phys. A **66**, 41 (2011) [arXiv:1002.2206 [hep-ph]].
- [197] W. A. Horowitz and B. A. Cole, “Systematic theoretical uncertainties in jet quenching due to gluon kinematics,” Phys. Rev. C **81**, 024909 (2010) [arXiv:0910.1823 [hep-ph]].
- [198] N. Armesto, B. Cole, C. Gale, W. A. Horowitz, P. Jacobs, S. Jeon, M. van Leeuwen and A. Majumder *et al.*, “Comparison of Jet Quenching Formalisms for a Quark-Gluon Plasma ‘Brick’,” Phys. Rev. C **86**, 064904 (2012) [arXiv:1106.1106 [hep-ph]].
- [199] T. Renk, “Constraining the Physics of Jet Quenching,” Phys. Rev. C **85**, 044903 (2012) [arXiv:1112.2503 [hep-ph]].
- [200] Y. Mehtar-Tani, J. G. Milhano and K. Tywoniuk, “Jet physics in heavy-ion collisions,” Int. J. Mod. Phys. A **28**, 1340013 (2013) [arXiv:1302.2579 [hep-ph]].
- [201] R. Abir, C. Greiner, M. Martinez and M. G. Mustafa, “Generalisation of Gunion-Bertsch Formula for Soft Gluon Emission,” Phys. Rev. D **83**, 011501 (2011) [arXiv:1011.4638 [nucl-th]].

-
- [202] R. Abir, “Jet-parton inelastic interaction beyond eikonal approximation,” *Phys. Rev. D* **87**, 034036 (2013) [arXiv:1301.1839 [hep-ph]].
- [203] R. Abir, C. Greiner, M. Martinez, M. G. Mustafa and J. Uphoff, “Soft gluon emission off a heavy quark revisited,” *Phys. Rev. D* **85**, 054012 (2012) [arXiv:1109.5539 [hep-ph]].
- [204] R. Abir, U. Jamil, M. G. Mustafa and D. K. Srivastava, “Heavy quark energy loss and D-Mesons at RHIC and LHC energies,” *Phys. Lett. B* **715**, 183 (2012) [arXiv:1203.5221 [hep-ph]].
- [205] T. Bhattacharyya, S. Mazumder and R. Abir, “Color synchrotron off heavy flavor jet deluges the ”dead cone”,” arXiv:1307.6931 [hep-ph].
- [206] U. W. Heinz and M. Jacob, “Evidence for a new state of matter: An Assessment of the results from the CERN lead beam program,” nucl-th/0002042.
- [207] R. Baier, A. H. Mueller, D. Schiff and D. T. Son, “’Bottom up’ thermalization in heavy ion collisions,” *Phys. Lett. B* **502**, 51 (2001) [hep-ph/0009237].
- [208] J. Alam, B. Sinha and S. Raha, “Successive equilibration in quark - gluon plasma,” *Phys. Rev. Lett.* **73**, 1895 (1994).
- [209] Z. Xu and C. Greiner, “Shear viscosity in a gluon gas,” *Phys. Rev. Lett.* **100**, 172301 (2008) [arXiv:0710.5719 [nucl-th]].

-
- [210] S. K. Das and J. -eAlam, “Soft gluon multiplicity distribution revisited,” *Phys. Rev. D* **82**, 051502 (2010) [arXiv:1007.4405 [nucl-th]].
- [211] S. J. Parke and T. R. Taylor, “An Amplitude for n Gluon Scattering,” *Phys. Rev. Lett.* **56**, 2459 (1986).
- [212] T. Bhattacharyya, S. Mazumder, S. KDas and J. -eAlam, “Examination of the Gunion-Bertsch formula for soft gluon radiation,” *Phys. Rev. D* **85**, 034033 (2012) [arXiv:1106.0609 [nucl-th]].
- [213] T. S. Biro, E. van Doorn, B. Muller, M. H. Thoma and X. N. Wang, “Parton equilibration in relativistic heavy ion collisions,” *Phys. Rev. C* **48**, 1275 (1993) [nucl-th/9303004].
- [214] S. Mazumder, T. Bhattacharyya and J. -eAlam, “Gluon bremsstrahlung by heavy quarks - its effects on transport coefficients and equilibrium distribution,” arXiv:1305.6445 [nucl-th].
- [215] M. Younus, C. E. Coleman-Smith, S. A. Bass and D. K. Srivastava, “Systematic Study of Charm Quark Energy Loss Using Parton Cascade Model,” arXiv:1309.1276 [nucl-th].
- [216] B. L. Combridge, “Associated Production of Heavy Flavor States in $p p$ and anti- $p p$ Interactions: Some QCD Estimates,” *Nucl. Phys. B* **151**, 429 (1979).
- [217] E. Eichten, I. Hinchliffe, K. D. Lane and C. Quigg, “Super Collider Physics,” *Rev. Mod. Phys.* **56**, 579 (1984) [Addendum-*ibid.* **58**, 1065 (1986)].

-
- [218] K. J. Eskola, V. J. Kolhinen and C. A. Salgado, “The Scale dependent nuclear effects in parton distributions for practical applications,” *Eur. Phys. J. C* **9**, 61 (1999) [hep-ph/9807297].
- [219] H. L. Lai, J. Huston, S. Kuhlmann, F. I. Olness, J. F. Owens, D. E. Soper, W. K. Tung and H. Weerts, “Improved parton distributions from global analysis of recent deep inelastic scattering and inclusive jet data,” *Phys. Rev. D* **55**, 1280 (1997) [hep-ph/9606399].
- [220] C. Peterson, D. Schlatter, I. Schmitt and P. M. Zerwas, “Scaling Violations in Inclusive $e^+ e^-$ Annihilation Spectra,” *Phys. Rev. D* **27**, 105 (1983).
- [221] U. Jamil and D. K. Srivastava, “Nuclear suppression of heavy quark production at forward rapidities in relativistic heavy ion collisions,” *J. Phys. G* **37**, 085106 (2010) [arXiv:1005.1208 [nucl-th]].
- [222] R. Abir and M. G. Mustafa, “Colour-singlet clustering of partons and recombination model for hadronization of quark-gluon plasma,” *Phys. Rev. C* **80**, 051903 (2009) [arXiv:0905.4140 [hep-ph]].
- [223] R. Abir and M. G. Mustafa, “On the critical exponent of η/s and a new exponent-less measure of fluidity,” arXiv:1001.0692 [hep-ph].
- [224] C. A. Islam, R. Abir, M. G. Mustafa, S. K. Ghosh and R. Ray, “SU(3) colorsingletness, Z(3) symmetry, Polyakov Loop and dynamical recombination,” arXiv:1208.3146 [hep-ph].